Novel tools for mast cell research: Mast cell-specific Cre-mediated gene inactivation and inducible ablation of mast cells *in vivo*

Inaugural-Dissertation

zur

Erlangung des Doktorgrades

der Mathematisch-Naturwissenschaftlichen Fakultät

der Universität zu Köln

vorgelegt von

Julia Scholten
aus Duisburg

Köln, 2009

Berichterstatter: **Prof. Dr. Dr. Thomas Krieg**

Prof. Dr. Manolis Pasparakis

Tag der mündlichen Prüfung: 5. Februar 2009

Summary

Mast cells are well known effector cells in allergic disorders. In the recent years, however, mast cells were demonstrated to play pivotal roles in initiating and modulating innate and adaptive immune responses. The animal models available until today for the investigation of mast cell functions are primarily the *Kit*-mutant $Kit^{W/Wv}$ and $Kit^{Wsh/Wsh}$ mouse strains. These mice are devoid of mast cells and can be reconstituted with mast cells from gene deficient mice. The phenotypic abnormalities, apart from mast cell deficiency, e.g. the profound perturbation of the hematopoietic system, however, limit the utility of these strains. Aiming at new models of mast cell-specific gene inactivation *in vivo* and of mast cell-deficiency, the Cre/*loxP* system was applied to allow Cre-mediated mutagenesis selectively in mast cells. BAC (bacterial artificial chromosome) transgenic animals were successfully generated that display Cre expression under the control of either the *Mcpt5* or *Mcpt6* promoter. Cre-mediated recombination as assessed by reporter gene expression in *Mcpt5-Cre* or *Mcpt6-Cre R26R-EYFP* double positive mice was found to be highly efficient in peritoneal and skin mast cells, but was not found in hematopoietic cell populations other than mast cells. Thus, the new mast cell-specific Cre transgenic mouse lines will provide useful tools for the investigation of mast cell-specific functions of individual genes.

Furthermore, the Mcpt5-Cre strain was used to establish a new model for inducible ablation of mast cells in adult mice. By crossing this line to the iDTR strain, which expresses the high affinity diphtheria toxin receptor (DTR) after Cre-mediated deletion of a stop element, mast cells were rendered diphtheria toxin (DT) sensitive. DT treatment of *Mcpt5-Cre iDTR* double positive mice resulted in successful ablation of connective tissue type mast cells (CTMC), but not of mucosal mast cells (MMC). The depletion of CTMC resulted in significant reduction of a passive, systemic anaphylactic response demonstrating that this system for mast cell ablation represents a useful model for the investigation of mast cell functions during immune responses. Interestingly, the repopulation of the peritoneal cavity and the skin with mast cells after DT-mediated mast cell depletion followed a very slow kinetic with a noteworthy recurrence of peritoneal mast cells three months after DT treatment. Skin mast cells do not return significantly within a period of four months. Thus, the long persistence of the mast cell-depleted state allows the application of this system for long-term experiments and should provide new insights into the mechanisms of mast cell homeostasis and recruitment.

Zusammenfassung

Mastzellen sind vor allem bekannt als Effektorzellen allergischer Erkrankungen. In den letzten Jahren wurde jedoch gezeigt, dass Mastzellen entscheidend zu der Mobilisierung und Modellierung von angeborenen und adaptiven Immunantworten beitragen. Die derzeitig verfügbaren Modelle für die *in vivo*-Analyse von Mastzellfunktionen, sind vorwiegend die *Kit*-mutierten, Mastzell-defizienten $Kit^{W/Wv}$ und $Kit^{Wsh/Wsh}$ Mäuse, die mit *in vitro* differenzierten Mastzellen von Gen-defizienten Mäusen rekonstituiert werden können. Phänotypische Abnormitäten zusätzlich zu der Mastzell-Defizienz, z. B. Störungen des hämatopoietischen Systems, erschweren jedoch das Experimentieren und die Interpretation der Daten. Aus diesem Grund wurde hier das Cre/*loxP*-System herangezogen, um *in vivo* Gene gezielt in Mastzellen zu inaktivieren und um neue Modelle für Mastzell-Defizienz zu generieren. BAC (bacterial artificial chromosome) transgene Mauslinien wurden erfolgreich hergestellt, die die Cre-Rekombinase unter der Kontrolle des *Mcpt5*- bzw. *Mcpt6*-Promotors ausprägen. In *Mcpt5-Cre* bzw. *Mcpt6-Cre R26R-EYFP* doppelt positiven Mäusen konnte eine höchst effiziente, Cre-mediierte Rekombination in Mastzellen der Peritonealhöhle und der Haut, jedoch nicht in anderen Zellpopulationen, nachgewiesen werden. Die neuen Mastzell-spezifischen Cre-transgenen Mauslinien werden daher in Zukunft die Untersuchung Mastzell-spezifischer Funktionen einzelner Gene erheblich erleichtern.

Des Weiteren wurde die Mcpt5-Cre Linie für die Etablierung eines neuen Models für induzierbare Ablation von Mastzellen *in vivo* verwendet. Die Kreuzung dieser Linie mit dem iDTR Mausstamm, der den hoch affinen Diphtherietoxin Rezeptor (DTR) nach Cre-mediierter Deletion eines Stop-Elements ausprägt, führt zu einer Sensibilisierung von Mastzellen gegenüber dem Diphtherietoxin (DT) in *Mcpt5-Cre iDTR* doppelt positiven Tieren. Die Behandlung mit DT resultierte in einer effizienten Depletion von Bindegewebs-mastzellen (CTMC), jedoch nicht von mukosalen Mastzellen (MMC). Die Ablation der CTMC reichte aus, eine passive, systemische anaphylaktische Reaktion signifikant zu reduzieren, was demonstriert, dass das System der induzierbaren Mastzell-Ablation ein geeignetes Modell für die Erforschung von Mastzell-Funktionen darstellt. Interessanter-weise folgte die Repopulation der Bauchhöhle und der Haut mit Mastzellen einer höchst langsamen Kinetik. Ein signifikanter Anstieg der Mastzell-Zahlen in der Bauchhöhle zeigte sich erst drei Monate nach Depletion. Eine deutliche Rückkehr der Hautmastzellen war auch nach vier Monaten noch nicht zu beobachten. Folglich erlaubt die langfristige Depletion der Mastzellen die Anwendung dieses Systems in Langzeitexperimenten und kann, des Weiteren, neue Einblicke in die Mechanismen der Homöostase und Rekrutierung von Mastzellpopulationen gewähren.

Table of contents

1 Introduction

1.1 Mast cells

Mast cells are highly granulated immune cells that reside in tissues and serosal cavities throughout the body but predominantly at inner and outer body surfaces, like the skin, the airways and the intestinal tract and also in close vicinity to blood vessels and nerves (Galli, 1990). At these locations they are well placed to serve as the first line of defense.
Mast cells were first described by Paul Ehrlich in the late 19th century based on the metachromatic staining properties of the large cytoplasmic granules (Ehrlich, 1878). The "well-fed appearance" led him to designate these cells as mast cells. Today we know that the granule content does not originate from an uptake but from the synthesis and storage of high amounts of proteoglycans, proteases and other mediators.
Mast cells are widely recognized as major effectors in allergic disorders and in responses to parasites. But in the last decade, it turned out that mast cells also serve other important functions. The essential role of mast cells in the immune system is also reflected by the fact that no human individual has been identified until today that lacks mast cells (Stevens and Adachi, 2007).

1.1.1 Mast cell development and heterogeneity

Mast cells originate from multipotent hematopoietic precursors in the bone marrow. Differentiated to committed mast cell progenitors (MCP), they are released to the blood and circulate until they extravasate into the tissue and serosal cavities where they finally differentiate to the mature tissue resident mast cells (Hallgren and Gurish, 2007; Rodewald et al., 1996). The spleen has also been demonstrated to be a source of MCPs in the adult mouse (Arinobu et al., 2005; Khalil et al., 1996). The earliest murine committed MCP has been identified in fetal blood at day 15.5 of gestation (Rodewald et al., 1996). In contrast, the direct identification of MCPs in the circulation of adult mice has not been accomplished by reason of their low frequency, i.e. 0.001% of mononuclear cells as determined by mast cell colony formation by blood cells *ex vivo* (Hallgren and Gurish, 2007). A sequential increase of MCPs first in the bone marrow, then in the blood and finally in the intestine, could be observed in worm infected mice demonstrating the recruitment of mast cells from the bone marrow to the site of infection (Pennock and Grencis, 2004). The development of MCPs to mature mast cells is strongly dependent on the microenvironment and, thus, on the production of growth factors at the site of differentiation. The most important factor for mast cell growth, differentiation, proliferation and survival is the stem cell factor (SCF) that binds to the receptor tyrosine kinase c-Kit and is expressed by stromal cells as a soluble or a membrane bound molecule in various

tissues (Galli et al., 1994; Longley et al., 1997). The *Kit* gene is a proto-oncogene originally discovered as the cellular homolog (*c-Kit*) of the feline sarcoma virus oncogene *v-Kit (Besmer et al., 1986)*. The Kit receptor is expressed on hematopoietic progenitor cells but is down regulated upon differentiation in all lineages except mast cells which express Kit and remain SCF responsive throughout their entire differentiation and life span (Metcalfe et al., 1997). The critical role of c-Kit/SCF interaction was demonstrated in mice with spontaneous mutations in the *c-Kit* locus (also known as *white spotting locus* (*W*)), e.g. in $Kit^{W/W\text{-}v}$ and $Kit^{Wsh/Wsh}$ mice (Grimbaldeston et al., 2005; Kitamura et al., 1978) or in mice with mutations of the *SCF locus, (*SI/SI^{d} mice (Kitamura and Go, 1979), see also section 1.1.5). In addition to SCF, the mediators Interleukin (IL)-3, IL-4, IL-9, IL-10 and nerve growth factor (NGF) contribute to mast cell growth and differentiation (Okayama and Kawakami, 2006).

Mast cells that reside in various tissues differ in their phenotypes. This heterogeneity among mast cells is due to the diverse microenvironments and the presence of various combinations of the above mentioned growth factors at these sites where the precursor cells differentiate into mature mast cells (Okayama and Kawakami, 2006). Histochemical differences among mast cells described by Enerbäck et al. led to the classification of two distinct mast cell subpopulations in rodents, i.e. connective tissue mast cells (CTMC) and mucosal mast cells (MMC) (Enerbäck et al., 1985). These mast cell phenotypes differ in their localization and secretory granule content. CTMCs are found predominantly in the subepithelial strata of the skin and the peritoneal cavity but also in the submucosal layers of the intestine. Characteristically, CTMCs store abundant heparin sulfate proteoglycan, chymases, tryptases and mast cell carboxypeptidase A (MC-CPA). In contrast, MMCs reside predominantly within the epithelia in the intestinal and respiratory tract, i.e. they are located above the basement membrane between the epithelial cells. They are smaller than CTMCs and have fewer granules. The MMC granules contain chonodroitin sulfate proteoglycan and chymases, but not tryptases (Metcalfe et al., 1997). An important finding was that the MMC population remarkably expands in T cell-dependent responses to certain intestinal parasites and that, in athymic mice, MMC numbers are reduced, while CTMC numbers are not, revealing a T cell dependence of MMCs, but not of CTMCs (Metcalfe et al., 1997). The intestine harbors a large reservoir of mast cell progenitors. Helminth infections cause a rapid expansion of the MMC population, likely facilitated by the presence of these intestinal precursors and by *de novo* production of mast cell progenitors in the bone marrow that are committed to enter the intestine from the blood (Gurish and Boyce, 2006; Pennock and Grencis, 2004). Within three weeks after expulsion of the pathogen, the number of intestinal mast cells decreases again suggesting a life span of most MMCs of only one to two weeks. On the contrary, an extraordinarily

long life span, i.e. probably more than one year, has been reported for CTMCs in the skin and peritoneal cavity (Kitamura, 1989).

Also in humans, two mast cell subpopulations, distinguished by their granule content, were described. The MC_T subpopulation contains only tryptases, whereas the MC_{TC} contain tryptase and chymase as well as cathepsin G-like protease and MC-CPA (Metcalfe et al., 1997). In terms of localization, MC_T correspond most closely to the MMC phenotype in rodents as they reside predominantly in the lung septa and small intestine mucosa. In contrast, the MC_{TC}, localized particularly in the skin and intestinal submucosa, resemble most closely the rodent CTMC population (Metcalfe et al., 1997).

1.1.2 Mast cell granules and proteases

The mast cell granules predominantly contain proteoglycans and proteases. The serglycin proteoglycans with heparin and chonodroitin sulfate site chains in the secretory granules are the most negatively charged molecules in the body (Huang et al., 1998b) and are the reason for the metachromatic staining properties of mast cells that can readily be detected with cationic dyes like Toluidine blue or Giemsa. The neutral proteases, which are active at a neutral pH, are synthesized as inactive zymogens containing a hydrophobic signal peptide for the translation into the endoplasmic reticulum followed by a propeptide. In the mature secretory granules the proteases are stored in their enzymatically active form that results from proteolytic cleavage of the propeptide and are ionically bound to the serglycin proteoglycans (Huang et al., 1998b). About 50% of the weight of a mature mast cell consists of the proteases/serglycin complexes (Thakurdas et al., 2007). The three major families of mast cell proteases are tryptases, chymases and mast cell carboxypeptidase A (MC-CPA) (Reynolds et al., 1989). Both, tryptases and chymases, belong to the family of serine proteases with endopeptidase activity whereas CPA is a metalloproteinase with exopeptidase activity.

In mice, two mast cell tryptases, mMCP-6 and mMCP-7 (McNeil et al., 1992b; Reynolds et al., 1991), and five chymases, mMCP-1, -2, -4, -5 and -9 (Hunt et al., 1997; McNeil et al., 1991; Serafin et al., 1990; Serafin et al., 1991; Trong et al., 1989), were described. In contrast to the MC-CPA, encoded on chromosome 3, the genes for the tryptases, *Mcpt6* and *Mcpt7*, are located in a 1.5 Mb complex on chromosome 17, which is a cluster of genes encoding for 13 mouse proteases all belonging to the serine protease superfamily. Among these, mMCP-6 and mMCP-7 are selectively expressed in mast cells (Wong et al., 2004). Like the tryptase genes, the genes encoding for the chymases, *Mcpt1*, *2*, *4*, *5* and *9*, are organized in a gene cluster which is located on chromosome 14 (Gurish et al., 1993). This cluster also includes the genes that encode cathepsin G and numerous granzymes (Huang et al., 1998b).

The mast cell proteases are differentially expressed in the mast cell subpopulations. CTMCs display abundant mMCP-4, -5 and -6 as well as MC-CPA expression whereas MMC express preferentially mMCP-1 and -2 (Pejler et al., 2007). The expression pattern of mast cell proteases shows that even the subpopulation of MMCs and CTMCs are not homogenous. MMCP-9, for instance, is preferentially expressed in uterine CTMCs (Hunt et al., 1997). Stevens and coworkers demonstrated that perivascular mast cells in BALB/c mice express mMCP-2 and high steady state levels of mMCP-7 in addition to mMCP-4, -5, -6 and MC-CPA (Stevens et al., 1994). Furthermore, a strain specific difference has been detected for mMCP-7. This protease is not expressed in C57BL/6 mice due to a point mutation leading to differential splicing and, thus, to an introduction of on additional stop codon (Hunt et al., 1996). The mast cell protease phenotype seems to be plastic during immune responses since Friend and coworkers showed that in *Trichinella spiralis*-infected BALB/c mice the phenotype of mast cells changed in respect to their protease content. Dependent on the time after infection and on the intestinal tissue layer they detected, in addition to mast cells expressing either mMCP-5 or mMCP-1/mMCP-2, transitional phenotypes that express either mMCP-5/mMCP-2 without mMCP-1, or only mMCP-2 (Friend et al., 1996).

The functions of mast cell proteases are versatile. Results of i*n vitro* studies implicated mast cell proteases in the activation of matrix metalloproteases, cleavage of angiotensin I to angiotensin II and extracellular matrix remodeling by cleavage of fibronectin (Pejler et al., 2007). *In vivo*, the tryptase mMCP-6 was demonstrated to be essential for the clearance of a *Klebsiella pneumonia* infection. By inducing IL-8 production from endothelial cells mMCP-6 indirectly mediates neutrophil extravasation and accumulation in the tissue (Thakurdas et al., 2007). The disruption of the *Mcpt1* gene, usually expressed in MMCs, leads to an impaired expulsion of the nematode *Trichinella spiralis* (Knight et al., 2000). Using mMCP-5 deficient mice, Abonia et al. demonstrated a critical role of mMCP-5 in ischemic tissue injury (Abonia et al., 2005). Furthermore, the CTMC proteases mMCP-4 and -6 were implicated in mast cell-mediated upregulation of angiogenesis in a model of epithelial cancer (Coussens et al., 1999). Interestingly, chymase-heparin complexes exocytosed into the dermal tissue seem to regulate mast cell numbers in the skin by converting membrane bound SCF expressed by keratinocytes to its soluble form. In addition these complexes mediate the accumulation of eosinophils in a model of dermatitis (Tomimori et al., 2002a; Tomimori et al., 2002b). Finally, using an *mc-cpa* mutant Schneider and coworkers could demonstrate the critical role of MC-CPA in the regulation of endothelin effects and in the protection against snake venom sarafotoxins (Schneider et al., 2007).

1.1.3 From mast cell activation to effector functions

Mast cells were widely recognized as key effector cells in type I hypersensitivity reactions or in responses to parasites. Especially in countries where parasite infections play a minor role, mast cells were primarily regarded as potentially harmful cells causing allergic disorders. Today it is well accepted that mast cells exert various other physiological functions. The strategical location close to the inner and outer body surfaces and their location close to blood vessels enable mast cells to quickly react to invading pathogens and to initiate immune responses by producing and secreting a broad spectrum of factors and by recruiting other effector cells from the circulation.

Mast cells are equipped with a multitude of receptors serving directly or indirectly as sensors of pathogen invasion. Many of these belong to the large family of pattern recognition receptors (PRR) that bind directly to pathogen associated molecular patterns (PAMPs) shared by distinct groups of pathogens. Toll-like receptors (TLR) are an important group of the PRR family. Via the TLR2/6 heterodimer, the TLR4 and via the intracellular TLR9 they are able to recognize gram positive bacteria (peptidoglycans), gram negative bacteria (lipopolysaccharide, LPS) and bacterial DNA containing *CpG* motives, respectively (Matsushima et al., 2004; McCurdy et al., 2001; Supajatura et al., 2002). Furthermore, mast cells release proinflammatory cytokines like type I interferons (IFN) when activated by dsRNA (Poly I:C, a mimic of viral infection) via TLR3 and ssRNA via TLR7 indicating a role of mast cells in anti-viral responses (Kulka et al., 2004; Matsushima et al., 2004).

The activation of mast cells via FcεRI was investigated extensively (Kinet, 1999). This receptor is constitutively expressed on mast cells and constantly loaded with IgE due to its high affinity to the invariable chain of this immunoglobulin class (Benoist and Mathis, 2002). The crosslinking of FcεRI bound IgE by multivalent antigens results in degranulation. In the presence of SCF and IFNγ mast cells additionally express the FcγRIII and FcγRI, respectively (Tkaczyk et al., 2004). The crosslinking of these receptors by IgG immune complexes can also induce degranulation. Beside these activating receptors, mast cells also express the inhibitory receptor FcγRIIB. Coaggregation of FcγRIIB with FcεRI or FcγRIII by IgG immune complexes results in downregulation of the secretory response (Ott and Cambier, 2000; Tkaczyk et al., 2004). Also the interaction of complement components or their cleavage products (C3a and C5a) with complement receptors on mast cells results in activation and release of mast cell mediators (Marshall, 2004).

Mast cells can be regarded as factories of a huge variety of mediators. Three major classes of mediators are produced by mast cells (Marshall, 2004): (1) The preformed and granule-associated mediators like histamine, serotonin, mast cell proteases as well as the

factors TNF, VEGF and FGF2; (2) the newly synthesized lipid mediators like leukotriene (LT)C_4, LTB_4, prostaglandin (PG)D_2 and PGE_2 and (3) *do novo*-synthesized cytokines and chemokines. The cytokines produced by mast cells can be grouped in pro-inflammatory and immunomodulatory cytokines. The huge variety of mast cell-mediators as well as their potential functions are listed in Table 1.1 which was taken from the review "Mast-Cell Responses To Pathogens" by Jean S. Marshall (Marshall, 2004).

Mediators	Examples of function
Granule-associated	
Histamine and serotonin	Alter vascular permeability
Heparin and/or chondroitin sulphate peptidoglycans	Enhance chemokine and/or cytokine function and angiogenesis
Tryptase, chymase, carboxypeptidase and other proteases	Remodel tissue and recruit effector cells
TNF, VEGF and FGF2	Recruit effector cells and enhance angiogenesis
Lipid-derived	
LTC_4, LTB_4, PGD_2 and PGE_2	Recruit effector cells, regulate immune responses, and promote angiogenesis, oedema and bronchoconstriction
Platelet-activating factor	Activates effector cells, enhances angiogenesis and induces physiological inflammation
Cytokine	
TNF, IL-1α, IL-1β, IL-6, IL-18, GM-CSF, LIF, IFN-α and IFN-β	Induce inflammation
IL-3, IL-4, IL-5, IL-9, IL-13, IL-15 and IL-16	Functions of T helper 2-type cytokines
IL-12 and IFN-γ	Functions of T helper 1-type cytokines
IL-10, TGF-β and VEGF	Regulate inflammation and angiogenesis
Chemokine	
CCL2, CCL3, CCL4, CCL5, CCL11 and CCL20	Recruit effector cells, including dendritic cells, and regulate immune responses
CXCL1, CXCL2, CXCL8, CXCL9, CXCL10 and CXCL11	Recruit effector cells and regulate immune responses
Other	
Nitric oxide and superoxide radicals	Bactericidal
Antimicrobial peptides	Bactericidal

Table 1.1 Mediators synthesized by mast cells. Table is taken from the review of Marshall, 2004 "Mast-Cell Responses To Pathogens". CCL, CC-chemokine ligand; CXCL, CXC-chemokine ligand; FGF2, fibroblast growth factor 2; GM-CSF, granulocyte/macrophage colony-stimulating factor; IFN, interferon; IL, interleukin; LIF, leukemia inhibitory factor; LT, leukotriene; PG, prostaglandin; TGF-β, transforming growth factor-β; TNF, tumor-necrosis factor; VEGF, vascular endothelial growth factor.

Dependent on the mode of activation, mast cells can release distinct cytokine and mediator profiles thereby enabling mast cells to initiate and modulate immune responses in a way appropriate to meet the pathogenic challenge.

The importance of mast cells for host defense against bacterial infection was demonstrated by studies of *Klebsiella pneumonia* infection and of a peritonitis model of cecal ligation and puncture (CLP) (Echtenacher et al., 1996; Malaviya et al., 1996). Using genetically mast cell-deficient mice (*Kit*-mutant mice, see below) it was shown that the rapid release of TNF from mast cells facilitated neutrophil recruitment necessary for clearance of infection. Mast cells are the only cells known to prestore TNF in their secretory granules, which can be immediately released upon activation (Gordon and Galli, 1990a), stressing the potential role of mast cell-derived TNF in the initiation of inflammatory responses. In addition to TNF, other mediators secreted by mast cells promote the recruitment of effector cells. These mediators include histamine that increases vascular permeability and enhances the expression of adhesion molecules on endothelial cells (Marshall and Jawdat, 2004), as well as mast cell proteases which play a critical role in the recruitment of neutrophils and eosinophils (Huang et al., 1998a; Schmidlin et al., 2002). *In vitro* studies showed that mast cells are capable of phagocytosing pathogens and that mast cells produce antimicrobial peptides suggesting also direct effector functions of mast cells in host defense (Abraham and Malaviya, 1997; Di Nardo et al., 2003). These data were confirmed by a report that revealed a mechanism used by mast cells to kill bacteria extracellularly. This study demonstrated *in vitro* that, upon exposure to *Streptococcus pyogenes*, mast cells released extracellular structures composed of DNA, histones, tryptase and antimicrobial peptides. This process was mediated by reactive oxygen species (ROS)-dependent cell death (von Köckritz-Blickwede et al., 2008). In addition to their critical role in host defense, several reports implicated mast cells in wound healing and tissue remodeling (Trautmann et al., 2000; Weller et al., 2006).

The data discussed so far illustrates that mast cells are the cells responsible for the immediate innate response to invading pathogens. There are many indications that mast cells also set the stage for adaptive immune responses and exert modulatory functions on T and B cell responses. Accordingly, mast cells can influence the migration, maturation and function of dendritic cells and in this line indirectly induce the polarization of naïve T cells towards T_H2 effector cells (Galli et al., 2005). McLachlan et al. could show that the T cell recruitment to lymph nodes draining at site of infection and the hypertrophy of these lymph nodes was substantially increased by mast cell-derived TNF (McLachlan et al., 2003). In addition, a recent study by McLachlan and coworkers suggested mast cells as the sensory arm of the adaptive immune system. They could show that small-molecule mast cell activators, administered together with vaccine antigen, evoked substantial increases of antigen-specific serum IgG, highlighting mast cell activators as a new class of adjuvants (McLachlan et al., 2008). Surprisingly, mast cells, best known as

immunostimulatory cells and promoters of inflammation, have recently been implicated in immunosuppression, based on experiments with *Kit*-mutant, mast cell-deficient mice. The immunosuppressive function of regulatory T cells in a model of transplant tolerance was found to be dependent on mast cells (Lu et al., 2006). Another study demonstrated that mast cell-derived IL-10 limits skin pathology during allergic contact dermatitis and chronic irradiation with UVB (Grimbaldeston et al., 2007).

1.1.4 Mast cell associated disorders

The most extensively studied disorder associated with mast cells is the type I hypersensitivity. Because of the extremely high affinity of the Fc receptor for IgE (FcεRI), mast cells are constantly coated with IgE (Benoist and Mathis, 2002). Crosslinking of the surface IgE molecules by multivalent antigens leads to degranulation and release of preformed mediators like histamine, prostaglandins, leukotrienes and TNF causing the immediate allergic response. Furthermore, mast cells have an important role in the manifestation of chronic allergic disorders like asthma, allergic rhinitis and atopic dermatitis. In mice, it was shown that the development of the typical features of asthma, i.e. excessive production of mucus, airway hyperresponsiveness, bronchoconstriction, chronic inflammation of airway mucosa and recruitment of eosinophils and other leukocytes, was dependent on mast cells expressing the γ-chain of the FcεRI and FcγRIII receptors (Yu et al., 2006). Anaphylaxis is a life-threatening condition caused by the sudden release of mast cell- and basophil-derived mediators into the circulation. This severe form of an immediate hypersensitivity reaction is classically mediated by IgE and FcεRI. In rodents, however, an alternative mode of mast cell activation via IgG and FcγRIII was described (Grimbaldeston et al., 2006).

In addition to antigen-specific IgE-mediated responses, antigen-nonspecific IgE can modulate mast cell functions as well. Mast cells and antigen-nonspecific IgE were both required for optimal sensitization in a model of contact hypersensitivity (CHS), a T cell-mediated immune response. The TNF released by mast cells in this model was important for the optimal migration of dendritic cells to the draining lymph nodes which present the contact allergen to T cells (Grimbaldeston et al., 2006).

Beside the IgE/FcεRI-mediated allergic disorders, a pathogenic role was suggested for mast cells in various other human diseases like multiple sclerosis, bullous pemphigoid and rheumatoid arthritis. Enhanced degranulation and accumulation of mast cells and their products at the affected sites in those patients indicated a contribution of mast cells to these diseases (Benoist and Mathis, 2002). The observations were supported by results obtained in mouse models for these disorders. Multiple sclerosis and the corresponding mouse model of experimental autoimmune encephalomyelitis (EAE) are both critically

dependent on proinflammatory T_H1 cells. Interestingly, mast cell-deficient (*Kit*-mutant) mice develop an only milder form of the disease (Secor et al., 2000). Rheumatoid arthritis induced by antibodies against the enzyme glucose-6-phosphate isomerase (GPI) was also shown to be dependent on mast cells as mast cell-deficient mice were resistant to arthritis induction (Lee et al., 2002). The same was found in another model of collagen-induced arthritis. The results have to be validated further since contradictory results were obtained with different mast cell-deficient mouse strains (see also section 1.1.5) (Zhou et al., 2007). The strong therapeutic effect of a β2-adrenergic agonist, that prevents mast cell degranulation, on experimental arthritis, however, supports a contribution of mast cells to this autoimmune disease (Malfait et al., 1999). Likewise, in a mouse model for bullous pemphigoid, mast cells were demonstrated to play a crucial role by recruiting neutrophils to the developing lesion (Chen et al., 2001).

Recently, the involvement of mast cells in tumorigenesis is gaining increasing attention. Mast cells accumulate in the microenvironment of many tumors (Theoharides and Conti, 2004). As mast cells can release mediators that are beneficial as well as mediators that are detrimental for the tumor, the overall effect of mast cells on tumorigenesis was not clear. Interestingly, in a model of adenomatous polyposis coli (APC), Khazaie and coworkers could show that the development of the polyps was mast cell dependent (Gounaris et al., 2007). Consistent with these results, mast cells accumulate around Myc-induced pancreatic islet tumors. Reduced tumor growth after administration of inhibitors of mast cell degranulation and impaired tumor progression in *Kit*-mutant, mast cell-deficient mice provided evidence for an important function of mast cells in tumor progression (Soucek et al., 2007). In a model of epithelial carcinogenesis involving mast cell-competent and mast cell-deficient (*Kit*-mutant) HPV16 transgenic mice, Coussens et al. demonstrated an implication of mast cells in the induction of premalignant neovascularization (Coussens et al., 1999).

1.1.5 Models for the investigation of mast cells

To investigate biochemistry and functions of mast cells *ex vivo* it is necessary to obtain pure suspensions of mast cells. The cultivation of primary mast cells isolated from mice was often hampered by the scarcity of mast cells in the various tissues. For *in vitro* studies, mast cell lines like the murine, growth factor-independent C57 or growth factor-dependent MC/9 and PT18 lines (Burd et al., 1989) and human mast cell lines like the immature HMC-1 line (Butterfield et al., 1988) are available. These lines, however, might not reflect the mast cell phenotypes found *in vivo*. An improvement was the finding that mast cells can be derived from bone marrow cells in the presence of IL-3 (Kitamura, 1989). These bone marrow-derived mast cells (BMMC) have a rather immature phenotype as judged by their production of chonodroitin sulfate and of the proteases mMCP-5 and -6

and MC-CPA but lack of mMCP-4 (Lunderius et al., 2000). The isolation and cultivation of fetal skin-derived mast cells (FSMC (Yamada et al., 2003)) and peritoneal cell-derived mast cells (PCMC (Malbec et al., 2007)) provided useful tools for the investigation of mast cells *in vitro* as these cultured mast cells closely resemble connective tissue type mast cells *in vivo*.

To investigate mast cell functions *in vivo*, researchers utilized mouse strains carrying spontaneous mutations of either the *c-Kit* gene (*white spotting locus*, *W*) or of the *steel* locus (*sl*) encoding for the Kit ligand (stem cell factor, SCF) which result, among other phenotypic abnormalities, in profound mast cell-deficiency (Galli and Kitamura, 1987). The most commonly used mouse model for mast cell investigation is the WBB6F1-$Kit^{W/Wv}$ mouse. *W* represents a point mutation at an exon-intron junction that causes an altered splicing of the mRNA, resulting in abrogation of surface Kit expression (Galli et al., 2005). Mice homozygous for the *W* allele are white and die before postnatal day ten. The *W* mutation is fixed to the WB background (W-spotted line B) due to a breeding program of continuous brother-sister matings of $Kit^{W/+}$ mice (Waskow et al., 2004). *Wv* is a loss-of-function point mutation in the tyrosine kinase domain of c-Kit, that significantly reduce (but does not abolish) kinase activity upon ligand binding. The F1-hybrid of the $Kit^{W/+}$ and $Kit^{Wv/+}$ mice (WBBL/6F1-$Kit^{W/Wv}$) is viable and profoundly lacks all mast cells with less than 1% of wild-type levels of skin mast cells (Kitamura et al., 1978). In addition, these mice suffer from several other phenotypic abnormalities like macrocytic anemia, sterility, lack of melanocytes and interstitial cells of Cajal and a high incidence of spontaneous dermatitis, squamous papillomas of the fore-stomach, gastric ulcera and dilatation of the duodenum (Grimbaldeston et al., 2005). The same phenotype is present in Sl/Sl^{d} mice in which a mutation of the gene encoding for SCF results in mast cell deficiency (Galli and Kitamura, 1987). Another mouse model that is gaining increasing popularity is the $Kit^{Wsh/Wsh}$ mouse. The "*Wsash*" (*Wsh*) mutation is an inversion mutation spanning 2.8 to 3.3 Mb (Nigrovic et al., 2008) in the region upstream of the transcription start of *c-Kit* that arose spontaneously in a cross between two inbred strains (C3H/HeH x 101/H) 23 years ago (Berrozpe et al., 2006; Grimbaldeston et al., 2005). Mast cells are present in newborn mice but their numbers decrease with age until, at the age of ten weeks, the mice are virtually mast cell-deficient (Wolters et al., 2005; Yamazaki et al., 1994). Grimbaldeston et al. detected in the back skin of ten to twelve week-old $Kit^{Wsh/Wsh}$ mice mast cell numbers that were about 1.2 to 7.2% of those observed in wild-type littermates. Surprisingly, it has been shown that after induction of chronic inflammatory responses, mast cell populations developed in $Kit^{Wsh/Wsh}$ but also in $Kit^{W/Wv}$ mice at the affected sites (Metz et al., 2007). In contrast to the $Kit^{W/Wv}$ mice, $Kit^{Wsh/Wsh}$ mice were considered to display less phenotypic abnormalities. They are viable and fertile but also lack the interstitial cells of Cajal and

demonstrated significant bile reflux into the stomach (Grimbaldeston et al., 2005). However, new data generated by Nigrovic et al. demonstrated hematopoietic abnormalities in *Kit*$^{Wsh/Wsh}$ mice (Nigrovic et al., 2008). Consistent with our own unpublished observations, they described significant splenomegaly in 12 week old mice along with expansion of the myeloid and megakaryocyte populations. In addition, the inversion mutation in *Kit*$^{Wsh/Wsh}$ mice disrupted the *corin* gene encoding for a serine protease that activates pro-atrial natriuretic peptide resulting in cardiac hypertrophy (Nigrovic et al., 2008).

In order to demonstrate that phenotypic differences between mast cell-deficient and congenic wild-type mice are indeed due to the lack of mast cells, mast cell-deficient mice were reconstituted with either bone marrow cells or with BMMCs derived from congenic wild-type or gene deficient mice. While the adoptive transfer of hematopoietic cells into *Kit*$^{W/Wv}$ and *Kit*$^{Wsh/Wsh}$ mice is possible, it is not in *Sl/Sl*^{d} mice because SCF is expressed predominantly by the microenvironment and not by the hematopoietic cells them self (Galli and Kitamura, 1987). For the reconstitution, the *in vitro* derived mast cells can be administered by intravenous, intraperitoneal, intradermal or by injection into the anterior wall of the stomach. The reconstituted mice were called “mast cell knock in mice” (Metz et al., 2007). Dependent on the anatomical site, the transferred BMMCs were reported to differentiate into mast cells resembling native mast cell populations at the corresponding site in wild type mice (Nakano et al., 1985). The reconstitution of mast cells in the different tissues is, dependent on the rout of administration, variable and mast cell numbers can differ from numbers in wild type mice. For example, more mast cells appear in the gastrointestinal tract when injected intravenously.

These reconstitution models yielded important insights into functions of mast cells but inherent technical problems limit experimentation and interpretation of data obtained with these systems. These vagaries became especially apparent when Zhou et al. revealed a profound difference in the development of antibody-mediated arthritis in *Kit*$^{W/Wv}$ and *Kit*$^{Wsh/Wsh}$ mice. While *Kit*$^{W/Wv}$ mice were resistant, *Kit*$^{Wsh/Wsh}$ mice developed full arthritis (Zhou et al., 2007). These discrepant results illustrate that *Kit*-mutant mice are not ideal models for the study of mast cell functions and that new models of mast cell-deficiency are urgently needed, which are independent of *Kit* mutations.

1.2 Generation of mouse models

The investigation of systems as complex as mammalian immune responses as well as the elucidation of the contributions of individual cell types to host defense, requires models that reflect *in vivo* situations. The mouse is such a suitable model since on the one hand murine immunology largely resembles the human situation and on the other hand there are enormous possibilities to manipulate the mouse genome. Gene-deficient mice as well as mice displaying a cell type specific gene knock out provide powerful tools to gain insights into immune functions.

1.2.1 Classical gene "Knock out"

To investigate gene functions *in vivo*, targeted mutations were introduced into the germline of the mouse in order to achieve inactivation of a gene of interest in all cell lineages in the mouse. For this purpose, the genome of embryonic stem (ES) cells was manipulated by homologous recombination. Injected into blastocysts, these ES cells can contribute to all cell lineages including germ cells, thus, resulting in heritable mutations (Capecchi, 1989; Koller and Smithies, 1992; Thomas and Capecchi, 1987).

This classical gene knock out methodology is a valuable tool that provided important information. Germline mutations, however, can be lethal and complete gene inactivation in the entire mouse often does not allow conclusions on cell type-specific functions. Therefore, spatial and temporal control of mutagenesis in the mouse was desired.

1.2.2 Conditional gene targeting

1.2.2.1 Site specific recombination systems

Conditional, i.e. cell type-specific or inducible mutagenesis *in vivo*, became possible by the introduction of site specific recombination (SSR) systems into the mouse. SSR relies on bacterial or yeast recombinases that cleave DNA at specific target sequences and ligate it to a second site (Kilby et al., 1993). The Cre/*loxP* recombination system proved particularly useful. The Cre recombinase (causes recombination) originates from the P1 bacteriophage and catalyzes recombination between two recognition sites, designated *loxP* (locus of crossing (X)-over of P1). This 34 bp sequence contains an eight bp core spacer region that determines the orientation of the *loxP* site, and two flanking 13 bp palindromes, the binding sites for the recombinase. The Cre enzyme deletes sequences flanked by *loxP* sites of identical orientation leaving a single recognition site behind. In case of sites with opposite orientation, the *loxP*-flanked sequence is inverted. In addition, translocation between *loxP* sites located on different chromosomes can occur (Nagy, 2000).

To achieve Cre-mediated mutagenesis *in vivo*, Cre transgenic lines are crossed to mouse strains containing *loxP*-flanked sequences. As shown by Vooijs et al., the success of Cre-mediated recombination *in vivo* is dependent on the position of the *loxP* sites in the genome and on the cell type in which SSR is desired (Vooijs et al., 2001). Furthermore, the level of Cre expression is critical for efficiency of recombination. As the Cre recombinase is derived from a prokaryotic organism its expression is not optimal in eukaryotic cells. The high frequency of *CpG* motives, for instance, can lead to epigenetic silencing during mammalian development. In order to adapt *Cre* cDNA to the transcription and translation system in eukaryotic cells, Shimshek et al. generated a codon-improved Cre recombinase (iCre (Shimshek et al., 2002)). This mutated *Cre* sequence contains silent base mutations corresponding to human codon-usage preferences and a minimized *CpG* content. Putative cryptic splice sites were eliminated and an optimal Kozak consensus sequence was included.

The temporal control of SSR *in vivo* was accomplished either using inducible promoters to drive Cre expression (Kuhn et al., 1995; St-Onge et al., 1996) or by chemically induced activation of an inactive form of the Cre protein. In the latter case, the Cre open reading frame was fused to the human estrogen receptor ligand binding domain (ER). The CreER fusion protein is trapped in the cytoplasm in an inactive state bound to the heat shock protein 90 (HSP 90) complex. Upon ligand binding, CreER is released from the complex and free to translocate into the nucleus where it can catalyze recombination. The estrogen binding domains used in this system are mutated (Cre-EBD (G521R) (Schwenk et al., 1998), $CreER^{T}$ (G521R) (Feil et al., 1996)) and have a high affinity to the synthetic compound 4-OH-Tamoxifen (OHT), but not to endogenous 17β-estradiol. The affinity to OHT was further improved by mutation resulting in the $CreER^{T1}$ and $CreER^{T2}$ fusion proteins (Feil et al., 1997).

Another site specific recombination system that has successfully been applied in mouse ES cells and gene targeting is the Flp/*frt* system derived from the yeast *Saccharomyces cerevisiae* (Dymecki, 1996b). The principle of Flp-mediated recombination resembles that of the Cre/*loxP*-system, although it is not as widely used as the Cre recombinase. The Flp recombinase is largely applied for the deletion of the selectable marker in ES cells after successful gene targeting (Kwan, 2002) or *in vivo* in combination with the Cre/*loxP* system.

1.2.2.2 Applications of the Cre/loxP system

To apply the Cre/*loxP* system to the mouse, genomic gene segments are flanked with *loxP* sites by classical gene targeting in ES cells. Conditional mutagenesis is then achieved by crossing the so called “floxed” mouse to a strain expressing the Cre recombinase under the control of a cell type-specific promoter. This binary system

represents a powerful tool to investigate gene functions by gene inactivation selectively in a cell population of interest. Since the first description of *in vivo* gene inactivation using the Cre/*loxP* system (Gu et al., 1994), an impressive number of floxed mouse lines have been generated as well as numerous tissue and cell type-specific Cre recombinase expressing strains, many of them listed on the webpage http://www.mshri.on.ca/nagy/.
Furthermore, the Cre/*loxP* system can be used to activate gene expression in selected cell types. For this purpose, the open reading frame of a gene of interest is separated from a promoter by a *loxP*-flanked stop element containing polyadenylation sequences (Lakso et al., 1992). The expression of the gene is inhibited until Cre-mediated excision of the stop cassette. This principle of cell type-specific gene activation has found multiple applications. It is largely used in Cre excision reporter strains in order to demonstrate the functionality of a Cre transgenic line (Soriano, 1999; Srinivas et al., 2001). In these strains, the expression of indicator proteins, like β-glalactosidase or fluorescent proteins, under the control of a ubiquitously active promoter (e.g. *ROSA26)* indicates successful Cre-mediated deletion of the stop element. The same was applied with success for depletion of individual cell populations *in vivo* by Cre-mediated derepression of a *diphtheria toxin fragment A* (*DTA*) gene (Ivanova et al., 2005; Voehringer et al., 2008). Temporally controlled ablation of cell populations was achieved by Cre-mediated control of expression of the simian diphtheria toxin receptor (DTR) resulting in sensitization of the DTR-expressing cells to exogenous diphtheria toxin (Buch et al., 2005). Furthermore, the conditional expression of oncogenes (Lakso et al., 1992) and of mutated versions of genes (Forlino et al., 1999; Gerbaulet et al., submitted), allowed insides into tumorigenesis and the effect of loss or gain of function mutations on a given cell type.

1.2.3 BAC transgene technology

The introduction of foreign genes into the germ line of mice was achieved either by homologous recombination in ES cells resulting in the expression of the foreign gene under the control of an endogenous promoter (i.e. knock-in) or by pronucleus injection resulting in random integration of the construct into the genome. Thus, the construct for random integration must include the complete promoter in addition to the open reading frame.
In the past, transgenes were limited in size and usually contained the cDNA of a gene of interest and a minimal promoter sequence. This restriction was due to the limited availability of DNA-engineering methods for large DNA molecules. Consequently, the lack of *cis*-regulatory elements in the promoter or intronic sequences could affect the expression level. Furthermore, small transgenes are notably prone to position effects exerted by regulatory elements present at the site of random integration. Effects of promoters, enhancers and silencers at the integration site may override those of the

transgenic promoter. Expression may also be hampered by integration into a heterochromatin rich site (Heaney and Bronson, 2006).

To overcome these chromosomal position effects, the transgenes were either targeted to a certain site by homologous recombination in ES cells or, alternatively, the size of the randomly integrated transgenes was considerably increased, for instance, by using bacterial artificial chromosomes (BAC). These vectors can accommodate DNA fragments of up to 300 kb and are, therefore, used for the generation of mouse genomic BAC libraries (Osoegawa et al., 2000). Since large BAC clones can contain the entire genomic sequence of a gene including all *cis*-regulatory elements, BAC based transgenes are usually not affected by position effects (Giraldo and Montoliu, 2001).

Conventional cloning methods, relying on the use of restriction endonucleases and DNA ligases, cannot routinely be applied for the manipulation of BAC clones as the size limits the availability of suitable (rare) restriction sites. Today, BAC modification is facilitated by homologous recombination in *E. coli*. A powerful tool applied for BAC recombineering is the Red®/ET® Recombination system ("ET-cloning") (Muyrers et al., 1999; Zhang et al., 1998). The process of recombination is catalyzed by one of the phage-derived enzyme pairs, either Redα and Redβ from the λ-phage or RecE and RecT derived from the Rac prophage. Redα and RecE are 5'-3' exonucleases producing single-stranded overhangs at the 3' end of double-strand breaks. Redβ and RecT are ssDNA-binding proteins with annealing and strand exchange activity. These equivalent enzyme pairs efficiently mediate recombination in *E. coli* BAC hosts between a circular BAC clone and a linear DNA fragment at homologous sequences shared by these two DNA molecules. Thus, this method is completely independent of restriction sites. Furthermore, as the regions of homology can be chosen freely, the BAC clone can precisely be modified at any desired position. Since only 50 bp are sufficient to serve as homology region, this short sequence can be included into oligonucleotide primers for amplification of a linear DNA fragment that is to be inserted into a BAC vector. The intrinsic recombination pathway in *E. coli* involves the strand invasion protein RecA and the RecBCD complex as the major cellular exonuclease. One function of the RecBCD is the destruction of foreign linear DNA and, thus, would render a recombination event between the BAC and linear DNA impossible. Therefore, the λ-derived Redγ protein, which inhibits the RecBCD exonuclease activity, is expressed along with Redα/Redβ or RecE/RecT (Zhang et al., 1998). The applications of this method are versatile. It allows the insertion and/or deletion of DNA and even single base changes. In addition, DNA can be subcloned from diverse sources, which can be BAC vectors, the *E. coli* chromosome or even mouse genomic DNA, into a minimal vector in one recombination step in *E. coli* (Zhang et al., 2000).

1.3 Objectives

Recent research demonstrated that mast cells are not only central effectors of allergic disorders but play pivotal roles in orchestrating innate and adaptive immune responses by exerting immunostimulatory as well as immunosuppressive functions. Until today, most knowledge about mast cell functions was gained by *in vitro* studies or *in vivo*, using genetically mast cell-deficient mice, in particular the $Kit^{W/Wv}$ and recently also the $Kit^{Wsh/Wsh}$ strain.

The reconstitution of these mice with *in vitro* cultured mast cells derived from gene deficient mice provided valuable information about mast cell-specific gene functions. However, these models were not ideal since *Kit*-mutant mice, in addition to mast cell deficiency, are characterized by complex perturbation of the hematopoietic system. The vagaries of these models became in particular apparent when contradictory results were obtained from different mast cell-deficient strains. Thus, a new mouse model that allows mast cell-specific mutagenesis *in vivo* would represent an important improvement.

The first aim of this thesis was, therefore, to generate a mouse line expressing Cre recombinase selectively in mast cells. This line should allow for selective inactivation but also activation of individual genes in mast cells *in vivo*.

A second aim was to employ the new Cre expressing line to generate a new mouse model of mast cell deficiency. This is possible by Cre-mediated deletion of a stop element thereby derepressing the expression of the high affinity diphtheria toxin receptor (DTR) rendering Cre-expressing cells diphtheria toxin sensitive. In order to demonstrate biological effects of the induced mast cell-ablation *in vivo*, the impact of mast cell depletion on a typical mast cell-mediated immune response, i.e. systemic anaphylaxis, was investigated. Conditional expression of the DTR in mast cells should provide an alternative model to *Kit*-mutant mice, mentioned above, in which, apart from mast cell-deficiency, no other phenotypic abnormalities perturb interpretation of the data.

2 Results

2.1 Generation and analysis of mast cell-specific Cre transgenic mice

2.1.1 Generation of the *Mcpt5-Cre(ER^{T2})* and *Mcpt6-Cre* gene constructs

In order to express the Cre recombinase selectively in mouse mast cells *in vivo* we used the *Mcpt5* and *Mcpt6* promoters, respectively. The constructs were generated by modification of BAC vectors by homologous recombination. BAC clones encompassing either the entire *Mcpt5* gene (clone RP23-284A14) or the *Mcpt6* gene (clone RP23-240F3) were identified using the NCBI tools “Map viewer” and “clone finder” of the mouse genome resources. Both clones are part of the mouse BAC library RPCI-23 (Roswell Park Cancer Institute (Osoegawa et al., 2000)) and consists of the pBACe3.6 vector backbone and a 210 kb and 173.2 kb large insert of C57BL/6 genomic DNA, respectively (Fig. 2.1 and Fig. 2.2). The clones were purchased from the RZPD (Deutsches Ressourcen-zentrum für Genomforschung GmbH, Berlin, Germany).

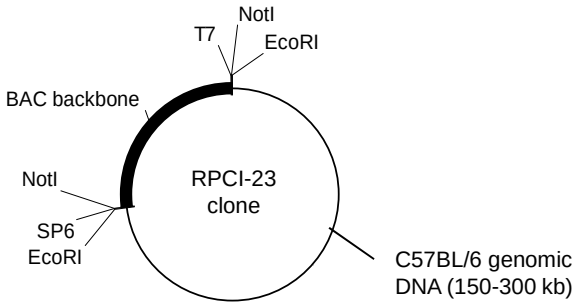

Fig. 2.1 Scheme of a BAC clone of the RPCI-23 mouse BAC library. *T7* and *SP6* are promoters located at the end of the BAC backbone of the pBACe3.6 vector (bold line). C57BL/6 genomic DNA fragments of about 150-300 kb were cloned into *Eco*RI sites of the pBACe3.6 vector.

For transgene construction we used a modified improved Cre (*iCre* (Shimshek et al., 2002)) gene cassette that consists of the coding sequence of *iCre* followed by an *frt* site-flanked *ER^{T2}* cassette and a SV40 polyadenylation (PolyA) signal. The *iCre-frt-ER^{T2}-frt-SV40-PolyA* cassette was kindly provided by Dr. Giuseppe Testa, Milan. This cassette provides the option to induce Cre activity in adult mice by the application of tamoxifen but also the possibility to remove the *ER^{T2}* domain by Flp recombinase-mediated deletion either in *E. coli* or in the mouse in order to obtain constitutive Cre activity.

All cloning steps were done by Red/ET recombination in *E.coli*. The primers containing the homology regions (HR) for each recombination step are listed in Table 2.1 and Table 2.2 for construction of the *Mcpt5-Cre* and the *Mcpt6-Cre* construct, respectively. Clones which

had undergone the desired recombination events during each of the cloning steps (described in section 2.1.1.1 and 0) were identified by PCR (data not shown).

application/template	primer name	primer sequence
shaving of the insert at *T7* end of the vector backbone	T7HR-Amp-FOR	5′GCTTGACATTGTAGGACTATATTGCTCTAATAAATTTGCGGCCGCTAATAGGTCTGACGCTCAGTGGAAC
template: pBluescript II KS+	InsertRP23-284A14HR-*Not*I-Amp-REV	5′TGCCTGTTGGCCTGTGGGAGCCCAGCGAGGTTGGGGCCAGCAGCGGGTGCGCGGCCGCGTGCGCGGAACCCCTATTTG
shaving of the insert at *SP6* end of the vector backbone	InsertRP23-284A14HR-*Not*I-Zeo-FOR	5′GGGCAGAAAGGCTCAGAAGTTGAGACTCAGCAGGGCCTCAGAAAGCTGGTGCGGCCGCCTCCCTTGGAGCCTACCTAGACTCA
template: psiRNA-hH1zeo	SP6HR-Zeo-REV	5′TTTCTATCCTCCCGAATTGACTAGTGGGTAGGCCTGGCGGCCGCCTGGCCAATGCACTGACCTCCCACATTCCCTT
subcloning of *CreER^{T2}*	HR(3'End of Cre)subcloning-HR(last 50bp of *Mcpt5*-exon1)-*Not*I-minimal vector-FOR	5′ACGCCTATTTTTATAGGTTAATGTCATGATAATAATGGTTTCTTAGACGTGTGAGTGCTGGGGTCGCTCCCTCTCCAATCTGCAGGGTCAGCTCCTAAAAGCGGCCGCGCCCTGCACCATTATGTTCCGGA
template: pACYA184	HR(5'End of Cre)subcloning-HR(50bp 5' of *Mcpt5*-ATG)-*Not*I-minimal vector-REV	5′ACAGGGAGGGCAGGCAGGTTTTGATGCACAGTCAGCAGGTTGGACACCATATTTGGGCCTTAGGCTTATTACTCCCAGCGGGCAGGGGAGTGGCAGAGCTGCGGCCGCGCCCCGGCAGTACCGGCATAACCA
insertion of *Neo* into the minimal vector between *iCre* and 3'HR of *Mcpt5*	HR(3'End of Cre)-loxm2-NeoFOR	5′ACGCCTATTTTTATAGGTTAATGTCATGATAATAATGGTTTCTTAGACGTATAACTTCGTATATGGTTTCTTATACGAAGTTATCGGCCGCATTCTACCGGGTAGG
template: pPGK-gb2-neo	HR(last 50bp of *Mcpt5*-Exon1)-loxm2-Neo-REV	5′TTTTAGGAGCTGACCCTGCAGATTGGAGAGGGAGCGACCCCAGCACTCACATAACTTCGTATAAGAAACCATATACGAAGTTATCGCGTTTAAACGGCGCGCCGCACACAA

Table 2.1 Primers used for *Mcpt5-Cre*(*ER^{T2}*) transgene construction by Red/ET recombination**.** The respective 50 bp homology regions (HR) were included into the primers used for the amplification of selection markers or the minimal vector.

application/template	primer name	primer sequence
shaving of the insert at T7 end of the vector backbone	T7HR-Amp-FOR	5′GCTTGACATTGTAGGACTATATTGCT CTAATAAATTTGCGGCCGCTAATAGGTC TGACGCTCAGTGGAAC
template: pBluescript II KS+	InsertRP23-240F3HR-*Not*I-Amp-REV	5’GGGGTCAGGATGAGGGGCGGGGCAC ACCTGGTGCCCTCCTGCTCCTCCTCG CGGCCGCGTGCGCGGAACCCCTATTTG
shaving of the insert at SP6 end of the vector backbone	InsertRP23-240F3HR-*Not*I-Zeo-FOR	5’AGCCCATCACCATCTCCCAGGAGCA AGACCCCCCTAACATCAAATGGGGTG CGGCCGCCTCCCTTGGAGCCTACCTAGA CTCA
template: psiRNA-hH1zeo	SP6HR-Zeo-REV	5′TTTCTATCCTCCCGAATTGACTAGTG GGTAGGCCTGGCGGCCGCCTGGCCAATG CACTGACCTCCCACATTCCCTT
subcloning of *CreER^{T2}*	HR(3’End of Cre) subcloning-HR(last 50bp of *Mcpt6*-exon1)-*Not*I-minimal vector-FOR	5’ACGCCTATTTTTATAGGTTAATGTCAT GATAATAATGGTTTCTTAGACGTGTAAG TTGTCTTGAGCCCTCCCTGTCTCTCC CTCACCTTCACAGGCCACAGCGGCCGC GCCCTGCACCATTATGTTCCGGA
template: pACYA184	HR(5’End of Cre) subcloning-HR(50bp 5’ of *Mcpt6*-ATG)-*Not*I-minimal vector-REV	5’ACAGGGAGGGCAGGCAGGTTTTGATGC ACAGTCAGCAGGTTGGACACCATCTGGA AGCAGTGAGGAGCACAGCCTGAGTCC AGCTAAAAGACAGGGCTAGGCGGCCGC GCCCGGCAGTACCGGCATAACCA
insertion of *Neo* into the minimal vector between *iCre* and 3’HR of *Mcpt5*	HR(3’End of Cre)-*loxm2*-Neo-FOR	5′ACGCCTATTTTTATAGGTTAATGTCA TGATAATAATGGTTTCTTAGACGTATAA CTTCGTATATGGTTTCTTATACGAAGTT ATCGGCCGCATTCTACCGGGTAGG
template: pPGK-gb2-neo	HR(last 50bp of *Mcpt6*-Exon1)-*loxm2*-Neo-REV	5’TGTGGCCTGTGAAGGTGAGGGAGAG ACAGGGAGGGCTCAAGACAACTTACA TAACTTCGTATAAGAAACCATATACGAA GTTATCGCGTTTAAACGGCGCGCCGCAC ACAA

Table 2.2 Primers used for *Mcpt6-Cre* transgene construction by Red/ET recombination. The respective 50 bp HRs were included into the primers used for the amplification of selection markers or the minimal vector.

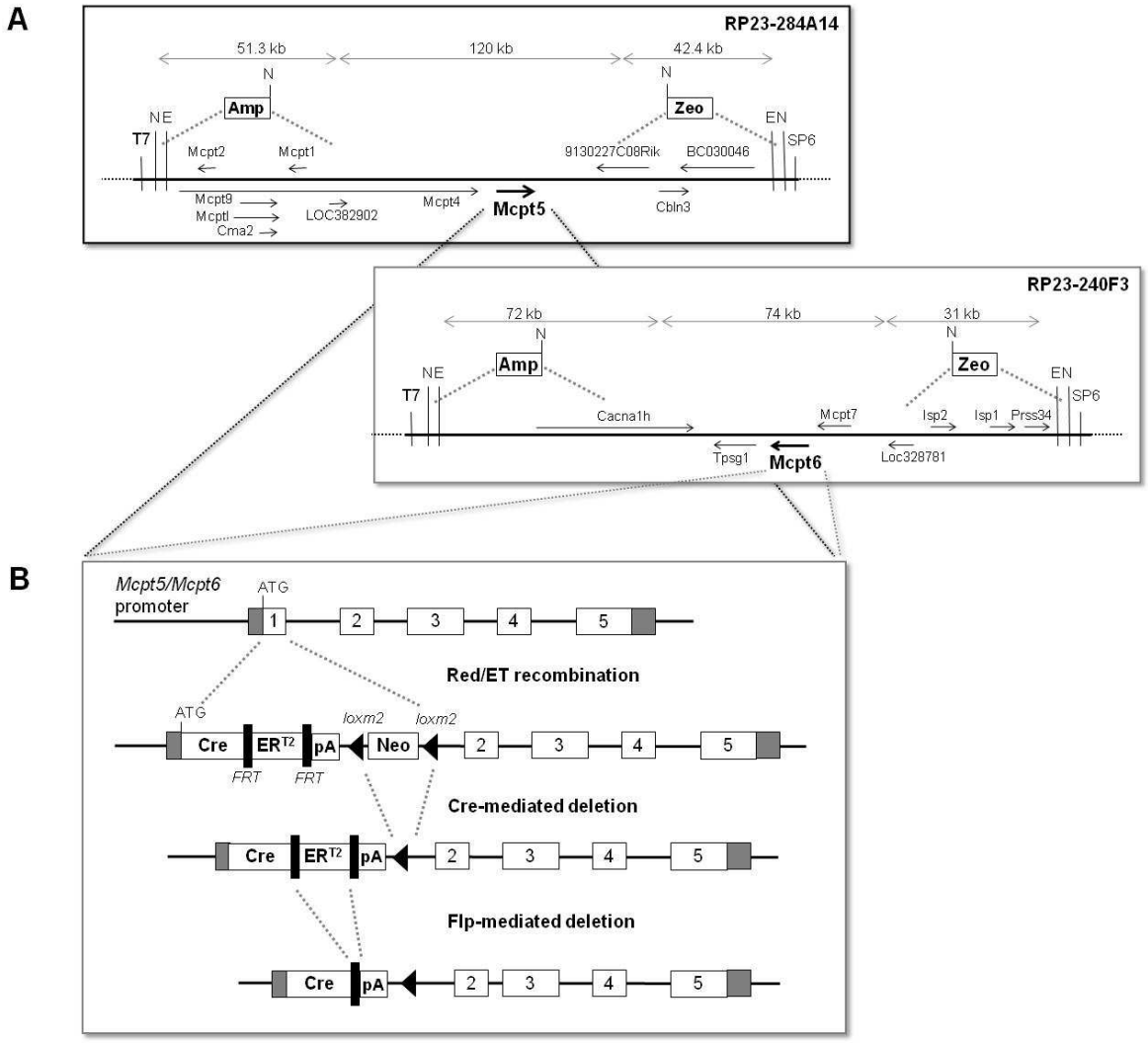

Fig. 2.2 Cloning strategy for the construction of the *Mcpt5-CreER^{T2}*, *Mcpt5-Cre* and *Mcpt6-Cre* transgenes. (A) Scheme of the mouse BAC clones RP23-284A14 and RP23-240F3 containing the entire genomic sequences of the *Mcpt5* and *Mcpt6* gene, respectively. Both clones were shortened by replacing several kb at the *T7* and at the *SP6* end by an *ampicillin* (*Amp*) or a *zeocin* (*Zeo*) resistance cassette, respectively. Lengths of the replaced and remaining sequences are indicated. (B) Insertion of *Cre* into *Mpct5*/*Mcpt6* genes by replacing the coding part of the first exon of the respective genes by an *iCreER^{T2}-loxm2-Neo-loxm2* cassette by homologous recombination and subsequent excision of *Neo* by Cre-mediated deletion. For constitutive Cre activity in transgenic mice, the *ER^{T2}* cassette was removed by Flp-mediated deletion in *E. coli*. Finally, the constructs *Mcpt5-CreER^{T2}*, *Mcpt5-Cre* and *Mcpt6-Cre* were used for pronucleus injection. (N, *Not*I; E, *Eco*RI; shaded boxes, 5' and 3' untranslated region)

2.1.1.1 Shortening ("shaving") of the BAC inserts

Beside the *Mcpt5* and *Mcpt6* genes, the inserts of the BAC clones included many genes most of which encoded for other mast cell proteases. In order to avoid possible effects of altered gene dosages in the transgenic mice, these neighboring genes were excluded from the transgenic constructs by shortening the BAC inserts at both ends (Fig. 2.2, A). The *Mcpt5* containing BAC was trimmed by replacing 51.3 kb of the *T7* and 42.4 kb of the *SP6* end of the genomic DNA insert by an *ampicillin* (*Amp*) and *zeocin* (*Zeo*) resistance cassette, respectively, leaving 67.4 kb upstream of the ATG start codon and 46.8 kb downstream of the 3'UTR of the *Mcpt5* gene (Fig. 2.2, A). The *Mcpt6* containing BAC was shortened by replacing 72 kb of the *T7* and 31 kb of the *SP6* end of the insert by *Amp* and *Zeo* cassettes, leaving 39 kb upstream of the translation start codon and 29.9 kb downstream of the 3'UTR of the *Mc*pt6 gene (Fig. 2.2, A).

2.1.1.2 Assembly of CreER^{T2}-Neo and insertion into the Mcpt5 and Mcpt6 genes

In order to assemble the *CreER^{T2}-Neo* cassette and to attach the HRs for the insertion into the *Mcpt5* or the *Mcpt6* genes, the *CreER^{T2}* cassette was first subcloned from plasmid pCreER^{T2}Amp (a gift from Giuseppe Testa, Milan) into a minimal vector (Fig. 2.3, A). This vector consists of an origin of replication and a chloramphenicol resistance cassette amplified from plasmid pACYA184. The primers used for the amplification contain the HRs for both, the subcloning of the *CreER^{T2}* cassette and for the insertion of *CreER^{T2}* into *Mcpt5* or *Mcpt6* (see Table 2.1 and Table 2.2). The subcloning step resulted in plasmid pMinCreER^{T2}, which was modified by insertion of a *loxm2*-flanked *PGK-gb2-Neo* cassette (*Neo*) 3' of *CreER^{T2}* and 5' of the 3'*Mcpt5/Mcpt6* HR (Fig. 2.3, B). The primers for the amplification of *Neo* contained the *loxm2* sites in addition to the HRs for the 3' end of *Cre* and the 3'*Mcpt5/Mcpt6-HR*. These mutated *loxP* sites can recombine with each other, but not with wild type *loxP* sites (Langer et al., 2002). Finally, the *HR-CreER^{T2}-loxm2-Neo-loxm2-HR* cassette was released from the minimal vector by *Not*I digestion and recombined into the BAC by replacing the coding part of exon 1 of the *Mcpt5* gene or the *Mcpt6* gene (Fig. 2.3, C and Fig. 2.2, B). The *Neo* cassette was subsequently removed by Cre-mediated deletion in *E. coli* resulting in the *Mcpt5/Mcpt6-CreER^{T2}* constructs that should allow for an induction of Cre activity in the adult mouse. The *Mcpt5*/*Mcpt6-Cre* constructs for constitutive Cre activity were generated by removing the *ER^{T2}* cassette by Flp-mediated recombination in *E. coli* (Fig. 2.2, B).

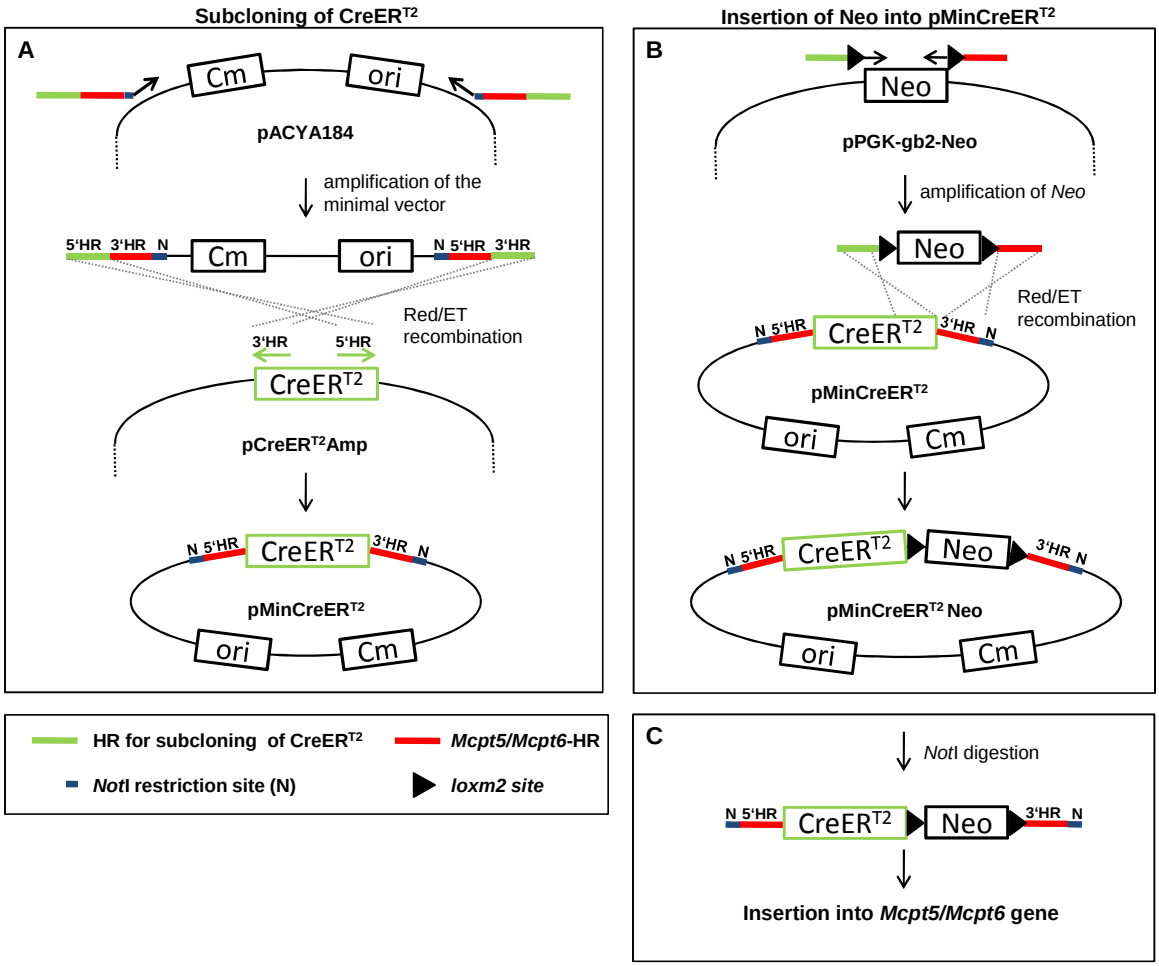

Fig. 2.3 Assembly of the *HR-CreER^{T2}-loxm2-Neo-loxm2-HR* cassette by subcloning of *CreER^{T2}* and subsequent insertion of a *loxm2*-flanked *Neo* cassette. (A) In order to attach the *Mcpt5*/*Mcpt6* HRs to *Cre*, a minimal vector encompassing a *chloramphenicol* resistance cassette (*Cm*) and an origin of replication (ori) was amplified using primers containing both, the HRs for subcloning Cre (green line) and the HRs for the insertion into the *Mcpt5/Mcpt6* gene (red line) and a *Not*I restriction site (N, blue line (B) The *Neo* cassette was inserted 3' of *Cre* and 5' of the 3'*Mcpt5/Mcpt6-HR*. (C) The *HR-CreER^{T2}-loxm2-Neo-loxm2-HR* cassette, released from the minimal vector by *Not*I digestion, was ready for the replacement of the coding part of the first exon of *Mcpt5/Mcpt6.*

2.1.1.3 Test for precision and fidelity of BAC modification

During BAC modification by homologous recombination unwanted recombination events may occur in addition to the intended modification. To test for recombination events the modified BAC clones and the original unmodified clones are usually digested with restriction enzymes and the resulting DNA fragment patterns are compared. As the *Mcpt5-Cre* containing BAC was shortened by 94 kb and the *Mcpt6-Cre* BAC by 103 kb, the comparison with the unmodified clones was not meaningful. To ensure integrity of the promoter region, 4.5 kb upstream of the translation start codon of the original RP23-284A14 and RP23-240F3 and of the respective modified BAC clones were sequenced. The comparison of the sequences revealed no mutations in these regions of the *Mcpt5-Cre* and *Mcpt6-Cre* BAC clones (data not shown).

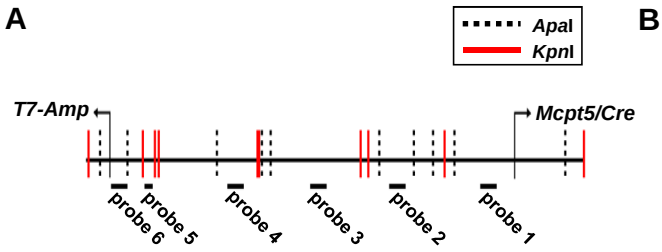

B

probe	ApaI		KpnI	
	RP23-284A14	Mcpt5-Cre construct	RP23-284A14	Mcpt5-Cre construct
1	18720 bp	10124 bp	23186bp	13027 bp
2	5778 bp		11965 bp	
3	18317 bp		16996bp	
4	7617 bp		16616 bp	
5	15157 bp		2014 bp	
6	4515 bp	9985 bp	9258 bp	10886 bp

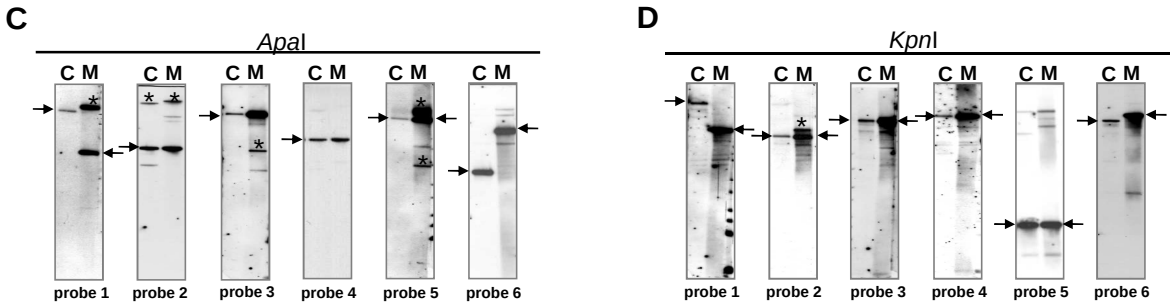

Fig. 2.4 Test for unwanted recombination events in the *Mcpt5-Cre* BAC construct by Southern blot analysis. (A) The scheme displays the *Mcpt5* translation start, with the upstream region of the clone RP23-284A14. The start of the *Amp* cassette in the modified BAC followed by the *T7* promoter of the BAC backbone is indicated. Six probes and the restriction sites for *Apa*I and *Kpn*I as predicted from the database sequence of the unmodified BAC clone are indicated. (B) The expected DNA fragment sizes for each restriction enzyme are listed. (C and D) The original and *Mcpt5-Cre* BAC were either digested with *Apa*I or *Kpn*I. The blots were hybridized with probe 1 to 6. The expected bands are marked by arrows. C, control RP23-284A14 BAC; M, modified BAC; *, additional signals due to unspecific binding of the probes or incomplete digest.

In addition, 67 kb and 39 kb upstream of the translation start codon of the *Mcpt5* and *Mcpt6* genes, respectively, were tested for unwanted recombination events by Southern blot analysis. For this purpose, the *Mcpt5-Cre* construct and the respective unmodified BAC clone were digested either with *Apa*I or *Kpn*I. The blots were hybridized with six different probes (Fig. 2.4, A) and the labeled DNA fragments of the original and the modified BAC were compared. The primers for the generation of the probes are listed in Table 4.3, section 4.3. As it is displayed in Fig. 2.4 C and D all DNA fragments of the modified BAC showed the expected sizes (Fig. 2.4, B), indicating that no major unwanted recombination events had occurred within this part of the construct. As the tested *Mcpt5-Cre* construct was based on the *Mcpt5-CreER*^{T2} BAC, unwanted recombination in the latter construct can be excluded. The same strategy was pursued for the *Mcpt6-Cre* BAC using either *Sac*I or *Eco*RV for the digestion. The blotted *Sac*I digested DNA was hybridized with six and the *Eco*RV digested DNA with four probes. The comparison of the detected DNA fragments of the unmodified and modified BAC revealed no unwanted recombination events within the analyzed region (Fig. 2.5, A-D).

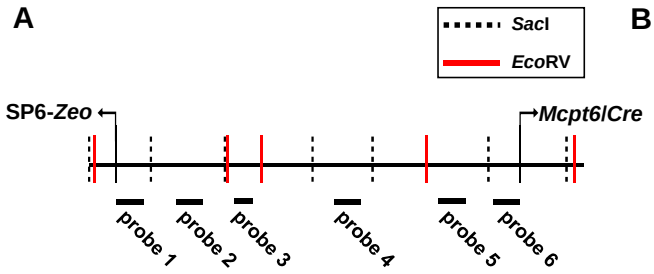

B

	*Sac*I		*Eco*RV	
probe	RP23-240F3	Mcpt6-Cre construct	RP23-240F3	Mcpt6-Cre construct
1	5053 bp	14884 bp	12900 bp	11394 bp
2	7123 bp			
3	8510 bp		3263 bp	
4	5757 bp		15908 bp	
5	11162 bp		14449 bp	16184 bp
6	7507 bp	9242 bp		

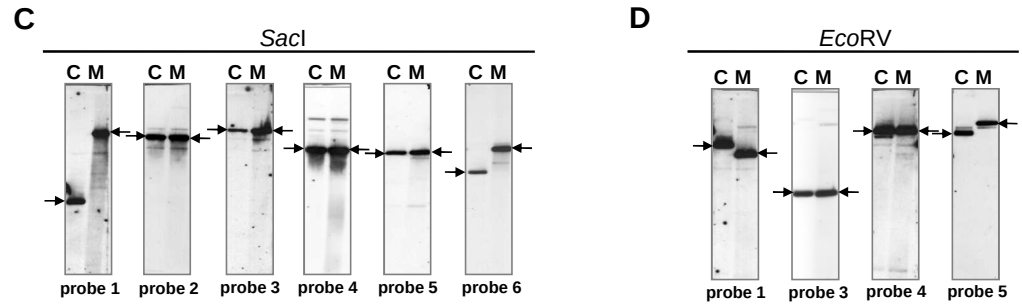

Fig. 2.5 Test for unwanted recombination events in the final *Mcpt6-Cre* BAC by Southern blot analysis. (A) The scheme displays the *Mcpt6* translation start with the upstream region of clone RP23-240F3. The start of the *Zeo* cassette in the modified BAC followed by the SP6 promoter is indicated. Six probes and the restriction sites for *Sac*I and *Eco*RV as predicted from the database sequence of the unmodified BAC clone are indicated. (B) The expected DNA fragment sizes for original and *Mcpt6-Cre* construct for each restriction enzyme are listed. (C and D) The original and *Mcpt6-Cre* BAC were either digested with *Sac*I or *Eco*RV. The blots were hybridized with six and four probes, respectively. The expected bands are marked by arrows. C, control, RP23-240F3 BAC clone; M, modified BAC.

Fig. 2.6 Alignment of the original coding sequence of the Cre recombinase with the *Cre* sequence in the final *Mcpt5-Cre* construct. Shown are the last 295 bp of the *CreER*^{T2} cassette. Both, the original *Cre* and the *Mcpt5-Cre* were sequenced. In the *Mcpt5-Cre* sequence, a single base pair insertion (red box) was found downstream of the SV40 polyadenylation signal (black box). Green box: part of the 3' *Mcpt5* homology region.

Finally the *Cre* cassettes of the *Mcpt5-Cre* and *Mcpt6-Cre constructs and the ER^{T2}* cassette of *Mcpt5-CreER^{T2}* were analyzed for point mutations by sequencing overlapping PCR products (primers are listed in Table 4.3, section 4.3). No mutations were found in *Mcpt6-Cre* and in the *ER^{T2}* cassette of the *Mcpt5-CreER^{T2}* construct (data not shown). A single point mutation detected in the *Mcpt5-Cre* construct downstream of the PolyA signal was considered irrelevant (Fig. 2.6). This single base pair insertion is probably due to a mutation in the primer used for the subcloning of *Cre*.

2.1.2 Generation of transgenic mice

The constructs for constitutive and inducible Cre activity with Cre expression under the control of the *Mcpt5* promoter were used for the generation of transgenic mice. The BAC inserts were separated from the vector backbone and from the *ampicillin* and *zeocin* resistance cassettes by *Not*I digestion and agarose gel electrophoresis. After further purification by electroelution and drop dialysis (see Material and Methods) the constructs were tested for the correct size and purity by pulsed-field gel electrophoresis (data not shown). The *Mcpt5-CreER^{T2}* and the *Mcpt5-Cre* constructs were finally pronucleus-injected into fertilized C57BL/6 oocytes which were then transferred into foster mice. The pronucleus injections were performed by Ronald Naumann, Transgenic Core Facility, MPI of Molecular Cell Biology and Genetics, Dresden. 25 and 38 offspring were obtained for the *Mcpt5-Cre* and *Mcpt5-CreER^{T2}* constructs, respectively.

In order to express the Cre recombinase under the control of the *Mcpt6* promoter *in vivo*, only the construct for constitutive Cre activity was pronucleus-injected. The *Mcpt6-Cre* containing insert was separated from the BAC backbone by a double digestion with *Asc*I and *Bsp*BI leaving the *ampicillin* and *zeocin* cassettes attached to the insert. These resistance cassettes can be detected by PCR in transgenic mice in order to test for full length integration of the transgene, which was not possible in case of the *Mcpt5-Cre* constructs. 34 offspring were obtained by pronucleus injection of the *Mcpt6-Cre* construct.

Tail DNA of all offspring was tested for the presence of the transgenes by PCR. Primers for the detection of *Cre* and the *ER^{T2}* cassette are indicated in Fig. 2.7. The respective BAC constructs, which were diluted and mixed with wild type genomic tail DNA resulting in a molar ratio of BAC to genomic DNA of 1:1, served as positive control. Six animals were identified as *Mcpt5-Cre* and also six animals as *Mcpt5-CreER^{T2}* transgenic. The ID numbers of these founder animals are indicated in Fig. 2.7 (bold numbers). The *Mcpt5-CreER^{T2}* transgenic founder 525624 died before the shipment to Cologne. In order to test for germ line transmission, all remaining founder mice were crossed to C57BL/6 wild type animals. As all Mcpt5-CreER^{T2} and Mcpt5-Cre founders had transgenic offspring, germline transmission was evident for eleven transgenic lines.

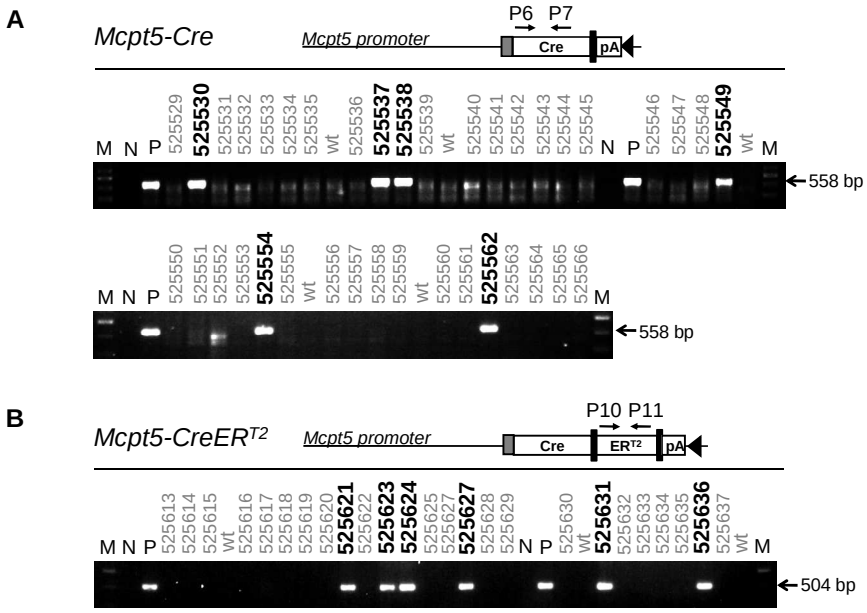

Fig. 2.7 Genotyping PCR for *Mcpt5-Cre* and *Mcpt5-CreER*^{T2} of animals generated by pronucleus injection of the respective constructs. Diluted BAC DNA served as positive control (P). Negative control reactions (N) did not contain DNA. Primers used for genotyping are indicated in the schemes representing the *Mcpt5-Cre* (A) and the *Mcpt5-CreER*^{T2} (B) constructs (arrows). Primer sequences are displayed in Table 4.3, section 4.3 under the respective numbers. (A) Genotyping of mice derived from the pronucleus injection of the *Mcpt5-Cre* construct. *Cre*-positive mice (bold numbers) were identified by a 558 bp product. No product was expected in wt animals. (B) Genotyping of mice derived from the *Mcpt5-CreER*^{T2} pronucleus injection. *CreER*^{T2}-positive mice were identified by a 504 bp product. M, 100 bp DNA ladder, Fermentas life sciences.

In case of the *Mcpt6-Cre* construct, ten transgenic animals were identified (Fig. 2.8, A), six of which carried a full length integration as demonstrated by PCR using primers specific for the *ampicillin* and *zeocin* resistance cassettes (Fig. 2.8, B). *Mcpt6-Cre*-specific amplification of tail DNA of founder 526844 repeatedly resulted in only very weak bands, most likely indicating that the transgene is found only in a fraction of the cells (Fig. 2.8, A, lane 526844 upper and lower panel). Therefore, this founder animal was not further analyzed. Germline transmission was evident for seven of the nine remaining founder lines after crossing them to C57BL/6 wild type animals.

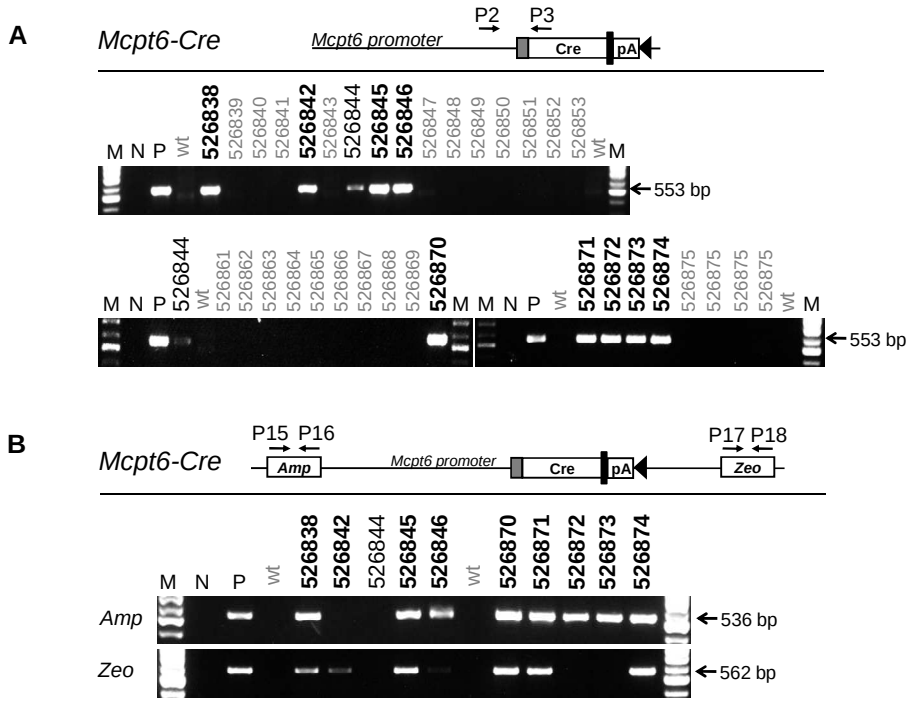

Fig. 2.8 Genotyping PCR of mice generated by pronucleus injection of the *Mcpt6-Cre* construct. Primers for PCR are indicated in the schemes (arrows), the sequences can be found in Table 4.3, section 4.3 under the respective numbers. (A) The identification of positive founder animals (IDs are indicated) was done by PCR on genomic tail DNA resulting in a PCR product of 553 bp. (B) Full length integration of the transgene was tested by the amplification of the *ampicillin* (A*mp*) and *zeocin* (Z*eo*) resistance cassettes resulting in PCR products of 536 bp and 562 bp, respectively. M, 100bp DNA ladder, Fermentas life sciences; N, negative control (without DNA); P, positive control (diluted BAC DNA mixed with genomic DNA resulting in molar ratio of BAC to genomic DNA of 1:1).

2.1.3 Screening of Mcpt5-Cre founder lines for Cre-mediated recombination

In order to test for the efficiency and mast cell-specificity of Cre-mediated recombination, the six *Mcpt5-Cre* transgenic lines were mated to the R26R-EYFP reporter line (Srinivas et al., 2001). This reporter line expresses the enhanced yellow fluorescent protein (EYFP) under the control of the ubiquitously active *ROSA26* promoter provided a *loxP*-flanked stop cassette is removed by Cre-mediated deletion (Fig. 2.9).

Screening of the six lines was done by flow cytometric analysis of peritoneal mast cells for EYFP expression. In three lines, no or in less than 10% of mast cells EYFP expression could be detected (data not shown). One of the six lines showed EYFP expression in only 80% of the peritoneal mast cells and was not further investigated (data not shown). In contrast, in two lines reporter gene expression could be detected in close to 100% of peritoneal mast cells (Mcpt5-Cre lines 525530 and 525537, for results see section 2.1.4). Because of autosomal inheritance of the transgene in the 525530 line and X-linked

inheritance in the 525537 line, these lines were designated A-Mcpt5-Cre and X-Mcpt5-Cre, respectively.

Fig. 2.9 Principle of reporter gene expression in *Cre/R26R-EYFP* double positive mice. Mcpt5-Cre mice were crossed to the R26R-EYFP reporter strain. EYFP is expressed under the control of the ubiquitously active *ROSA26* promoter provided a *loxP*-flanked stop cassette is removed by Cre-mediated deletion.

2.1.4 Detailed analysis of *A-Mcpt5-Cre* and *X-Mcpt5-Cre* transgenic mice

2.1.4.1 Efficient Cre-mediated recombination in mast cells

Highly efficient Cre-mediated reporter gene expression in peritoneal mast cells, defined as $CD117^+Fc\varepsilon RI\alpha^+$ cells, was detected in seven *A-Mcpt5-Cre R26R-EYFP* double positive mice (99.1±0.31%, Fig. 2.10, upper panel) but not in Cre-negative R26R-EYFP single transgenic control mice (littermates in most instances). In skin cell suspensions, mast cells were defined as $CD117^+CD45^+$ cells and were detected in low numbers, on average 0.32% of total skin cells. (FcεRIα staining was not reliable likely due to loss of epitopes during enzymatic tissue dissociation.) In the five animals, for which this mast cell population was investigated, the majority of the few $CD117^+CD45^+$ cells gated was EYFP positive (43/47, 54/64, 32/39, 23/27 and 77/88 gated events, Fig. 2.10, lower panel). Given that the mast cell gate will inevitably collect some non-mast cells upon analysis of high total cell numbers (40,000 events), the percentage of skin mast cells expressing EYFP is probably close to 100%.

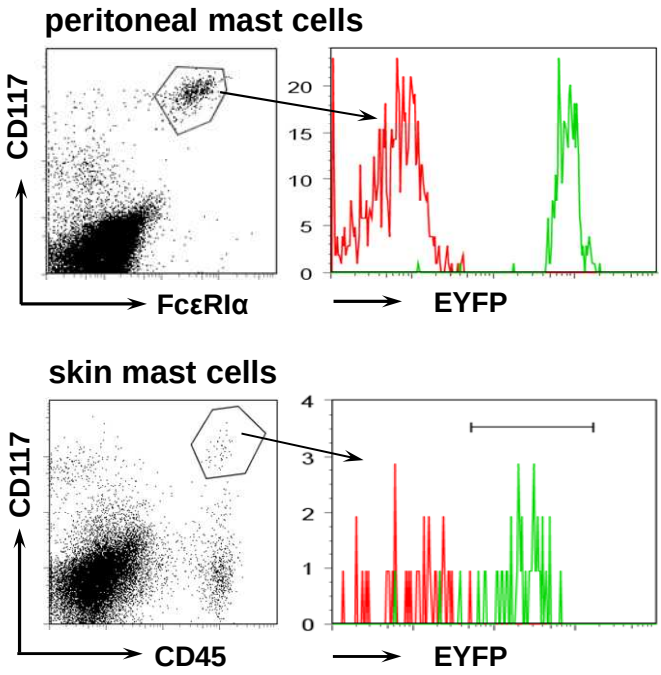

Fig. 2.10 Efficiency of Cre-mediated activation of EYFP reporter gene expression in mast cells. EYFP expression is demonstrated in cells from peritoneal lavage fluid and single cell suspension of skin of *Mcpt5-Cre R26R-EYFP* double positive mice. Peritoneal mast cells were identified as CD117 and FcεRIα and skin mast cells as CD117 and CD45 double positive cells. Mast cell populations were gated and EYFP fluorescence intensitiy was displayed in histogram plots. The green graph represents the *Mcpt5-Cre/R26R-EYFP* mouse, the red graph the *Cre*-negative but *R26R-EYFP* positive control animal (a littermate in most instances). Results are representative for seven (peritoneal mast cells) and five (skin mast cells) A-Mcpt5-Cre mice.

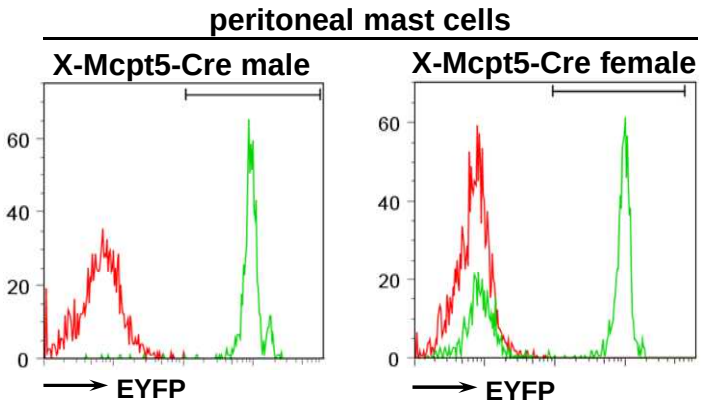

Fig. 2.11 EYFP Reporter gene expression in peritoneal mast cells of male and female *X-Mcpt5-Cre R26R-EYFP* double positive mice. EYFP fluorescence intensity of $CD117^{+}Fc\varepsilon RI\alpha^{+}$ mast cells was displayed in histogram plots. The Green graph represents *Mcpt5-Cre R26R-EYFP* double positive mice, the red graph represents the *Cre*-negative but *R26R-EYFP*-positive controls.

A similar efficiency of Cre-mediated deletion in mast cells was observed in three male *X-Mcpt5-Cre R26R-EYFP* double positive mice (98.5±0.6%, Fig. 2.11). The mast cell population in the skin was analyzed in three males and showed efficient activation of EYFP expression (46/58, 61/66 and 48/55 gated events, data not shown). In contrast to the males, in two female *X-Mcpt5-Cre R26R-EYFP* double positive mice analyzed, a reporter gene expression was only observed in 61% and 32% of peritoneal mast cells consistent with random X-chromosome inactivation (Fig. 2.11).

2.1.4.2 Investigation of mast cell-specificity of Cre-mediated recombination

Various hematopoietic non-mast cell populations were investigated for potential Cre-mediated activation of EYFP expression. In peritoneal macrophage and B cell (n=3 for each, A-Mcpt5-Cre and X-Mcpt5-Cre) as well as in splenic basophil, eosinophil, neutrophil, dendritic cell, macrophage, B cell and T cell populations (n=3 for each, A-Mcpt5-Cre and X-Mcpt5-Cre) no or very few EYFP positive cells could be detected (i.e. below 1%, Fig. 2.12). In addition, analysis of the non-hematopoietic fraction of skin cell suspensions (composed primarily of fibroblasts and keratinocytes) did not reveal Cre-mediated activation of EYFP expression (Fig. 2.12).

A low percentage of EYFP expressing cells was detected in the CD49b (α2-Integrin) positive compartment of the spleen in A-Mcpt5-Cre mice, stained with the anti-49b antibody clone DX5 (on average 3.67±1.88%, n=4). This monoclonal antibody stains natural killer (NK) cells as well as NK T cells (Arase et al., 2001). We further examined the NK and NK T cell populations in peripheral blood samples of one *A-Mcpt5-Cre R26R-EYFP* double positive animal. As shown in Fig. 2.13, 8.96% of the $CD49b^+NKG2D^+$ NK cell subset, but only 1.29% of NK T cells, defined as $CD49b^+CD3^+$ cells, displayed EYFP reporter gene expression (Fig. 2.13, A and B). Only 0.78% of NKG2D single positive NK cells were EYFP positive (Fig. 2.13, B). In conclusion, a small fraction of the $CD49b^+NKG2D^+$ NK cells is the only hematopoietic cell population other than mast cells that delete loxP-flanked DNA.

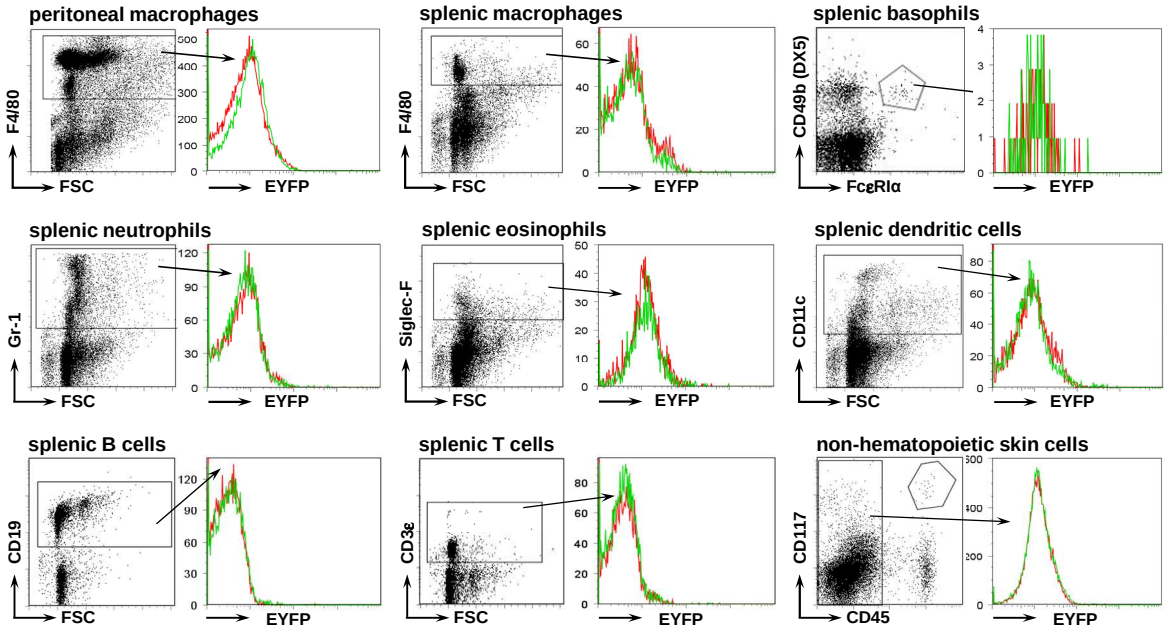

Fig. 2.12 Absence of EYFP reporter gene expression in hematopoietic cells other than mast cells and in non-hematopoietic skin cells. EYFP expression was analyzed in hematopoietic cells from peritoneal lavage fluid and spleen cell suspensions of *Mcpt5-Cre R26R-EYFP* double positive mice. In order to enrich granulocytes, splenocytes were separated into lymphocyte and non-lymphocyte fractions by MACS. Basophils were detected as CD49b and FcεRIα double positive cells. Macrophages, neutrophils, eosinophils, dendritic cells, B cells and T cells were stained using antibodies against F4/80, Gr-1, Siglec-F, CD11c, CD19 and CD3ε, respectively.

EYFP fluorescence intensity of these populations and CD45-negative cells of the skin was displayed in histogram plots. The green graph represents *Mcpt5-Cre R26R-EYFP* double positive mice and the red graph Cre-negative but *R26R-EYFP*-positive controls (littermates in most instances). Results are representative for three A- and three X-Mcpt5-Cre mice.

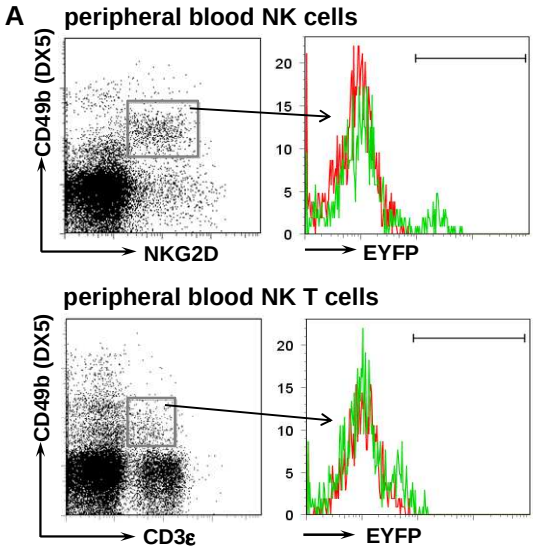

B

	EYFP⁺ cells
total CD49b⁺	5.8%
CD49b⁺ NKG2D⁺	8.96%
CD49b⁻ NKG2D⁺	0.78%
CD49b⁺ NKG2D⁻	4.41%
CD49b⁺ CD3ε⁺	1.29%

Fig. 2.13 Cre-mediated reporter gene expression in NK and NK T cells of one *A-Mcpt5-Cre R26R-EYFP* double positive mouse. Peripheral blood samples were taken from the lateral tail vein of one animal and erythrocytes were lysed. NK cells and NK T cells were identified as CD49b (clone DX5) and NKG2D or CD49b and CD3ε double positive cells, respectively. (A) EYFP fluorescence intensity of these cell populations was displayed in histogram plots. The green graphs represent the *A-Mcpt5-Cre R26R-EYFP* double positive animal and the red graph the Cre-negative control. (B) The table displays the percentages of EYFP expressing cells among the indicated populations of the *A-Mcpt5-Cre R26R-EYFP* double positive animal.

A

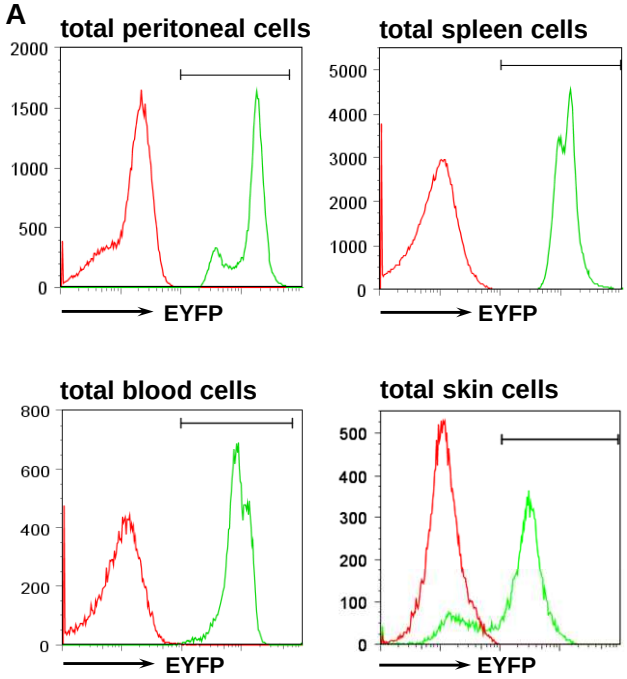

B

% of EYFP expressing cells		n
total cell populations:		
peritoneal cells	99.30%	2
spleen cells	99.31%	2
blood cells	99,71%	1
skin cells	67,41%	2
splenic cell populations:		
macrophages	98.70%	2
basophils	99.68%	2
eosinophils	98.55%	2
neutrophils	99.42%	2
dendritic cells	98.07%	2
B cells	99.75%	2
T cells	98.17%	2
CD49b$^+$	99.98%	2

Fig. 2.14 Cre-mediated activation of EYFP reporter gene expression in *tg(CMV-Cre) R26R-EYFP* double positive mice. (A) EYFP fluorescence of total cell populations of peritoneal lavage fluid, spleen, peripheral blood and skin was assessed by flow cytometry and displayed in histogram plots. The green graphs represent *tg(CMV-Cre) R26R-EYFP* double positive, the red graphs represent control mice. (B) Average percentage of EYFP expressing cells of total peritoneal, splenic, peripheral blood and skin cells. Macrophages, basophils, eosinophils, neutrophils, dendritic cells, B cells and T cells were stained with antibodies against F4/80, CD49b/FcεRIα, SiglecF, Gr-1, CD11c, CD19 and CD3ε, respectively. The EYFP expressing percentage of each cell population was assessed by flow cytometry. Results are representative of two double positive mice except for blood cells (n=1).

In a control experiment we used mice with a germ line deletion of the stop element of the R26R-EYFP reporter obtained by crossing the reporter strain to the X-linked Cre-deleter strain *tg(CMV-Cre)* (Schwenk et al., 1995). Analysis of *tg(CMV-Cre) R26R-EYFP* double positive mice demonstrated that all non-mast cell populations analyzed for reporter gene expression in the *Mcpt5-Cre* mice can, in principle, express EYFP (Fig. 2.14, A and B).

In contrast to six A-Mcpt5-Cre mice (described above), one *Mcpt5-Cre* transgenic animal displayed non-specific reporter gene expression in 15%-25% of all cell types analyzed including non-hematopoietic cells of the skin (data not shown). This animal was the progeny of a different F1 animal from the cross of the founder animal to the reporter strain. All littermates showed non-specific reporter gene expression to a variable extent (data not shown). This non-specific Cre-mediated recombination in cells other than mast cells was restricted to this substrain which was, therefore, not analyzed further. No non-specific reporter gene expression could be detected (in all subsequent experiments) in the substrain that was finally designated as A-Mcpt5-Cre.

As the A-Mcpt5-Cre line shows efficient and mast cell-specific Cre-mediated recombination and as this line has an advantage over the X-linked Cre line in terms of

breeding strategies and Cre-mediated deletion in female mice, this line will be used predominantly in the future for breeding with other floxed lines.

2.1.4.3 Exclusion of Cre-mediated genotoxicity in Mcpt5-Cre mice

In order to exclude a reduced viability of mast cells in *Mcpt5-Cre* mice due to Cre-mediated genotoxic effects, the percentage of mast cells in peritoneal lavage fluid was compared in *Mcpt5-Cre R26R-EYFP* double positive and wild type animals. Numbers of peritoneal mast cells in double positive mice did not differ from those of wild type animals (Fig. 2.15, A).

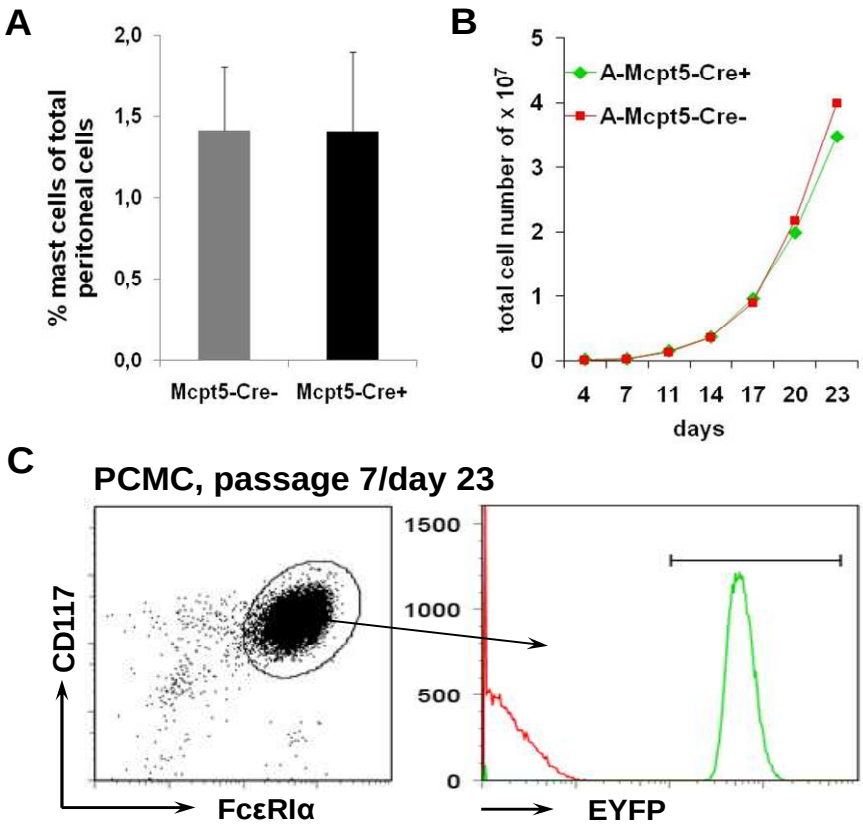

Fig. 2.15 Numbers and proliferative potential of peritoneal mast cells in *Mcpt5-Cre* transgenic mice. (A) Mast cells were quantified in percent of total peritoneal cells in peritoneal lavage fluid from control (n=9) and *Mcpt5-Cre* (seven A-Mcpt5-Cre and three male X-Mcpt5-Cre) mice. (B) Peritoneal cell-derived mast cells (PCMC) were generated from total peritoneal cells of one control and one A-*Mcpt5-Cre R26R-EYFP* double positive mouse by incubating these cells in medium supplemented with SCF-conditioned medium (Malbec et al. 2007). Cell numbers were quantified at each passage every 3-4 days by counting trypan blue excluding cells. (C) At passage seven, PCMCs were analyzed by flow cytometry by staining for CD117 and FcεRIα. $CD117^{+}FcεRIα^{+}$ cells were gated and analyzed for reporter gene expression (displayed in a histogram plot). The green graph represents the *Mcpt5-Cre R26R-EYFP* double positive mouse and the red graph the control animal.

To assess whether the proliferative potential of mast cells in *Mcpt5-Cre* transgenic animals was reduced by genotoxic Cre effects, total peritoneal lavage cells of *Mcpt5-Cre R26R-EYFP* double positive and *Cre*-negative mice were cultured in presence of stem cell

factor (SCF) as described (Malbec et al., 2007). After 23 days, these cultures contained 98% mast cells designated as PCMCs (peritoneal cell derived mast cells) as judged by expression of the CD117 and FcεRIα surface markers (Fig. 2.15, C). By this time, absolute cell numbers had increased more than 200-fold in both cultures (Fig. 2.15, B). Importantly, the mast cells grown from the *Mcpt5-Cre R26R-EYFP* mouse uniformly expressed EYFP ruling out an overgrowth of the culture by a (hypothetical) minor population of mast cells, which do not express Cre (Fig. 2.15, C). These results show that *Mcpt5-Cre* positive mast cells are viable like wild type mast cells, and that they are not growth retarded. Therefore, mast cells of *Mcpt5-Cre* transgenic mice do not seem to be significantly affected by Cre-mediated genotoxicity.

2.1.5 Screening of *Mcpt6-Cre* transgenic mice for Cre-mediated recombination

Seven of the Mcpt6-Cre founder lines that transmitted the transgene to the germline were mated to R26R-EYFP reporter mice and *Mcpt6-Cre R26R-EYFP* double positive offspring were obtained from five breedings and tested for Cre-mediated recombination by flow cytometry. Since the staining of mast cells with a new lot of the anti-FcεRIα antibody proved unreliable, in most of the following experiments mast cells were identified as CD117 and IgE positive cells. Given that, due to its high affinity for IgE, basically all FcεRI receptors are loaded with immunoglobulin E (Benoist and Mathis, 2002), cells which are positive for IgE can be considered as $FcεRI^+$ and designated as $FcεRI/IgE^+$.

In two of the five lines, efficient Cre-mediated activation of EYFP expression was observed in $CD117^+FcεRIα/IgE^+$ peritoneal mast cells as well as in $CD117^+CD45^+$ skin mast cells (Fig. 2.16, A). As these lines were derived from the founder animals 526873 and 526874 and as they displayed an autosomal pattern of transgene inheritance these two lines were designated as A73-Mcpt6-Cre and A74-Mcpt6-Cre. 95.92±0.96% and 96.5±1.39% of $CD117^+FcεRIα^+$ peritoneal mast cells of the A73- and A74-Mcpt6-Cre line, respectively, displayed reporter gene expression (n=4 for both lines, Fig. 2.16, A). In one animal of the A73-Mcpt6-Cre line and two mice of the A74-Mcpt6-Cre line, the $CD117^+CD45^+$ skin mast cell population was analyzed for reporter gene expression. The majority of the few $CD117^+CD45^+$ cells gated was EYFP positive (51/59, 15/28 and 42/45 gated events). Although a full length integration of the transgene could not be demonstrated for the A73-Mcpt6-Cre mice (Fig. 2.8, B), this line displayed almost identical efficiency of Cre-mediated recombination compared to the A74-Mcpt6-Cre line containing the full length transgene. This shows that the missing part of the transgene (of unknown size downstream of the *Mcpt6-Cre* sequence) was not important for transgene expression. In both Mcpt6-Cre lines, the expression of the Cre recombinase was restricted to mast

cells, since in two animals analyzed for each line reporter gene expression could be detected, if at all, in minimal numbers in hematopoietic cell populations other than mast cells (below 1%, Fig. 2.16, B and C). In contrast to the finding in *Mcpt5-Cre/R26R-EYFP* mice, peripheral blood CD49b$^+$ cells were basically all EYFP negative (below 0.1%, Fig. 2.16, B).

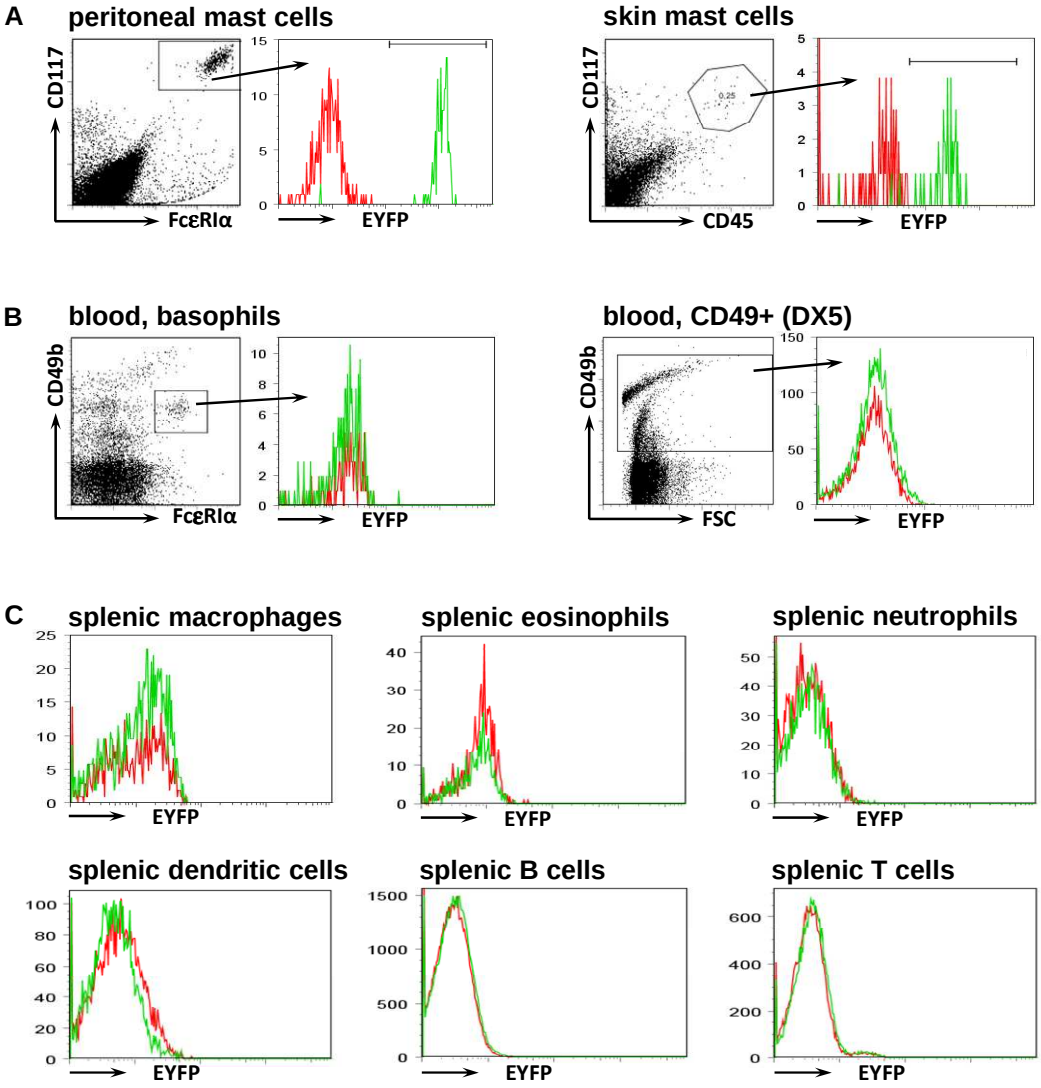

Fig. 2.16 Efficiency and specificity of Cre-mediated activation of EYFP reporter gene expression in A73- and A74-Mcpt6-Cre mice. EYFP expression was analyzed by flow cytometry of cells from peritoneal lavage fluid and skin cell suspensions (A), peripheral blood samples (B) as well as spleen cell suspensions (C) of *Mcpt6-Cre R26R-EYFP* double positive animals. (A) Peritoneal mast cells were stained for CD117 and FcεRI bound IgE (n=4 for each Mcpt6-Cre line) and skin mast cells for CD117 and CD45 (n=1 for A73- and n=2 for A74-Mcpt6-Cre). Mast cell populations were gated and their EYFP fluorescence was displayed in histogram plots. (B) Basophils were identified as CD49b (clone DX5) and FcεRIα double positive cells in erythrocyte lysed blood samples. The basophil population as well as total CD49b$^+$ cells were gated and displayed in histogram plots (n=2 for A73-Mcpt6-Cre and n=1 for A74-Mcpt6-Cre). (C) Macrophages, eosinophils, neutrophils, dendritic cells, B cells and T cells were identified in total spleen cell suspensions as F4/80, Siglec-F, Gr-1, CD11c, CD19 and CD3ε positive cells, respectively, (n=2 for each, A73- and A74-Mcpt6-Cre). EYFP fluorescence of the respective cell populations was displayed in histogram plots. The green graphs represent *Mcpt6-Cre R26R-EYFP* double positive animals, the red graphs *Cre*-negative but *R26R-EYFP* positive control animals (littermates in most instances).

A potential effect of Cre expression on the proliferative potential has not yet been determined for Mcpt6-Cre mice. However, both, A73- and A74-Mcpt6-Cre, displayed reduced mast cell numbers in the peritoneal cavity (0.8±0.38% mast cells of total peritoneal cells for the A73-Mcpt6-Cre line (n=4) and 0.73±0.29% for the A74-Mcpt6-Cre line (n=4) compared to 1.57±0.72% mast cells in control animals (n=6, Fig. 2.17). This result may be due to genotoxic effects of the Cre recombinase in mast cells of *Mcpt6-Cre* transgenic mice and will be analyzed further.

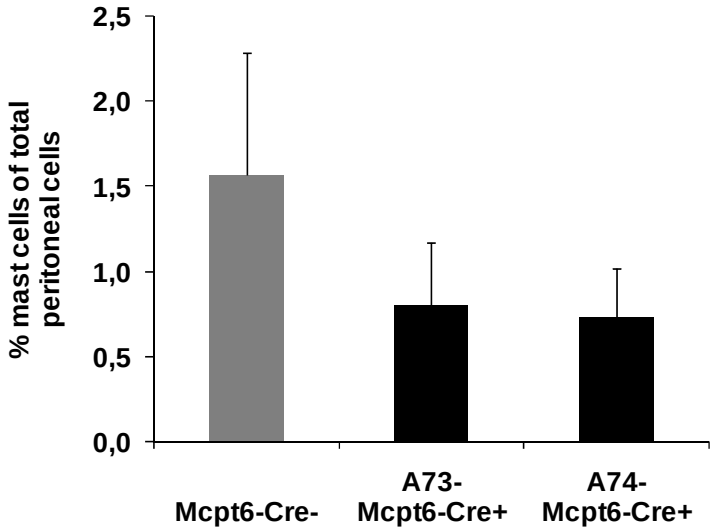

Fig. 2.17 Number of peritoneal mast cells in Mcpt6-Cre mice. Mast cells were quantified as percent of total peritoneal cells in peritoneal lavage fluid from control (n=6), A73-Mcpt6-Cre (n=4) and A74-Mcpt6-Cre (n=4) mice.

2.1.6 Test for Cre-mediated EYFP expression in BMMCs

In vitro cultured bone marrow-derived mast cells (BMMC) are immature mast cells as judged by the proteoglycan and mast cell protease content of their granules (Lunderius et al., 2000). They contain chondroitin sulfate, but not heparin sulfate, as well as the mast cell proteases mMCP-5, -6 and CPA. The IL-3 dependent differentiation of bone marrow cells to BMMCs resulted in 91.9±1.84% of $CD117^{+}Fc\varepsilon RI^{+}$ cells after eight weeks of culture as shown in Fig. 2.18, A, for BMMCs derived from *R26R-EYFP* and *A-Mcpt5-Cre*, *X-Mcpt5-Cre*, *A73-Mcpt6-Cre, A74-Mcpt6-Cre* and *tg(CMV-Cre)* double positive mice.

Various studies demonstrated significant transcription of *Mcpt5* and *Mcpt6* in BMMCs by northern blot analysis (Gurish et al., 1992; Lunderius et al., 2000; McNeil et al., 1991; Reynolds et al., 1991) and mMCP-5 and -6 expression on the protein level (Eklund et al., 1994; McNeil et al., 1992a; Wolters et al., 2001). However, only 7-35% of the $CD117^{+}Fc\varepsilon RI^{+}$ BMMCs derived from either *Mcpt5-Cre* or *Mcpt6-Cre R26R-EYFP* double positive mice display Cre-mediated activation of EYFP expression (Fig. 2.18, B and C).

Thus, in most of the cells the *Mcpt5* and *Mcpt6* promoters are either not active or active at such a low level that Cre expression is not sufficient for the deletion of the stop element. After twelve weeks in culture the percentage of EYFP expressing BMMCs was not significantly increased (8-41%, Fig. 2.18, C) demonstrating that neither Cre-expressing cells nor the EYFP-negative cells have a growth advantage.

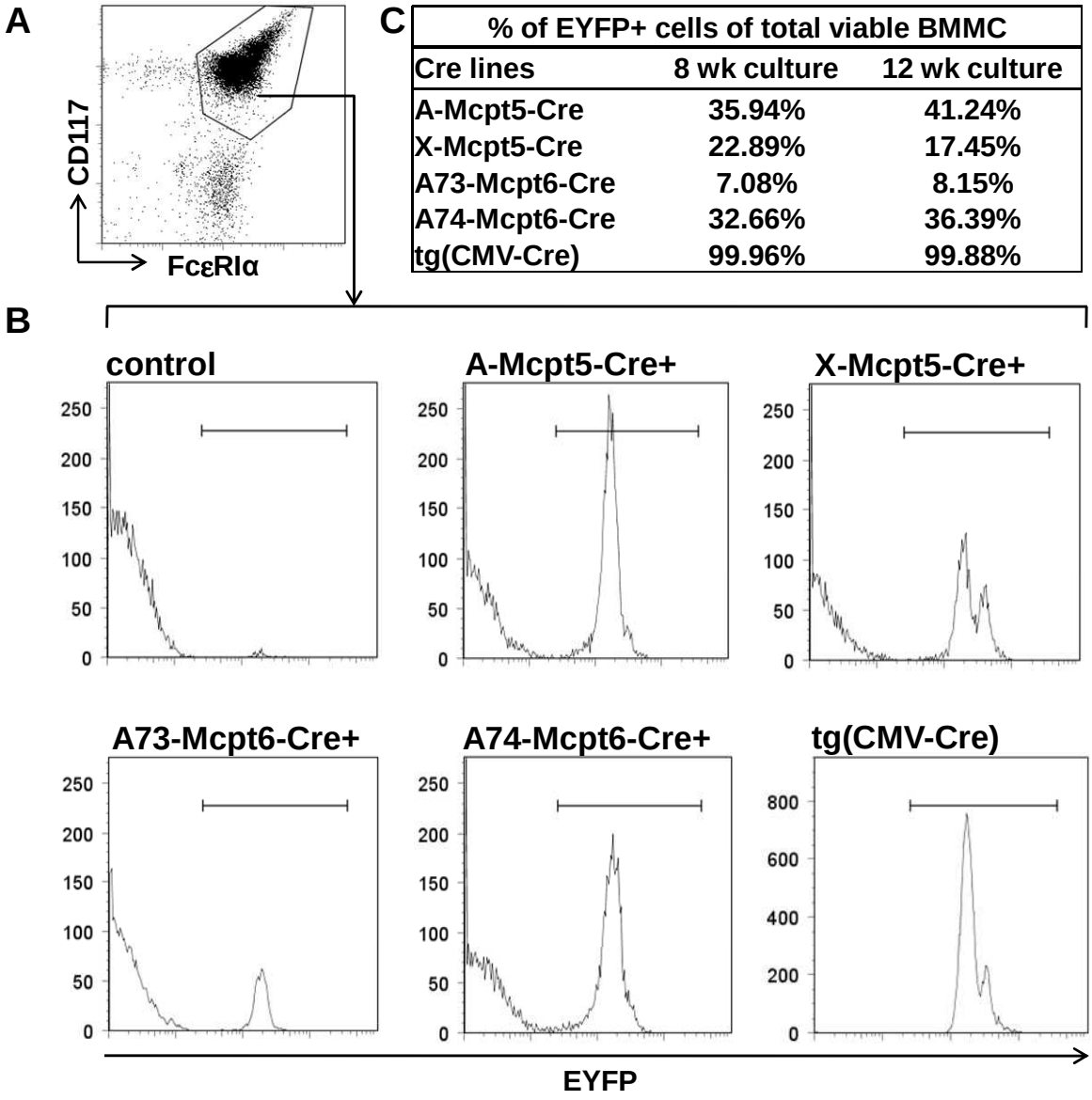

C

% of EYFP+ cells of total viable BMMC		
Cre lines	**8 wk culture**	**12 wk culture**
A-Mcpt5-Cre	**35.94%**	**41.24%**
X-Mcpt5-Cre	**22.89%**	**17.45%**
A73-Mcpt6-Cre	**7.08%**	**8.15%**
A74-Mcpt6-Cre	**32.66%**	**36.39%**
tg(CMV-Cre)	**99.96%**	**99.88%**

Fig. 2.18 EYFP reporter gene expression in bone marrow-derived mast cells (BMMC) derived from *A-* and *X-Mcpt5-Cre*, *A73-* and *A74-Mcpt6-Cre* and *tg(CMV-Cre) R26R-EYFP* double positive mice. Bone marrow cells were cultured in WEHI-3B conditioned medium. (A) After eight weeks (wk) in culture, cells were stained with antibodies against CD117 and FcεRIα and analyzed by flow cytometry. (B) $CD117^{+}Fc\varepsilon RI\alpha^{+}$ cells of the indicated genotype (n=1 for all lines) were gated and displayed in histogram plots to show the fraction of EYFP expressing BMMCs. (C) The table specifies the percentages of EYFP expressing cells in the respective BMMC populations after eight and twelve weeks of culture.

In order to demonstrate that BMMCs can, in principle, express EYFP under the control of the *ROSA26* promoter, the X-linked Cre-deleter strain *tg(CMV-Cre)* (Schwenk et al., 1995) was crossed with the R26R-EYFP strain. As displayed in the lower right histogram plot of Fig. 2.18 (B and C), EYFP expression could be detected in basically all $CD117^{+}Fc\varepsilon RI^{+}$ tg(CMV-Cre)/R26R-EYFP BMMCs after eight and twelve weeks of culture.

2.1.7 Screening of *Mcpt5-CreER^{T2}* transgenic mice for Cre-mediated recombination

CreER^{T2} lines are characterized by constitutive expression of a $CreER^{T2}$ fusion protein that is retained in the cytoplasm. Upon application of the estrogen analogon tamoxifen, the fusion protein translocates into the nucleus where it can mediate deletion of *loxP*-flanked sequences. To assess whether peritoneal mast cells show Cre-mediated activation of EYFP expression upon tamoxifen induction, *Mcpt5-CreER^{T2} R26R-EYFP* double positive mice and *Cre*-negative littermates were orally treated with tamoxifen for five days using a feeding needle. Peritoneal lavage fluid cells were analyzed by flow cytometry three days or four weeks after the last tamoxifen application. In none of these lines, EYFP expression could be detected in mast cells (data not shown). To investigate whether the tamoxifen induction was unsuccessful or whether the expression of the fusion protein was ineffective, the *frt* site-flanked *ER^{T2}* element was removed using a mouse strain expressing an ubiquitously active Flp recombinase (hACTB::FLP mice (Dymecki, 1996a)). In *Mpct5-Cre(ER^{T2}del) R26R-EYFP Flp-Deleter* triple positive mice the Cre recombinase should be constitutively active without tamoxifen application. The efficiency of the *ER^{T2}* deletion was demonstrated by PCR on tail tip DNA (data not shown). Peritoneal mast cells were analyzed for reporter gene expression, but even after deletion of the *ER^{T2}* cassette no or only about 14 % of the mast cells showed Cre-mediated activation of EYFP expression (data not shown). Similar results were obtained for all four lines analyzed. From one line, we did not obtained triple transgenic animals. These results indicate that all five Mcpt5-$CreER^{T2}$ lines are not functional, e.g. due to a defective transgene integration or an unfavorable integration site. New founder lines will be generated in the future.

2.2 A new model for inducible ablation of mast cells in adult mice

The currently used mouse models for the investigation of mast cells, i.e. mast cell-deficient mice, like the *Kit*$^{W/W\text{-}v}$ and *Kit*$^{Wsh/Wsh}$ mutant lines, yielded valuable information but suffer from important limitations. Therefore, we established a new model for inducible mast cell-ablation by crossing A-Mcpt5-Cre mice to the iDTR strain (inducible diphtheria toxin receptor, (Buch et al., 2005)), which is characterized by the conditional expression of the high affinity simian diphtheria toxin receptor (DTR), i.e. the heparin-binding epidermal growth factor-like growth factor (HB-EGF). The receptor is necessary for the internalization of the toxin into the cell. Rodents usually are diphtheria toxin (DT) resistant because of the low affinity of the rodent HB-EGF to DT. In contrast, iDTR mice express the simian diphtheria toxin receptor under the control of the ubiquitously active *ROSA26* promoter provided a *loxP*-flanked stop element was removed by Cre-mediated recombination. Upon diphtheria toxin injection, all cells that express the DTR internalize the DT via its B subunit. Within the cell, the A subunit inactivates elongation factor 2 and thereby terminates protein synthesis and causes apoptotic death (Buch et al., 2005).

2.2.1 Ablation of peritoneal and skin mast cells

In order to test the efficiency of the ablation of peritoneal mast cells, *A-Mcpt5-Cre iDTR* double positive, *Cre*-negative *iDTR* single transgenic and wild type mice were treated with a single intraperitoneal (i.p.) injection of 25 ng DT/g bodyweight. 24 h later, peritoneal lavage fluid cells were analyzed for the presence of mast cells by flow cytometry. In the *Cre*-negative *iDTR* single positive as well as in wild type mice, normal numbers of CD117^{+}FcεRIα^{+} cells could be detected (2.75±0.22% mast cells of total peritoneal cells, n=3) while in double positive mice only 0.035±0.01% mast cells were present reflecting successful ablation of 99.1±0.18% of CD117^{+}FcεRIα^{+} cells (n=2, Fig. 2.19, A and B). Peritoneal macrophages, defined as F4/80^{+}, and peritoneal B cells, defined as CD19^{+} cells, were not affected by DT treatment (Fig. 2.19, A and C). The results show that mast cells can be efficiently depleted in the peritoneal cavity with a single injection of the toxin.

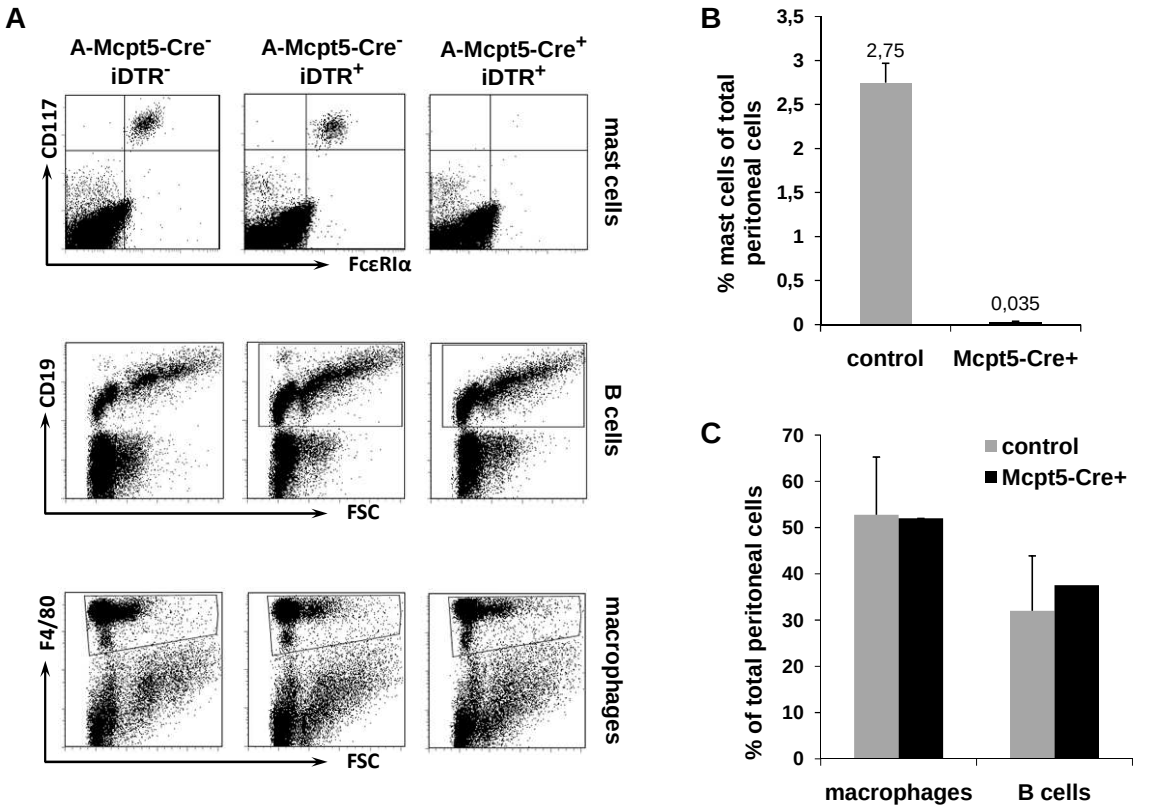

Fig. 2.19 Efficiency of ablation of peritoneal mast cells. Mice were injected i.p. with a single dose of 25 ng DT/g bodyweight. 24 h after the injection mice were sacrificed and peritoneal cells were isolated. (A) In peritoneal lavage fluid of wild type, *iDTR* single transgenic and *A-Mcpt5-Cre iDTR* double positive animals mast cells, B cells and macrophages were identified as CD117 and FcεRIα double and CD19 and F4/80 single positive cells, respectively, and analyzed by flow cytometry. (B) The average percent mast cells of total peritoneal cells in three control mice and two *A-Mcpt5-Cre iDTR* double positive mice are displayed. (C) Percent macrophages and B cells of total peritoneal cells in two control animals and one *A-Mcpt5-Cre iDTR* double positive mouse.

The efficiency of mast cell depletion in the skin after DT injections was examined on either skin biopsies or skin samples from the back, abdomen or ear post mortem. In Giemsa stained paraffin sections mast cells appear dark purple due to the metachromatic staining of the mast cell granules. Mast cell numbers per mm^2 were calculated by counting mast cells in the region between epidermis and panniculus carnosus and by software-supported determination of area size. DT treated *Cre*-negative i*DTR* positive littermates served as controls. Mast cell numbers in control mice were highly variable. Therefore, mast cell numbers in *A-Mcpt5-Cre iDTR* double positive mice were compared with a control collective representing mast cell numbers in back skin of ten *Cre*-negative mice (39.8±14.7 mast cells/mm^2).

A

DT dosage	1x 25 ng/g	3x 25 ng/g daily interval	7x 25 ng/g daily interval	4x 50 ng/g daily interval	4x 25 ng/g weekly interval
Bx = biopsy/skin sample	Bx	Bx	Bx	Bx	Bx
injections (i. p.)	↓	↓↓↓	↓↓↓↓↓↓↓	↓↓↓↓	↓ ↓ ↓ ↓
days	0 3	0 1 2 5	0 1 2 3 4 5 6 9	0 1 2 3 6	0 6 13 20 27
depletion efficiency	72,57%	76,23%	96,18%	99,83%	94,27%
mice	n=3	n=1	n=1	n=3	n=7

B

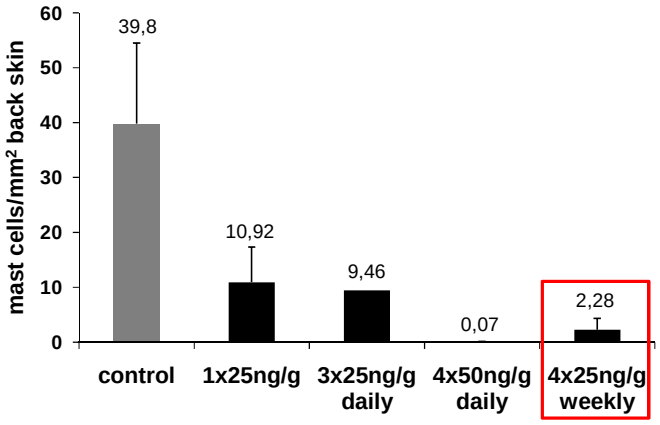

Fig. 2.20 Diphtheria toxin (DT) dosage finding experiments for depletion of skin mast cells in *A-Mcpt5-Cre iDTR* double positive animals. Mice were treated with different DT dosages and number of DT injections. 4 mm biopsies (Bx) of the back skin from anesthetized animals or about 2 cm^2 of back skin post mortem were taken three or seven days after the last DT injections. Mast cells were quantified per mm^2 in Giemsa stained paraffin sections. The area between epidermis and panniculus carnosus was determined using Diskus 4.50 software (A) Scheme for the tested DT injection protocols. The corresponding average depletion efficiencies and animal numbers are listed. (B) Mast cell numbers per mm^2 after injection of DT with the respective protocol were compared to mast cells per mm^2 of a control collective (mast cell numbers in back skin of ten Cre-negative control mice).

24 h after a single injection of 25 ng DT/g bodyweight we found no reduction in mast cell numbers in the skin (data not shown). Interestingly, three days after a single injection, skin mast cells were reduced to 10.92±6.41 mast cells/mm^2 (n=3, Fig. 2.20, A and B). In order to achieve efficient ablation of skin mast cells, different dosages, multiple injections and various injection intervals were tested. The different protocols are depicted in Fig. 2.20, A. The treatment with high doses, e.g. 3x 100ng/g (data not shown) or 4x 50ng/g bodyweight as well as frequent injections (7x 25 ng/g at daily intervals) turned out to be toxic or lethal for both, control and double positive mice. A reason for this toxic effect could be a contamination of the DT solution with endotoxins thereby causing a systemic inflammatory response. Also an effect mediated by the murine low affinity DTR cannot be excluded. Importantly, higher doses of DT resulted in complete elimination of skin mast cells (Fig. 2.20, A and B), showing that, in principle, 100% of skin mast cells express Cre recombinase and undergo Cre-mediated deletion of the *loxP*-flanked allele. Given the toxicity of higher doses and frequent injections (daily intervals) and also the slow kinetics

of skin mast cell depletion, we decided to follow a regimen of four injections of 25 ng/g bodyweight at weekly intervals. In skin samples taken one week after the last injection, mast cell numbers were reduced to 2.28±2.02 mast cells/mm^2 (n=7), i.e. with an average depletion efficiency of 94.27 % compared to the control collective (Fig. 2.20, A and B).

As mentioned above, all animals, controls and double positive mice, treated with high DT dosages (50 – 100 ng/g bodyweight) showed severe clinical signs like lethargy, significant weight loss and hunch back over a period of one to two weeks until they finally died. In contrast, after four injections of 25 ng DT/g bodyweight at weekly intervals control and *A-Mcpt5-Cre iDTR* double positive mice did not show any sign of disease. Nevertheless, some animals died within three days after the first injection. This problem occurred exclusively in *A-Mcpt5-Cre iDTR* double positive animals, 21.52% of which died (17 of 79 double positive mice and 0 of 69 controls, Fig. 2.21).

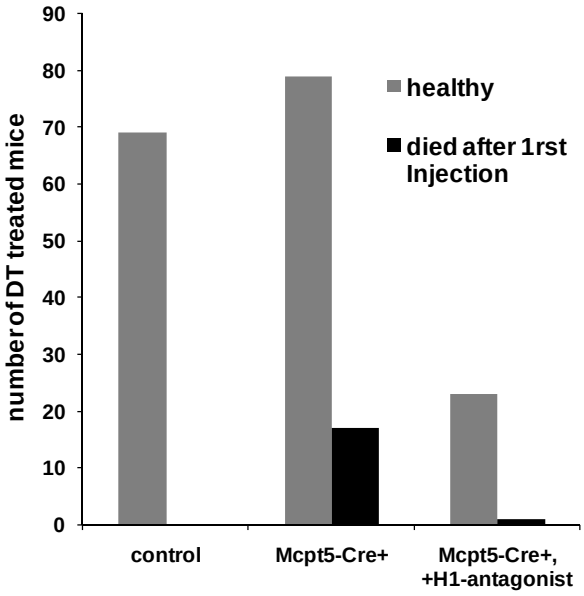

Fig. 2.21 Survival after the first injection of DT. *A-Mcpt5-Cre iDTR* double positive mice were either treated with DT alone or with DT together with the H1-antagonist pyrilamine (5µg/g bodyweight). The grey bar represents surviving and healthy DT treated animals. Black bar represents animals that died after the first DT injection within three days.

This finding led to the assumption that mast cells might degranulate before dying by apoptosis resulting in high systemic levels of mast cell mediators leading to lethal anaphylaxis. Therefore, control and *A-Mcpt5-Cre iDTR* double positive mice were treated with DT following the same protocol but this time the H1-antagonist pyrilamine (5 µg/g bodyweight) was injected together with the first toxin injection. Among the animals treated with DT plus H1-antagonist, i.e. 21 controls (data not shown) and 23 *Cre*-positive mice (Fig. 2.21), only one (*Cre*-positive) mouse died indicating a significant reduction of lethality to 4.35%. This result suggests that histamine release was in fact the cause of the lethal effects of mast cell ablation and that this problem can be avoided by blocking histamine effects. Since the pyrilamine is injected only along with the first DT dosage and since mast cell depleted mice will be used for experiments only four weeks later, it can be assumed

that the H1-antagonist treatment will not affect the experiments. Despite the evidence for systemic mast cell mediator release, we never observed any sign of local inflammation on histological tissue analysis of DT-injected double positive mice (with or without H1-antagonist treatment) (data not shown).

As skin mast cell numbers vary between different locations, reduction of mast cell numbers (achieved by the final DT injection protocol) was also determined at other sites than back skin, i.e. abdomen and ear. Mast cell depletion in abdominal skin of *A-Mcpt5-Cre iDTR* double positive mice was comparable to that in back skin with 1.34±1.16 residual mast cells/mm^2 (n=6) representing an average depletion efficiency of 96.58% compared to a control collective (39.2±14.16 mast cells/mm^2, n=4, Fig. 2.22, A). Ear skin mast cell density of control mice was about 3-fold higher than in other skin regions (107±16.24 mast cells/mm^2, n=4, Fig. 2.22, B) and depletion was least efficient in this location. Seven days after the last injection, 18.25±12.11 mast cells/mm^2 remained (n=6) corresponding to an average depletion efficiency of 84.33% compared to the control (Fig. 2.22, B).

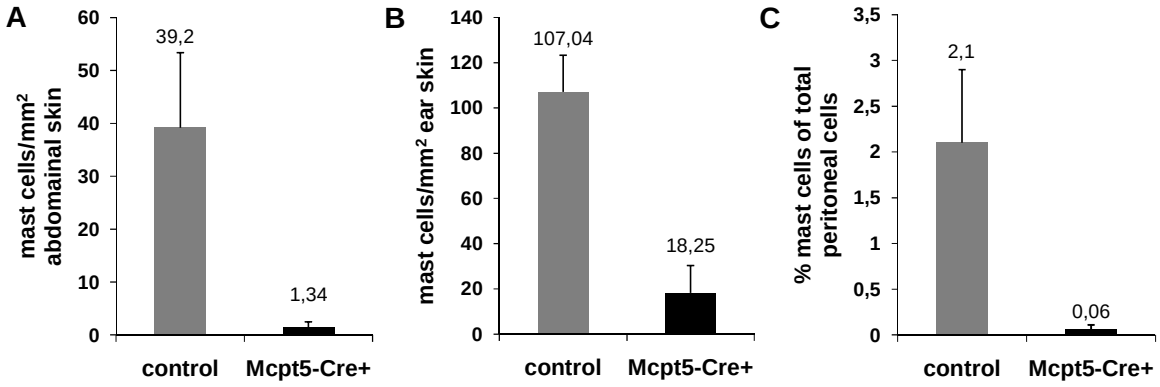

Fig. 2.22 Depletion of mast cells in abdominal skin, ear and peritoneal cavity by four injections of 25 ng DT/g at weekly intervals. Animals were analyzed seven days after the last injection. (A) Mast cells were quantified in the area between epidermis and panniculus carnosus of belly skin of six *A-Mcpt5-Cre iDTR* double positive and four *Cre*-negative control mice. (B) Mast cell numbers were determined in an area that represents the whole ear section of six double positive and four Cre-negative mice. (C) Mast cells in peritoneal lavage fluid were stained for CD117 and FcεRI bound IgE and analyzed by flow cytometry.

To further validate successful depletion of peritoneal mast cells using the final injection protocol, peritoneal lavage fluid cells were analyzed by flow cytometry seven days after the last injection. Seven *A-Mcpt5-Cre iDTR* double positive animals displayed an average depletion of 97% of CD117$^+$FcεRIα/IgE$^+$ mast cells corresponding to 0.06±0.05% mast cells of total peritoneal cells compared to 2.1% in control animals (n=13, Fig. 2.22, C).

In order to assess whether the four injections of 25 ng DT/g bodyweight at weekly intervals affected hematopoietic cells other than mast cells, the percentages of CD49b$^+$

cells, eosinophils and basophils of total blood leukocytes (Fig. 2.23, A) and of T cells, B cells, neutrophils, macrophages and dendritic cells of total splenocytes (Fig. 2.23, B) were determined by flow cytometry. The results indicated that the DT treatment did not cause a reduction of these cell populations in *A-Mcpt5-Cre iDTR* double positive mice (n=3 for peripheral blood cells and n=2 for splenocytes) compared to control animals (n=3 for peripheral blood cells and one animal for splenocytes). Although a small fraction of $CD49b^+$ cells were shown in *A-Mcpt5-Cre R26R-EYFP* double positive mice to express the Cre recombinase, a reduction of this cell population after DT treatment of *A-Mcpt5-Cre iDTR* mice was not detectable. The increased number of splenic neutrophils in double positive mice compared to the control (Fig. 2.23, B, right panel) has to be verified by analyzing more mice especially more DT-treated control animals.

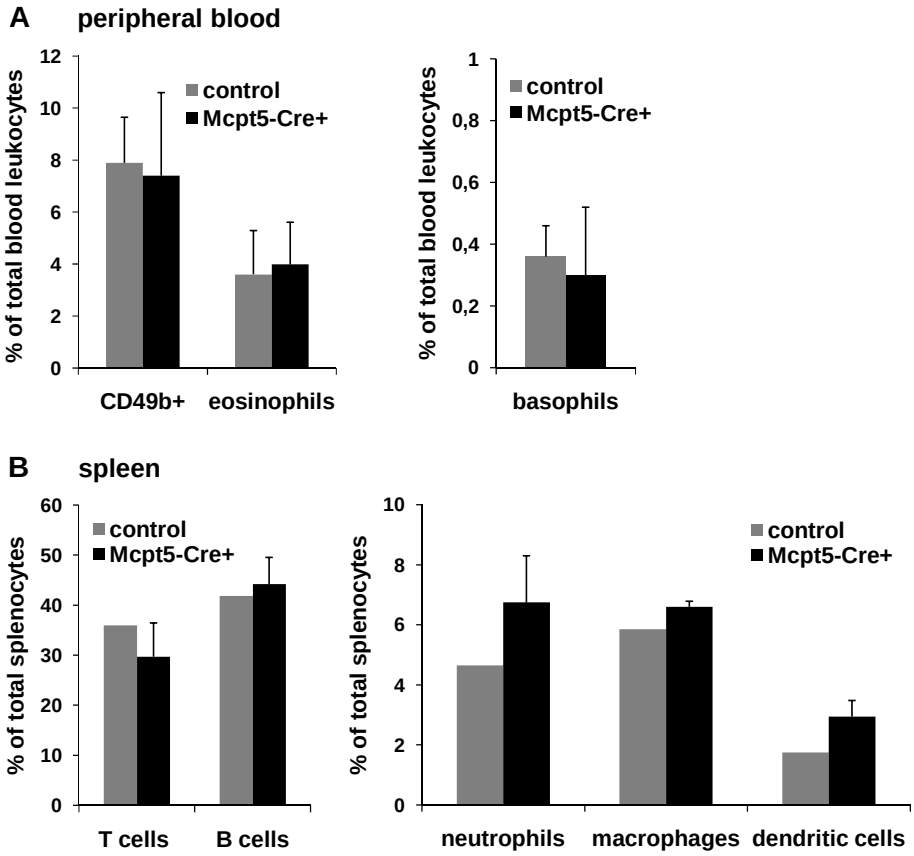

Fig. 2.23 DT does not affect hematopoietic cell populations other than mast cells. Control and *A-Mcpt5-Cre/iDTR* mice were treated 4x with 25 ng DT/g bodyweight i.p. at weekly intervals. The percentages of each cell population of total blood leukocytes (A) and total splenocytes (B) were determined by flow cytometry after erythrocyte lysis. (A) In peripheral blood samples of *A-Mcpt5-Cre iDTR* double positive mice (n=3) and Cre-negative controls (n=3) $CD49^+$ cells, basophils and eosinophils were stained with anti-CD49b (clone DX5), DX5 and anti-IgE and anti-Siglec-F, respectively. (B) In spleen cell suspensions of one Cre-negative and two *A-Mcpt5-Cre iDTR* double positive mice T cells, B cells, neutrophils, macrophages and dendritic cells were stained with antibodies against CD3ε, CD19, Gr-1, F4/80 and CD11c, respectively.

In conclusion, the A-Mcpt5-Cre/iDTR system allows efficient ablation of mast cells in the peritoneal cavity and skin without affecting other cell populations. However, mast cell depletion in the skin occurs slowly and requires multiple i.p. injections compared to the complete depletion of peritoneal mast cells after a single injection.

2.2.2 Depletion of gastrointestinal mast cells

In mice two mast cell phenotypes can be distinguished, connective tissue type mast cells (CTMC) and mucosal mast cells (MMC). The CTMCs are located predominantly in the skin and peritoneal cavity but also in the connective tissue of most organs including the submucosal layers of the gastrointestinal tract and are characterized by storage of the proteoglycan heparin sulfate and the proteases mMCP-4, -5, -6 and MC-CPA. MMCs reside within epithelia of the gastrointestinal and respiratory tracts, i.e. above the basement membrane between the epithelial cells. Their granules contain the proteoglycan chonodroitin sulfate and mMCP-1 and -2. In order to test whether Cre recombinase is also expressed in the MMC subset, mast cell depletion was analyzed in the stomach. This organ was chosen because in C57BL/6 mice, hardly any MMCs can be found in the small intestine and colon while high numbers are usually encountered in the stomach. Paraffin sections were stained histochemically for the chloroacetate esterase activity using AS-D chloroacetate as a substrate. In the sections, mast cells can be recognized by their dark red stained granules. The stomach can be divided into the squamous portion characterized by squamous epithelium and the presence of CTMCs but not MMCs and the glandular portion that contains both, CTMCs in the submucosa and MMCs in the mucosal epithelium. Seven days after the last of four injections of 25 ng DT/g bodyweight at weekly intervals, the CTMCs were depleted efficiently in the squamous as well as in the glandular portion of the stomach. CTMC numbers were reduced to 1.46±0.65 mast cells/mm^2 (n=3) corresponding a depletion efficiency of 94.2% compared to control mice (25.1±5.11 mast cells/mm^2, n=2, Fig. 2.24, A (upper and middle panel) and B). In contrast, no significant reduction in MMC numbers could be detected in the mucosal layer (26.13±0.61 mast cells/mm^2 in control animals (n=2) versus 20.63±5.2 mast cells/mm^2 in *A-Mcpt5-Cre iDTR* double positive mice (n=3), Fig. 2.24, A (middle and lower panel) and B). These results indicate that under the control of the *Mcpt5* promoter Cre recombinase is not expressed in mucosal mast cells or in progenitor cells that can give rise to MMCs.

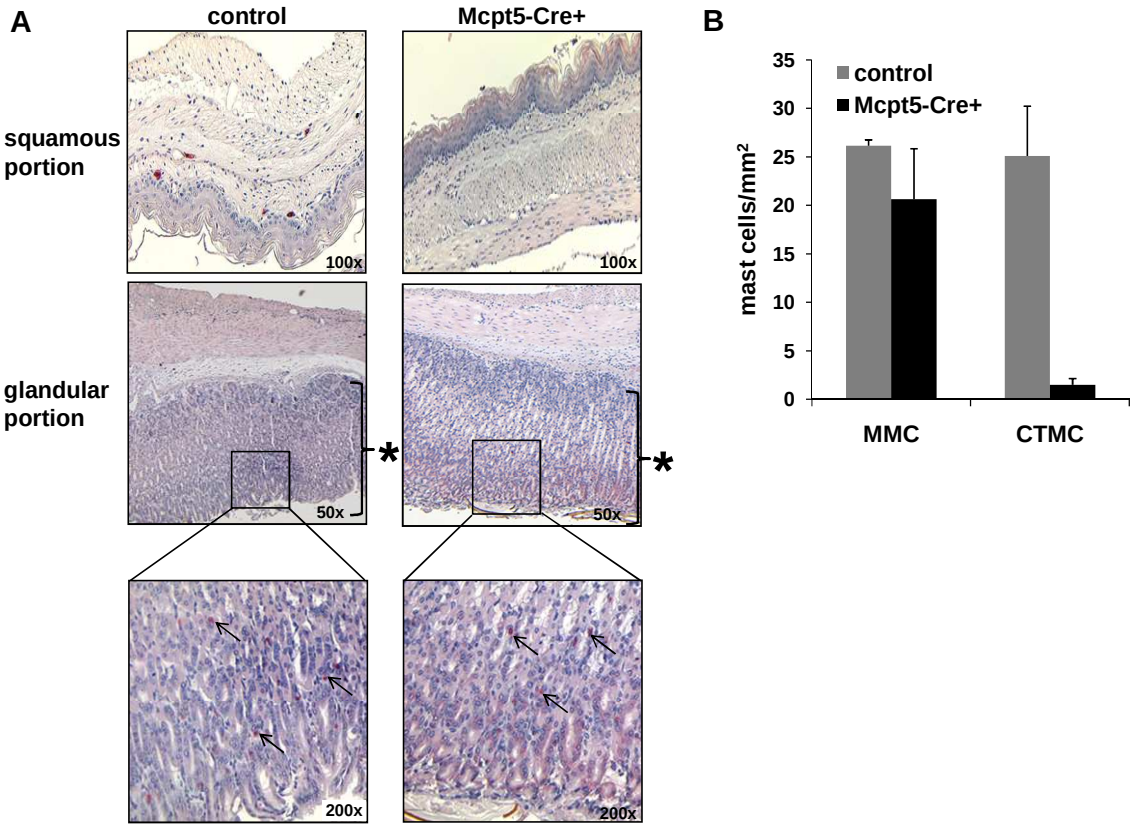

Fig. 2.24 Depletion efficiency of connective tissue mast cells (CTMC) and mucosal mast cells (MMC) in the stomach. Mice were treated with four injections of 25 ng DT/g bodyweight at weekly intervals and were sacrificed seven days after the last injection. The stomach was washed with PBS and fixed with Carnoy's solution. Paraffin sections were stained for chloroacetate esterase. (A) Squamous and glandular portion of either control mice or *A-Mcpt5-Cre iDTR* double positive mice are shown in 100-fold and 50-fold/200-fold magnification, respectively. Asterisks indicate the mucosal epithelium within the glandular portion of the stomach. Arrows indicate to chloroacetate esterase positive MMCs. Pictures were generated using a Leika DM 4000 B microscope. (B) CTMCs in the squamous and glandular portion and MMCs in the mucosal epithelium of the glandular portion were quantified as mast cells/mm^2. Grey bars represent control mice (n=2), black bars represent *A-Mcpt5-Cre iDTR* double positive mice (n=3).

2.2.3 Effect of mast cell depletion on passive systemic anaphylaxis

Anaphylaxis is a life threatening syndrome encompassing symptoms like bronchospasm, hypotension, laryngeal edema and hyperperistalsis. These clinical signs can be caused by the crosslinking of IgE antibodies bound to the high affinity IgE receptor (FcεRI) on mast cells and basophils which triggers the release of histamine, prostaglandins and leukotrienes (Kemp and Lockey, 2002). In order to test whether the ablation of connective tissue mast cells by DT injections also has an effect on a typical mast cell-mediated immune response, like anaphylaxis, the model of passive systemic anaphylaxis was applied to mast cell-depleted mice. In this model, the animals are first sensitized by injection of a monoclonal IgE antibody specific for the allergen dinitrophenyl (DNP). 24 h after sensitization, the mice are challenged with DNP coupled to human serum albumin (DNP-HSA). The transient drop of the body temperature is a widely used indicator of the intensity of the anaphylactic response. *A-Mcpt5-Cre iDTR* double positive mice and *Cre*-negative controls, treated four times with 25 ng DT/g bodyweight at weekly intervals (without pyrilamine), were sensitized with IgE seven days after the last DT injection and were challenged 24 h later with either DNP-HSA or vehicle. The body temperature was measured using a rectal probe before and every ten minutes over a period of three hours after challenging. The *Cre*-negative controls which were challenged with DNP-HSA developed a severe anaphylactic response. Within 20 min the body temperature decreased by 5.3±0.57°C and reached a minimum after 40 min (reduction of 6±1.1°C, Fig. 2.25). On the contrary, mast cell-depleted mice displayed a reduced anaphylactic response. After a drop of the body temperature by 3.3±1.03°C at 20 min after challenging, the double positive mice quickly recovered (Fig. 2.25). While 60 minutes after DNP injection the temperature of controls was still low (33.7±1.55°C), the mast cell-depleted mice almost reached normal temperatures (37.5±0.52°C compared to 38 ±0.35°C before challenging). Depletion efficiency of mast cells was tested in the peritoneal cavity for six of eleven *A-Mcpt5-Cre iDTR* double positive mice. Hardly any peritoneal mast cells (0.035±0.03% of total peritoneal cells) could be detected in these mice reflecting an average depletion efficiency of 98.33%. Since sensitization as well as challenge was applied intraperitoneally, it was expected that peritoneal mast cells are the predominant effectors of this response. These results show that, although peritoneal mast cells were efficiently ablated, the mice still developed a minor anaphylactic response. This residual response may be due to the activation of residual connective tissue mast cells in other tissues, mucosal mast cells or basophils.

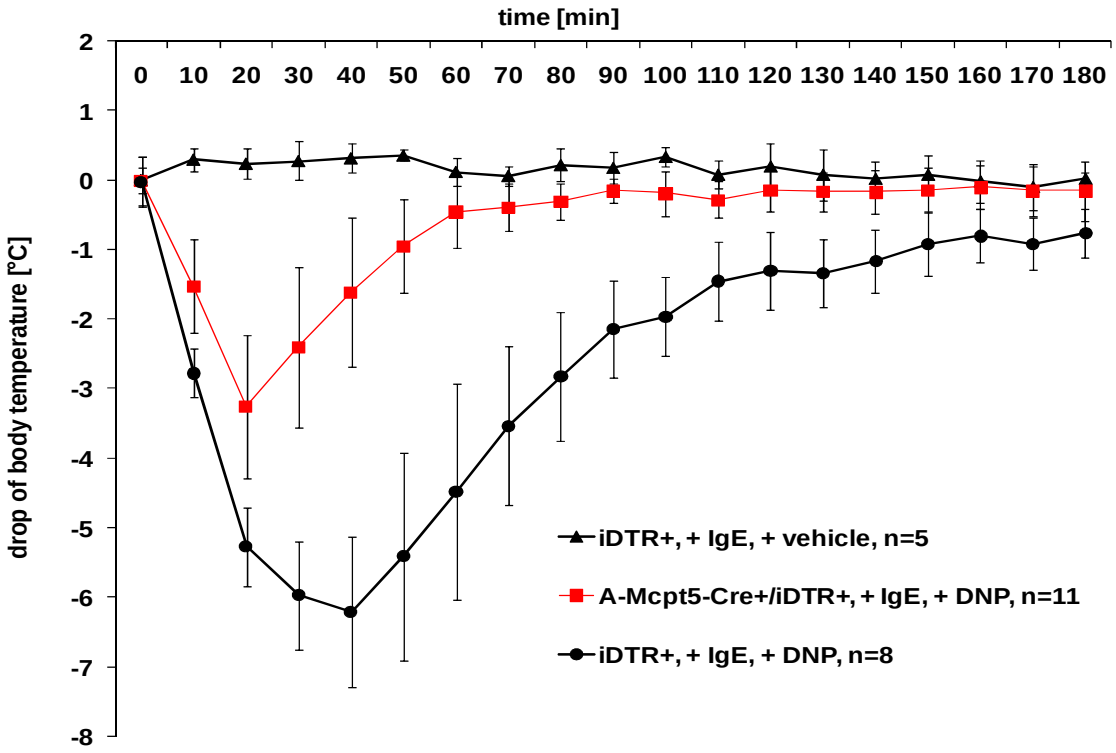

Fig. 2.25 Passive systemic anaphylaxis in mast cell depleted mice. *A-Mcpt5-Cre iDTR* double positive and *Cre*-negative control mice were injected i.p. four times with 25 ng DT/g bodyweight at weekly intervals. Seven days after the last injection, mice were sensitized i.p. with 12.5 µg anti-DNP-IgE. 24 h later, mice were either challenged i.p. with 400 µg DNP-HSA or injected with vehicle (saline). The body temperature was measured using a rectal probe before and every ten minutes after challenge over a period of three hours. For each time point, the drop of body temperature is displayed in each group as the mean reduction of the average body temperature before challenge. Black circles represent control mice treated with vehicle, red squares challenged double positive, mast cell depleted mice and black triangles challenged control mice. Numbers of animals in each group are indicated.

2.2.4 Repopulation of mast cells after DT-induced ablation

Repopulation of peritoneal cavity and skin with mast cells was investigated by FACS analysis of peritoneal lavage fluid and metachromatic staining of sections from skin biopsies. DT-treated *A-Mcpt5-Cre iDTR* double positive mice and *Cre*-negative control animals were sacrificed one (n=3), seven (n=7), 14 (n=4), 21 (n=4), 28 (n=2), 42 (n=2), 56 (n=3) and 84 (n=2) days after the last DT injection and peritoneal cells were isolated. The percentage of $CD117^{+}FcεRI/IgE^{+}$ mast cells of total peritoneal cells was compared to that of control mice (2.1±0.8% mast cells of total peritoneal cells, n=13, Fig. 2.26, A). Surprisingly, we did not observe a significant repopulation of the peritoneal cavity with mast cells within eight weeks after depletion. After an initial increase to 7% of control mast cell numbers three weeks after the last DT injection, the restoration of the peritoneal mast cell numbers seemed to stagnate and reached only 8% after 56 days. (Fig. 2.26, A). Between week eight and twelve, mast cells started to return gradually to 34% of control

mast cell numbers 84 days after the last DT injection. Even though animal numbers for each time point were very low, these results clearly demonstrate that mast cells repopulate the peritoneal cavity in significant numbers only twelve weeks after DT treatment. To further validate the data, more mice and later time points have to be analyzed.

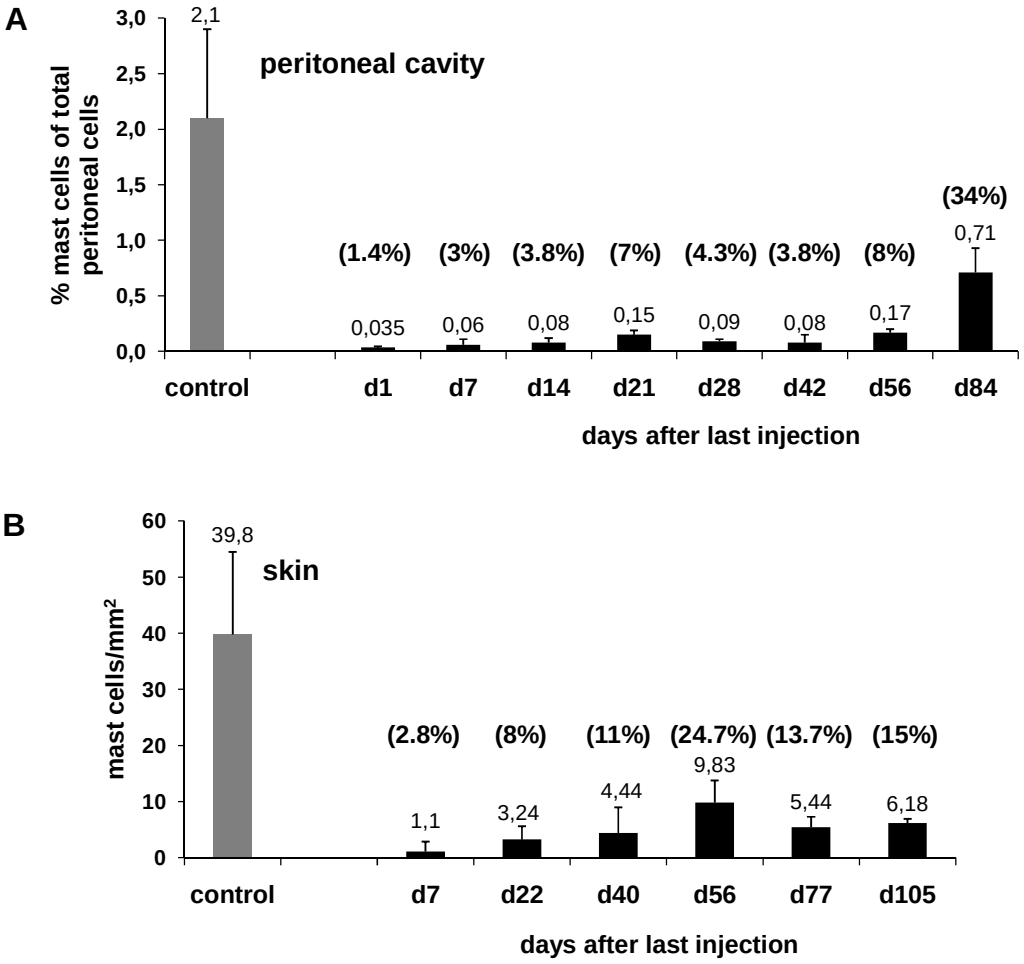

Fig. 2.26 Mast cell repopulation of the peritoneal cavity and skin after DT-induced mast cell ablation. (A) *A-Mcpt5-Cre iDTR* double positive and *Cre*-negative control mice were injected i.p. four times with 25 ng DT/g bodyweight at weekly intervals. Mice were sacrificed one (n=3), seven (n=7), 14 (n=4), 21 (n=4), 28 (n=2), 42 (n=2), 56 (n=3) and 84 (n=2) days after the last injection and peritoneal cells were isolated. Cells were analyzed for the presence of mast cells (defined as $CD117^{+}Fc\varepsilon RI/IgE^{+}$ cells) by flow cytometry. Mast cell numbers were displayed as percentages of total peritoneal cells and compared to those of control mice (n=13). Percentages in parentheses reflect percent mast cells of control mast cell numbers. (B) Numbers of skin mast cells were quantified as mast cells/mm^2 in Giemsa stained paraffin sections of back skin from double positive animals treated with three i.p. injections of 35 ng DT/g bodyweight at weekly intervals. 4 mm punch biopsies from the back skin were taken on day seven, 22, 40, 56, 77 and 105 (n=5 for each time point except d77 with n=4) after the last DT injection. Mast cell numbers in sections of these biopsies were compared to the average mast cell number per mm^2 of back skin of ten *Cre*-negative control animals. Percentages in parentheses reflect percent mast cells of control mast cell numbers.

Similar observations were made in the skin. In order to test the repopulation of skin with mast cells, biopsies from back skin of DT-treated mice were taken at two to four week intervals. For this experiment, mice were used that had received three i.p. injections of 35ng DT/g bodyweight at weekly intervals. Seven days after the last injection mast cell numbers were reduced to 1.1±1.76 mast cells/mm^2 reflecting an average depletion efficiency of 97.2% (n=5, Fig. 2.26, B). Mast cell numbers slightly increased until eight weeks after the last DT injection to 9.83±3.94 mast cells/mm^2. Thus, mast cell numbers were restored to 24.7% on average. For later time points we expected that the gradual increase in mast cell numbers would continue, but surprisingly, three weeks later (77 days after the last DT injection) mast cell numbers decreased again to 13.6% of control numbers (n=4, Fig. 2.26, B). Even 15 weeks after the last injection (d105, n=5) the mast cell numbers remained at the same level (15% of control numbers) demonstrating that the decrease of the mast cell numbers at time point d77 was not due to heterogeneity of mast cell numbers at different sites of the skin from which the biopsies were taken. Future experiments will demonstrate whether at later time points mast cell numbers recover to normal values or whether the induced ablation profoundly disturbed the steady state homeostasis of mast cell populations.

3 Discussion

Mast cells are one of the most versatile cells of the body. They express an enormous spectrum of mediators of which distinct profiles are released dependent on the mode of mast cell activation. Mast cells have been demonstrated to be essential initiators of innate immune responses against pathogens and important modulators of adaptive immunity. Even immunosuppressive mast cell functions were shown. The currently used mouse models for the investigation of mast cell biology, i.e. the reconstitution of *Kit*$^{W/Wv}$ or *Kit*$^{Wsh/Wsh}$ mice with *in vitro* differentiated mast cells derived from gene deficient mice, provided important information, but inherent technical problems limit experimentation and interpretation of the data. In addition, the availability of viable knock-out mice that can serve as a source of cultured mast cells for the reconstitution of mast cell-deficient mice is limited.

This thesis reports the successful generation of mast cell-specific Cre transgenic mouse lines that allow inactivation of genes selectively in mast cells *in vivo*. Two lines express Cre under the control of the *Mcpt5* promoter. The A-Mcpt5-Cre line is characterized by autosomal inheritance of the transgene, while the X-Mcpt5-Cre line shows X-linked inheritance (Scholten et al., 2008). Another two lines express Cre recombinase under the control of the *Mcpt6* promoter. Application of these *Mcpt6-Cre* transgenic lines (A73- and A74-Mcpt6-Cre) might be restricted due to Cre-mediated genotoxic effects on mast cells in these lines. All lines uniformly express Cre recombinase in all connective tissue type mast cells (CTMC) in a highly mast cell-specific manner resulting in efficient deletion of *loxP*-flanked DNA. To examine the mast cell-specific functions of individual genes, a diverse spectrum of mouse lines carrying *loxP*-flanked genes is available for mast cell-specific Cre-mediated mutagenesis *in vivo* using the Mcpt5-Cre lines. The A-Mcpt5-Cre line was applied for the establishment of a new model for inducible mast-cell ablation in adult mice as demonstrated in this thesis. A significant reduction of the mast cell-mediated systemic anaphylactic response in mast cell-depleted animals demonstrated the usefulness of this model for mast cell research. Recently, another Cre line was published by Müsch et al. that reportedly expresses Cre recombinase under the control of a baboon chymase promoter in mucosal mast cells (MMC) of lung and intestine (Müsch et al., 2008). Thus, this strain might complement our system.

3.1 Novel transgenic strains for mast cell-specific Cre-mediated mutagenesis *in vivo*

3.1.1 Design and construction of the transgene

To achieve mast cell-specific Cre-mediated deletion *in vivo*, Cre recombinase has to be expressed under the control of a mast cell-specific promoter. Ideally, a novel Cre-transgenic mouse would allow deletion of genes in all mast cells, i.e. CTMCs as well as MMCs. Promising candidate promoters were the promoters of mast cell protease genes which are abundantly expressed in mast cells while there is little evidence for expression in other cell types. In this thesis, *Mcpt5* and *Mcpt6* promoters were used for the generation of the transgenes. Both proteases, mMCP-5 and mMCP-6, are expressed in CTMCs and also in bone marrow derived mast cells (BMMC) as shown on transcriptional and translational levels (Gurish et al., 1992; Lunderius et al., 2000; Wolters et al., 2001). Other mast cell proteases could be excluded like e.g. mMCP-8, which is predominantly expressed in basophils (Lunderius and Hellman, 2001), mMCP-9, which can be detected in uterine mast cells (Hunt et al., 1997), or mMCP-1 and -2, which are predominantly expressed in MMCs (Pejler et al., 2007). mMCP-4 is considered to be a terminal differentiation marker of CTMCs (Pejler et al., 2007). Thus, Cre expression in a precursor that can differentiate into both, CTMCs and MMCs, seemed unlikely. In addition, mMCP-7 is not expressed in C57BL/6 mice at all due to a point mutation in this strain (Hunt et al., 1996). The *mc-cpa* promoter was not chosen in order to avoid Cre expression in related cell types that we reasoned may occur since the *mc-cpa* is one of the first mast cell protease genes to be expressed during mast cell differentiation (Pejler et al., 2007).

The construction of the transgene was facilitated by the advances in BAC recombineering. The advantage of BAC-based transgenes is that BAC vectors can accommodate large genomic DNA fragments which encompass the entire genomic sequence of a gene of interest (in this work *Mcpt5* and *Mcpt6*) along with abundant flanking sequence containing all *cis*-acting regulatory elements with high probability. In addition, these large molecules, when randomly integrated into the genome, are less, if at all, prone to position effects at the integration site. To drive Cre expression under the control of the *Mcpt5* or *Mcpt6* promoter, only exon 1 of these genes was replaced by the *Cre* cassette avoiding deletion of possible regulatory elements located within the introns of these genes.

Mcpt5 and *Mcpt6* are both encoded in protease gene clusters, *Mcpt5* within the chymase locus on chromosome 14 and *Mcpt6* within the tryptase locus on chromosome 17 (Gurish et al., 1993; Wong et al., 2004) and are, therefore, flanked by several other genes, mostly protease genes, many of which were included in the BAC clones. Given that, most probably, multiple copies of the gene constructs integrate into the genome, it seemed advisable to

remove other genes from the BAC inserts as far as possible in order to avoid effects of altered gene dosage in the transgenic mice. Therefore, the BAC inserts were shortened. In case of the *Mcpt5* containing BAC insert, all known open reading frames could be removed still leaving abundant upstream and downstream sequence flanking *Mcpt5*. In the *Mcpt6* BAC, two genes, *Tpsg1* and *Tpsab1*, encoding for the membrane bound protease mTMT and for mMCP-7, respectively, were located in close proximity of the *Mcpt6* gene and were, therefore, not eliminated. In case of the *Tpsab1* gene, no gene dosage effects were expected as mMCP-7 is not expressed in C57BL/6 mice due to a point mutation (Hunt et al., 1996).
The neighboring chymase and tryptase genes of the original BAC inserts are homologous to each other in variable extend (Gurish et al., 1993; Wong et al., 2004) which may increase the risk of undesired recombination events during the construction process. Therefore, homologous regions for modification of the BAC were carefully chosen to avoid unwanted recombination events and, after the last modification step, i.e. removal of the ER^{T2} cassette, it was essential to test the integrity of the BAC clones. The shortening of the BAC inserts precluded informative comparison of restriction digest patterns of the modified with those of the original BAC clones. Therefore, the integrity of the sequences upstream of the translation start of *Mcpt5* and *Mcpt6* was investigated with Southern blot analysis. Even though, the final constructs had undergone at least five modification steps, integrity of the BAC transgenes within the analyzed regions could be demonstrated. It seems likely that the risk for unwanted recombination had been minimized by the initial elimination of neighboring genes with a high grade of homology.

3.1.2 The *Mcpt5* and *Mcpt6* promoters allow efficient Cre expression in mast cells

The four new Cre transgenic lines demonstrated that the *Mcpt5* and *Mcpt6* promoters allow efficient and cell type-specific expression of Cre recombinase in mast cell since in *Mcpt5-Cre* and *Mcpt6-Cre R26R-EYFP* double positive mice, a Cre-mediated activation of reporter gene expression could be detected in dermal as well as in peritoneal mast cells. These results could be confirmed in the model for inducible ablation of mast cells in *A-Mcpt5-Cre iDTR* double positive mice. In these animals, peritoneal and dermal mast cells as well as CTMCs located in the submucosal layers of the stomach were efficiently depleted reflecting Cre expression in basically all CTMCs located at these anatomical sites. The detection of EYFP reporter gene expression in skin mast cells by flow cytometry was hampered by the low numbers of mast cells in the skin cell suspensions. However, in *A-Mcpt5-Cre/iDTR* mice treated with high dosages of diphtheria toxin (DT), it could be demonstrated that all skin mast cells are susceptible to DT-induced cell depletion and, therefore, must express Cre. In the X-Mcpt5-Cre line, females showed Cre-mediated recombination in only about half of the mast

cells most likely due to random inactivation of the X-chromosome carrying the transgene. Incomplete inactivation of particular genes may be advantageous if an attenuation of a severe phenotype is desired.

Importantly, in *Mcpt5-Cre iDTR* double positive mice treated with DT, CTMCs of the stomach were efficiently depleted whereas the MMCs within the mucosal epithelium were still present. This result clearly demonstrates that the *Mcpt5* promoter is not active in MMCs and neither in mast cell progenitors that can give rise to both, CTMCs and MMCs. This result was unexpected since *Mcpt5* expression was demonstrated on the RNA and protein levels in BMMCs as well as on RNA level in BMCPs, a common precursor for basophils and mast cells, found in the spleen of adult mice (Arinobu et al., 2005). Both, BMMCs and BMCPs, were shown to give rise to CTMCs as well as MMCs *in vivo (Arinobu et al., 2005; Nakano et al., 1985)*. Therefore, we expected to observe Cre-mediated recombination in both mast cell populations in Mcpt5-Cre mice. However, only a small portion of BMMCs showed Cre-mediated activation of reporter gene expression in all four Cre lines (A- and X-Mcpt5-Cre as well as A73- and A74-Mcpt6-Cre) after eight weeks of culture. These results were supported by a report about expression and localization of mMCP-5 in secretory granules of BMMCs. The analysis of cytospins of an eight week old BMMC culture revealed mMCP-5 only in BMMCs carrying electron dense granules which could be detected only in a fraction of BMMCs (McNeil et al., 1992a). Various reports suggest that the classification of murine mast cells into two subpopulations, with CTMCs expressing the proteases mMCP-4, -5, -6 and MC-CPA and MMCs expressing mMCP-1 and -2, may be too static. Friend et al. could show that mast cells can change their protease expression pattern during infection with the helminth *Trichinella spiralis*. In addition to the mast cell populations expressing either mMCP-5 or mMCP-1 and -2, these authors detected populations with a transitional phenotype displaying either mMCP-5 and mMCP-2 or mMCP-2 expression alone (Friend et al., 1996). Furthermore, the typical localization of these cell populations can deviate during immune responses. In a model for colon cancer that suggests an important role for mast cells in tumor formation, mMCP-6 but also mMCP-2 positive mast cells were found abundantly within the mucosal epithelium of the polyps in $Rag^{-/-}$ mice (animals devoid of T and B cells) (Gounaris et al., 2007). Whether these mMCP-6 expressing cells are MMCs with an altered protease pattern or CTMCs that moved into the epithelial layer was not determined. However, both examples, *T. spiralis* injection and polyp formation, show that protease expression is not necessarily restricted to a distinct mast cell population and that both, Mcpt5- and Mcpt6-Cre mice, may be useful also in the elucidation of mast cell functions during immune responses at the mucosal surfaces.

3.1.3 Cre-mediated deletion is restricted to mast cells

Analysis of hematopoietic cells other than mast cells revealed that the *Mcpt5* and *Mcpt6* promoters are highly specific for mast cells. When choosing these promoters, we were aware of the risk of non-mast cell-specific Cre expression in cell types that share a common precursor with mast cells. Until today it is controversially discussed whether committed mast cell progenitors (MCP) are directly derived from multipotential progenitors in the bone marrow (Chen et al., 2005) or whether they can originate from myeloid precursors (Arinobu et al., 2005). In the hands of Arinobu et al. the common myeloid progenitor (CMP) as well as the granulocyte/monocyte progenitor (GMP) could also differentiate to mast cells. The absence of Cre expression in cells of the myeloid lineage in Mcpt5- and Mcpt6-Cre mice argued against expression of mMCP-5 and -6 in CMPs or GMPs. Furthermore, Arinobu and coworkers detected a basophil/mast cell progenitor (BMCP) in the spleen. In culture, these cells, defined as $Lin^{-}c\text{-}Kit^{+}Fc\gamma RII/III^{hi}\beta7^{hi}$, exclusively gave rise to committed MCP and basophil progenitor cells (BaP) which differentiated into mast cells and basophils, respectively. They found *Mcpt1* and *Mcpt5* mRNA in BMCPs as well as in MCPs suggesting that an expression of the Cre recombinase in these progenitor cells had to be expected in *Mcpt5-Cre* transgenic mice, in which case Cre-mediated deletion of *loxP*-flanked sequences would occur not only in mast cells but also in basophils. Interestingly, splenic basophils did not display any Cre-mediated activation of reporter gene expression. Additionally, in *A-Mcpt5-Cre iDTR* double positive mice treated with DT basophils were still present in normal numbers. Therefore, the detection of *Mcpt5* RNA in BMCPs might reflect a fraction of these cells that already is committed for mast cells or the activity of the *Mcpt5* promoter is too low for successful Cre-mediated recombination. Given that BMCPs also can supply the intestine with MCPs which differentiate into MMCs, it is more likely that the *Mcpt5* promoter is active at low level that is not able to drive Cre expression at levels necessary for Cre-mediated recombination.

The only notable Cre expression outside the mast cell compartment was detected in NK cells of Mcpt5-Cre but not in Mcpt6-Cre mice. NK cells were identified either as CD49b/NKG2D double positive or NKG2D single positive cells. About 9% of the $CD49b^{+}NKG2D^{+}$ subset of NK cells displayed Cre-mediated recombination while in less than 1% of NKG2D single positive cells reporter gene expression could be detected. The $CD49b^{+}$ NK cells represent a subset that is characterized by a high cytotoxic activity while CD49b is down regulated in proliferating NK cells (Arase et al., 2001). This suggests that mMCP-5 is up regulated in a fraction of activated NK cells.

All mice designated as A-Mcpt5-Cre are progeny of a single F1 animal derived from the original founder. However, the progeny of another F1 animal displayed non-specific Cre-mediated recombination in variable fractions of all non-mast cell populations analyzed. This

finding could reflect a chimerism of the founder animal. Two independent integrations might have occurred in the embryo in two different cells that both gave rise to germ cells. The additional transgene present in the unspecific substrain may have been subject to position effects that lead to ubiquitous expression of the transgene. In contrast, no unspecific reporter gene expression (except for the small fraction of the NK cell subset described above) could be detected in the substrain finally designated as A-Mcpt5-Cre.

3.1.4 Absence of Cre-mediated genotoxicity in Mcpt5-Cre mice

The Cre recombinase has been shown to mediate genotoxicity in some Cre transgenic or Cre knock in mice. Mammalian genomes contain cryptic or pseudo *loxP* sites which occur with an estimated frequency of 1.2 per megabase and which can serve as functional recognition sites for Cre (Schmidt-Supprian and Rajewsky, 2007). Permanent and high levels of Cre expression can, therefore, cause growth arrest or even cell death. Thus, the difficulty in *Cre* transgenic animals is to achieve Cre expression levels high enough for efficient Cre-mediated deletion of *loxP*-flanked target genes but low enough to avoid Cre-mediated genotoxicity. Even though the protease mMCP-5 is abundantly expressed in mast cells, in *Mcpt5-Cre* mice we found no difference in mast cell numbers or proliferation of mast cells *ex vivo* in response to stem cell factor indicating that Cre-mediated genome damage is not a prominent feature of these mice. Two factors could contribute to this finding. First, the transgene contains a *loxm2* site and, therefore, Cre-mediated recombination should reduce transgene copy number. This may result in initial high levels of Cre expression with subsequent reduction of Cre activity. Second, the analysis of the *Mcpt5* promoter suggests a silencer located between 470 bp and 2200 bp upstream of the transcription start. The expression of a luciferace reporter gene in a plasmid containing only the first 470 bp of the promoter was 30-fold higher than in a plasmid containing 2200 bp of the promoter region (Morii et al., 1997). Thus, the presence of a silencer and the reduction of copy numbers after Cre expression may result in ideal Cre expression levels.

In *Mcpt6-Cre* mice, the proliferative potential *ex vivo* has not been analyzed yet. However, the reduced frequency of mast cells in the peritoneal cavity of these mice could be due to Cre-mediated genotoxicity. Like the *Mcpt5-Cre* transgene, also the construct for the *Mcpt6-Cre* mice contains a *loxm2* site and one can, therefore, expect a similar reduction of copy numbers upon Cre expression as described above. The presence of a potential silencer element like in the *Mcpt5* promoter is not known (Morii et al., 1996; Ogihara et al., 1999). In the case of significant Cre-mediated genotoxicity potential applications of the Mcpt6-Cre lines will be limited. However, DT-mediated mast cell ablation may be particularly efficient in these mice which will, therefore, be crossed to the iDTR strain.

3.1.5 Attempt to generate mice with inducible, mast cell-specific Cre activity

In contrast to the mast cell-specific Cre lines with constitutively active Cre recombinase, no functional founder line for tamoxifen-inducible Cre recombinase activity could be identified. Since it is known that orally administered tamoxifen is metabolized in the liver to 4-OH-tamoxifen (Kamal and Goetz, 2007) which has a high affinity to the CreER^{T2} domain (Feil et al., 1997), it was expected that tamoxifen treatment will result in Cre activity in mast cells. To rule out that the CreER^{T2} cassette was non-functional, e.g. due to disturbed folding of the Cre polypeptide in the presence of the ER^{T2} domain, we deleted the *ER^{T2}* cassette by Flp-mediated recombination *in vivo.* However, also offspring from Mcpt5-CreER^{T2} R26R-EYFP Flp-deleter breedings did not show any or only very low reporter gene expression in peritoneal mast cells. Constitutive expression of Flp recombinase in the mice most likely results in a reduction of transgene copy numbers since *frt* sites of neighboring copies will recombine. This reduction of transgene copies may contribute to a low level of Cre expression. Thus, it is difficult to assess whether the inefficient Cre-mediated reporter gene activation was due to inefficient induction of Cre activity by tamoxifen application or whether the transgenes were not functional. Since after tamoxifen administration, significant reporter gene expression could not be detected in any of the animals, it is more likely that Cre expression from the transgenes was too low to drive tamoxifen-induced Cre-mediated recombination. This inefficiency could be due to the integration of truncated constructs or to position effects at the integration site. In conclusion all five *Mcpt5-CreER^{T2}* transgenic lines have been considered as non-functional and new founder lines will be generated.

3.2 A new model for inducible ablation of mast cells *in vivo*

The relevance of mast cells in innate as well as in adaptive immune responses has been investigated using mast cell-deficient *Kit$^{W/Wv}$* and *Kit$^{Wsh/Wsh}$* mice in most *in vivo* studies. These models suffer inherent technical limitations as described above. Alternatively, inducible ablation of mast cells was achieved by the administration of antibodies directed against the c-Kit receptor which abrogated the survival signal mediated by SCF (Brandt et al., 2003; Gekara and Weiss, 2008). As c-Kit is also expressed on hematopoietic progenitor cells, other hematopoietic lineages are invariably affected especially by long-term administration of the anti-c-Kit antibody (Gekara and Weiss, 2008). Therefore, mast cell research would benefit considerably from new models of mast cell deficiency that are not dependent on compromised Kit function. The availability of a mouse strain for conditional expression, i.e. controlled by Cre-mediated recombination, of a diphtheria toxin receptor (DTR) under the control of the *ROSA26* promoter (Buch et al., 2005) and of the novel mast cell-specific Cre

transgenic mouse lines generated in the setting of the present thesis, provided a possibility to inducibly ablate mast cells in adult mice without affecting other hematopoietic cell populations. In the second part of this thesis it could be demonstrated that in diphtheria toxin (DT) treated *A-Mcpt5-Cre iDTR* double positive mice, connective tissue type mast cells can be efficiently depleted. Interestingly, the recovery of the mast cell populations in the tissues was very slow. Thus, this system provides a useful tool for the investigation of mast cell functions even in long-term experiments.

3.2.1 Efficient ablation of connective tissue mast cells in adult mice

The DTR-based system for inducible ablation of cell populations has been successfully applied by other groups for depletion of hematopoietic cell populations like T cells, B cells (Buch et al., 2005), dendritic cells (Jung et al., 2002), Langerhans cells (Bennett et al., 2005) or regulatory T cells (Lahl et al., 2007). The regimens for the DT treatment differ depending on the target cell type. While efficient ablation of T or B cells required multiple administrations of DT, splenic dendritic cells as well as Langerhans cells were efficiently ablated within 24 h after a single DT injection. In *A-Mcpt5-Cre iDTR* double positive mice, close to 100% of peritoneal mast cells were depleted 24 h after a single DT injection, while skin mast cells were not affected at that time point. The depletion efficiencies obtained using the various injection protocols suggested that ablation of skin mast cells requires high doses of the toxin and that skin mast cells undergo DT induced apoptosis with a slow kinetic. The administration of high DT doses at short intervals caused clinical signs like lethargy, hunch back and substantial weight loss and finally resulted in lethality consistent with observation of Jung and coworkers (Jung et al., 2002). This lethality probably results from a systemic inflammatory response due to contamination of the DT solution by endotoxins or from DT effects mediated by the low affinity mouse DTR. While toxic and, therefore, not applicable for most experimental questions, the highly efficient ablation of even skin mast cells achieved by high DT doses showed that, in principle, all skin mast cells can be ablated demonstrating that close to 100% of mast cells in the skin express Cre recombinase under the control of the *Mcpt5* promoter. In the ear pinna mast cell depletion was most difficult, but with high DT dosages basically all mast cells could be eliminated at this location (data not shown) ruling out the possibility that the mast cell population in the ears do not express Cre. Our final injection regimen with four injections of 25 ng DT/g bodyweight at weekly intervals resulted in efficient depletion of skin mast cells, but did not cause macroscopically evident disease. Whether skin mast cells are less sensitive to the toxin or whether toxin delivery into the skin is inefficient is not clear. The efficient depletion with high doses supports the assumption of pharmacokinetic problems. However, Bennett and coworkers were able to deplete Langerhans cells (that reside in the epidermis) with a single i.p. injection of 16 ng/g bodyweight within 24 h (Bennett et al., 2005). It is known that DT induces apoptosis in

proliferating as well as in non-proliferating cells (Saito et al., 2001) indicating that the resting phenotype of skin mast cells is not the reason for the slow depletion.

With the final injection protocol, i.e. four times 25 ng/g bodyweight at weekly intervals, neither control nor double positive animals showed any macroscopic signs of slowly progressive disease observed after high dosage administration. However, some few and exclusively *Cre*-positive animals died within three days after the first injection. This sporadic lethality was most likely due to release of mediators from the dying mast cells that caused anaphylaxis. This assumption was supported by a successful prevention of this problem by administration of the H1-antagonist pyrilamine together with the first DT injection. The H1-antagonist reliably prevented death after the initial DT application. Mast cell degranulation upon DT exposure *in vivo* will be verified in future experiments by testing for degranulation markers in peritoneal lavage fluid, like e.g. β-hexosaminidase. An interference of pyrilamine treatment with experimental results is not expected since experiments will in general be started about four weeks after the injection of the H1-antagonist along with the first DT administration. Moreover, pyrilamine has a short half life of less than 24 hours (Kelly and Slikker, 1987).

Buch et al. raised the question whether repetitive DT injections induce a humoral response against the toxin. They demonstrated a moderate antibody response that was without neutralizing effect (Buch et al., 2005). Consistent with these results, we found that even the fourth DT injection three weeks after the first treatment further improved the depletion efficiency ruling out an antibody response with neutralizing effect in this regimen of DT application.

In summary, the Mcpt5-Cre/iDTR system allows reliable depletion of CTMC without affecting other cell types and without significant toxicity when using a single dose of an H1-antagonist along with the first DT treatment. Thus, this model for inducible ablation of mast cells in adult mice provides a useful and versatile tool for the investigation of mast cell functions.

3.2.2 Reduced anaphylactic response in mast cell-depleted animals

Anaphylaxis is an acute, life-threatening allergic reaction most commonly triggered by antigen crosslinking of IgE bound to the high affinity IgE receptor (FcεRI) on mast cells and is characterized by a systemic release of mediators like histamine, leukotrienes and prostaglandins. In the model for IgE-mediated passive systemic anaphylaxis, mice are sensitized by injection of an IgE antibody directed against an allergen resulting in loading of FcεRI with antigen-specific IgE. Upon antigen encounter, FcεRI are crosslinked via IgE and trigger the degranulation of mast cells. In the mast cell depleted *A-Mcpt5-Cre/iDTR* transgenic mice, we observed a significantly impaired anaphylactic response as compared to controls. However, the anaphylactic response was not completely abolished. This was most likely not due to low efficiency of CTMC depletion because efficient ablation of peritoneal mast cells was demonstrated in those mice. This finding raised the question whether residual

mast cells in other tissues than the peritoneal cavity, foremost MMCs, and/or other cell types are the reason for the residual anaphylactic response.

Choi et al. showed that mast cells were dispensable in a model of IgE-mediated active fatal anaphylaxis induced by penicillin V in *Kit*$^{W/Wv}$ mice (Choi et al., 1998). Since FcεRI in the mouse is exclusively expressed on basophils and mast cells (Kawakami and Galli, 2002), basophils were most likely the mediators of the anaphylactic response in the model of Choi and coworkers. In contrast, in another model of anaphylaxis an anti-IgE monoclonal antibody (mAb) failed to induce anaphylaxis in mast cell-deficient mice (Strait et al., 2002). In the same study it was demonstrated that MMCs respond with degranulation to anti-IgE mAb as assessed by increased serum levels of mMCP-1. In conclusion, in DT treated *A-Mcpt5-Cre iDTR* double positive mice which are basically devoid of CTMCs but have normal MMC and basophil numbers it seems likely that both cell types contribute to the residual anaphylactic response. Our result clearly demonstrates that the selective depletion of CTMCs has a significant impact on the anaphylactic response and that basophils and MMCs are not sufficient to completely substitute CTMC functions in this model.

3.2.3 Slow recovery of mast cell populations after induced ablation

The iDTR/DT system has been used previously for the ablation of other hematopoietic cell populations like dendritic cells, Langerhans cells and macrophages. In these models the DTR was expressed under the control of the *CD11c* promoter (Jung et al., 2002), *langerin* promoter (Bennett et al., 2005; Kissenpfennig et al., 2005) or *CD11b* gene regulatory elements for macrophage specific DTR expression (Cailhier et al., 2005). The restoration of these cell types after DT-mediated ablation was found to occur within six days for splenic dendritic cells and about four days for peritoneal macrophages after a single DT injection. While Bennett et al. reported that Langerhans cells do not repopulate the epidermis during four weeks after a single injection of DT, Kissenpfennig et al., who independently generated another langerin-DTR strain, demonstrated that Langerhans cell depletion persisted for only six to seven days.

We found that peritoneal mast cells did not repopulate the peritoneal cavity significantly before twelve weeks. Eight weeks after the last DT injection only 8% of normal mast cell numbers were found while after twelve weeks mast cell numbers reached 34% of normal.

The restoration of skin mast cells was even slower than the repopulation of the peritoneal cavity. Mast cell numbers in the skin gradually increased until eight weeks after DT treatment to 25% of normal mast cell numbers. But, unexpectedly, at the following two time points, i.e. eleven and 15 weeks, mast cell numbers substantially decreased again to only 13-15% of normal numbers. The consistent results for the week eleven and 15 demonstrated that the decline after eight weeks was not due to heterogeneity of mast cell numbers at the different sites of back skin from which the biopsies were taken. The decline after day 56 may suggest

an exhaustion of progenitor cells in the skin. The source of progenitors for the mast cell repopulation may be the multipotent stem cells residing in the bulge region of hair follicles (in case of skin repopulation (Kumamoto et al., 2003)), bone marrow or spleen, anatomical sites demonstrated to be reservoirs for mast cell progenitors (Arinobu et al., 2005; Chen et al., 2005; Pennock and Grencis, 2004). Upon infection of mice with either *Schistosoma mansoni* (Khalil et al., 1996) or *Trichinella spiralis* (Arinobu et al., 2005), an expansion of progenitors in the bone marrow and spleen has been detected. Whether an enlargement of these progenitor pools is also evident after induced mast cell depletion remains to be determined. The signals that are responsible for the recruitment of progenitors from these reservoirs are largely unknown. An important factor known to regulate mast cell numbers is SCF (Galli et al., 1994; Shelburne and Ryan, 2001). This is reflected in the absence of mast cells in the Kit receptor mutant (*Kit*$^{W/Wv}$ and *Kit*$^{Wsh/Wsh}$) or SCF mutant (*Sl/Sl*^{d}) mice. SCF is, therefore, a good candidate to locally act as a chemoattractant for mast cell precursors in the various tissues. In accordance with this concept, Tsai and coworkers demonstrated that the intradermal injection of SCF into mast cell-deficient Sl/Sl^{d} mice resulted in accumulation and proliferation of mast cells in the skin reflecting the recruitment, proliferation and/or maturation of mast cell progenitors (Tsai et al., 1991). In DT-treated mast cell-depleted mice the presence of SCF in the skin as well as the effects of recombinant SCF injected into the dermis has to be investigated in future experiments. Usually this growth factor is expressed in the skin as a transmembrane protein on keratinocytes that can be cleaved by mast cell chymases to its soluble form, which is as bioactive as the membrane bound form (Longley et al., 1997). Tomimori et al. demonstrated that the accumulation of mast cells in a model of dermatitis was abolished by application of chymase inhibitors and that the intradermal injection of a chymase resulted in an increased mast cell density (Tomimori et al., 2002b). Longley et al. and Tomimori et al., therefore, suggest that the release of chymases by mast cells represents a positive feedback loop in which increased amounts of soluble SCF boost mast cell proliferation and/or precursor recruitment and maturation and that this positive feedback might promote the pathogenesis for example of mastocytosis and various forms of inflammatory skin disease. Apart from the suggested pathological role of chymases, this mechanism may also play a role in the steady state homeostasis of mast cells in the skin. On the basis of these observations one can hypothesize that in DT-treated mice, a decline of released chymases might result in a reduction of soluble SCF that is necessary for the recruitment of progenitor cells.

The induction of dermatitis in *Kit*$^{W/Wv}$ mice by epicutaneous administration of phorbol 12-myristate 13-acetate (PMA) results in the development of mature mast cells in the skin at the treated site in this mast cell-deficient strain but not in Sl/Sl^{d} mice (Gordon and Galli, 1990b) demonstrating again that SCF is essential for the recruitment and maturation of mast cell

progenitors. Mast cell development in *Kit*$^{W/Wv}$ mice after induction of immune responses was also observed by other groups (Metz et al., 2007). Thus, it will be interesting to investigate whether repopulation of the skin and peritoneal cavity of DT-treated mast cell-depleted mice will be accelerated under inflammatory conditions. In future experiments using our Mcpt5-Cre/iDTR system it will be of great importance to assess whether an accumulation of mast cells occurs at sites of inflammation in the mast cell-depleted mice. In that case the DT treatment could be intensified and prolonged or DT could also be applied locally since we have shown that local administration results in highly efficient ablation of mast cells (data not shown).

Our new system for inducible ablation of mast cells represents a useful tool for the investigation of mast cell functions. The persistence of mast cell depletion makes the model suitable for long-term experiments. In addition, the A-Mcpt5-Cre/iDTR system should allow new insights into the mechanisms of steady state homeostasis of mast cell populations and mast cell homing to tissues in healthy mice and mast cell recruitment during immune responses.

4 Materials and Methods

4.1 Chemicals and enzymes

Unless otherwise specified, all standard chemicals were purchased from Roth (Karlsruhe), Merck Biosciences (Darmstadt), Serva (Heidelberg) or Sigma-Aldrich (München).
Restriction endonucleases, Taq polymerase, Shrimp Alkaline Phosphatase (SAP), Exonuclease I and Proteinase K including the respective buffers were obtained from NEB (Frankfurt am Main) or Fermentas life sciences (St. Leon-Rot).

4.2 Bacterial cell culture

4.2.1 LB (Luria Broth) medium and agar

1% peptone (w/v), 0.5% yeast extract (w/v), 1% NaCl (for high salt) or 0.5% NaCl (for low salt) (w/v), optional 1.5% Select Agar (w/v) (for LB agar plates, Invitrogen, Karlsruhe) in ddH_2O

4.2.2 Antibiotics

All antibiotics were purchased from Sigma except zeocin (InvivoGen, Toulouse).

antibiotic	stock solutions	final concentration for low copy vectors	final concentration for high copy vectors
chloramphenicol	30 mg/ml in 100% ethanol	15 µg/ml	50 µg/ml
ampicillin	100 mg/ml in ddH_2O	50 µg/ml	100 µg/ml
tetracycline	10 mg/ml in 75% ethanol	3 µg/ml	10 µg/ml
kanamycin	30 mg/ml in ddH_2O	15 µg/ml	50 µg/ml
zeocin	100 µg/ml in ddH_2O	25 µg/ml in low salt LB medium	

Table 4.1 Antibiotics applied for BAC modification and subcloning. The final concentration in LB medium as well as in LB agar plates is dependent on the copy number of the extra-chromosomal DNA except for zeocin that was always used in a concentration of 25 µg/ml.

4.2.3 *Escherichia coli* (*E. coli*) strains

E. coli strain	genotype
DH10B	F- *mcr*A Δ(*mrr-hsd*RMS-*mcr*BC) φ80*lac*ZΔM15 Δ*lac*X74 *rec*A1 *end*A1 *ara*D139 Δ (*ara*, *leu*)7697 *gal*U *gal*K λ- *rps*L *nup*G /pMON14272 / pMON7124
HS996	F- *mcr*A ∆(*mrr-hsd*RMS-*mcr*BC) φ80*lac*ZΔM15 Δ*lac*X74 *rec*A1 *deo*R *ara*D139 Δ(*ara-leu*)7697 *gal*U *gal*K *rps*L (StrR) *end*A1 *nup*G *fhu*A::IS2
DH5α	F- φ80lacZΔM15 Δ(lacZYA-argF) U169 recA1 endA1 hsdR17 (rk-, mk+) gal-phoA supE44 λ- thi-1 gyrA96 relA1

Table 4.2 *E. coli* strains used in this thesis as hosts for smaller plasmids or BAC vectors. DH10B were the BAC hosts for the clones purchased from the RZPD, HS996 was kindly provided by Youming Zhang (Gene Bridges) and DH5α were purchased from Invitrogen.

4.3 Oligonucleotides

Table 4.3 Oligonucleotides used in this thesis were purchased from Metabion (Martinsried)

No.	name	sequence	template
Sequencing of Cre and genotyping of Mcpt5-Cre, Mcpt6-Cre and Mcpt5-CreER^{T2} mice			
P1	Mcpt5-CreUP	5'ACAGTGGTATTCCCGGGGAGTGT	*Mcpt5* promoter
P2	Mcpt6-CreUP	5'AGACTCCTGGGATGAACCTGCCCT	*Mcpt6* promoter
P3	CreSeq1b-DO	5'GTCAGTGCGTTCAAAGGCCA	*iCre*
P4	Mcpt5-Ex1-DO3	5'GCTTTGGTGCTGGAACCCAGGA	*Mcpt5* Exon1
P5	Mcpt5-Ex1seq-DO	5'TGAGAAGGGCTATGAGTCCCA	*Mcpt5* Intron1
P6	CreSeq1-UP	5'CCCTGGTGATGAGGAGAATC	*iCre*
P7	CreSeq2b-DO	5'CCATGTCCCTGGCAGCACCCA	*iCre*
P8	CreSeq2-UP	5'GCCTGATCTATGGTGCCAAGG	*iCre*
P9	CreSeq3b-DO	5'CCACAAAGCCTGGCACCCTCTTC	*ER^{T2}*
P10	CreSeq3-UP	5'CCAGACCCTTCAGTGAAGCT	*ER^{T2}*
P11	CreSeq4b-DO	5'CCTCCAGCAGCAGGTCATAGAG	*ER^{T2}*
P12	CreSeq4-UP	5'CCCACATCAGGCACATGAGT	*ER^{T2}*
P13	CreSeq5b-DO	5'GGATCTCCATTCGCCATTCAG	SV40 *PolyA*
P14	CreSeq5-UP	5'GCACATCCCCCTTTCGCCA	SV40 *PolyA*
Test for full length integration in Mcpt6-Cre founder mice			
P15	AmpTest-UP	5'GTGCGCGGAACCCCTATTTG	*ampicillin* resistance cassette
P16	AmpTest-DO	5'GGTCCTCCGATCGTTGTCAGAAG	
P17	ZeoTest-UP	5'GGAAGTTCGTGGACACGACCTC	*zeocin* resistance cassette
P18	ZeoTest-DO	5'GCACAGTCAAGGCCGAGAATG	
Genotyping of mouse strains other than Mcpt5- and Mcpt6-Cre mice			
P19	ROSA26-UP	5'CCAAAGTCGCTCTGAGTTGTTATC	*ROSA26* promoter
P20	R26stopDO1	5'GCGAAGAGTTTGTCCTCAACC	*STOP* cassette
P21	ROSA26-DO2	5'GGAGCGGGAGAAATGGATATG	wt *ROSA26* locus
P22	Flp-UP	5'CACTGATATTGTAAGTAGTTT	*Flp* gene
P23	Flp-DO	5'CTAGTGCGAAGTAGTGATCAG	*Flp* gene
P24	DelCre-UP	5'GAAAGTCGAGTAGGCGTGTACG	*CMV* promoter
P25	DelCre-DO	5'CGCATAACCAGTGAAACAGCAT	*nlsCre*
P26	iDTR-UP1	5'GGAAAGTCCGTGACTTGCAAGAG	*iDTR*
P27	iDTR-DO	5'TCAGTGGGAATTAGTCATGCC	*iDTR*
Sequencing of the promoter region of *Mcpt5* and *Mcpt6* genes			
P28	M5ProSeq1-UP	5'CATATTTGGGCCTTAGGCTTATTACTC	*Mcpt5* promoter
P29	M5ProSeq1-DO	5'GGATGGTTAAGCAGAAAGGACCC	
P30	M5ProSeq2-UP	5'CCTGAAAGAGAAGAGATGGCATG	
P31	M5ProSeq2-DO	5'GCCAAGAGATATAAGCCAATGCTG	
P32	M5ProSeq3-UP	5'GCTCTGCATCGGTGAGAGCAAGC	
P33	M5ProSeq3-DO	5'CCCAACAGGCTTACAATGATGTAC	
P34	M5ProSeq4-UP	5'CCCAGTGTTCCAAGACATGAG	
P35	M5ProSeq4-DO	5'CCCCATCTGTTCTTCTGACAC	
P36	M5ProSeq5-UP	5'CCTTCCTAAAAATGTTTCCAGAGCTAC	
P37	M5ProSeq5-DO	5'CTTCTAACGGTCATGCTTAGGCAC	
P38	M5ProSeq6-UP	5'CTGCATGTGTCCCTCGCTGACC	
P39	M5ProSeq6-DO	5'GTGAAATACAAATCAGAGACAGGAGCG	
P40	M5ProSeq7-UP	5'CCTCTGCTAAGAAAAGACACCGCTC	
P41	M5ProSeq7-DO	5'CAGAAGGATGCCTGAGTTGGAC	

P42	M6ProSeq1-UP	5'GCATTTCCTTGGGCATTTCACCGC	
P43	M6ProSeq1-DO	5'CATCTGGAAGCAGTGAGGAGCAC	
P44	M6ProSeq2-UP	5'GCTGATGAAATGCTCTATGAAGGG	
P45	M6ProSeq2-DO	5'GGAAAGGGGTATCTTCTGAGGG	
P46	M6ProSeq3-UP	5'CAGAATTCTTGGGAGTACTAGGAG	
P47	M6ProSeq3-DO	5'GAGGGGGGTGGGTATCAGAC	
P48	M6ProSeq4-UP	5'GCATCCAGCAGCCCTGAATTCTG	*Mcpt6* promoter
P49	M6ProSeq4-DO	5'CCTGCATGCACCATTGAATCG	
P50	M6ProSeq5-UP	5'CTAGGCAGTCCTTGATCCGACC	
P51	M6ProSeq5-DO	5'GGCTGATAACCTCACTCTGAGTC	
P52	M6ProSeq6-UP	5'CCAGACCATGAGGTTGTGTGC	
P53	M6ProSeq6-DO	5'GTGTAGGACAGTGACTTAGCTATCC	
P54	M6ProSeq7-UP	5'GGCCTTGAGTGTTCAGCCAATGAG	
P55	M6ProSeq7-DO	5'GGGTCATTAGCTGTCATACAGTC	
Generation of the probes for Southern blot analysis			
P56	M5Probe1-UP	5'CTGGATAAGAGTTAGAAGTCTCAG	
P57	M5Probe1-DO	5'GCCCTGCCTAGAGTCAGGTAATG	
P58	M5Probe2-UP	5'GCCCAGAGATGGTCCCACCCA	
P59	M5Probe2-DO	5'CCTGCCACTAGCTCCACAGGT	
P60	M5Probe3-UP	5'CGGTCTATTTCCCCACAGGCT	
P61	M5Probe3-DO	5'CCCTAACGTCCGTCCAATGGTC	insert DNA upstream of *Mcpt5*
P62	M5Probe4-UP	5'CCCAGACATCCTGTACCTGGT	
P63	M5Probe4-DO	5'GGTTGTCCTCTGAGAGGCTCTAC	
P64	M5Probe5-UP	5'GGGCATAGTTTCCCTCCTTGTG	
P65	M5Probe5-DO	5'GCCCATGAACATACAAGAAGCC	
P66	M5Probe6-UP	5'GGCTGACTGTACGAATTGAAAGGC	
P67	M5Probe6-DO	5'CGGTTTGGATGGAGGTTGGTATC	
P68	M6Probe1-UP	5'CCCATCTGCTCAAGGCTCAGC	
P69	M6Probe1-DO	5'CCAGTGAGAGTCCTGTGGACC	
P70	M6Probe2-UP	5'GGCTCCTATCAATTTGCTGTGCTC	
P71	M6Probe2-DO	5'CCTGGATGAGCGAATCCTGTG	
P72	M6Probe3-UP	5'GGGTTGAGCTGAGCGTATCTG	
P73	M6Probe3-DO	5'GCCTTTGTCATGGTGTCTCTTC	insert DNA upstream of *Mcpt6*
P74	M6Probe4-UP	5'GGTCGTGCAGAGCACCAGGAAC	
P75	M6Probe4-DO	5'GCCAGCAATCTTGGTGAGTGTG	
P76	M6Probe5-UP	5'GGCACTCAGAACCATACCAGATTC	
P77	M6Probe5-DO	5'CCATGTTGAGGTGAGACTGTTAG	
P78	M6Probe6-UP	5'GCCAGGAGCCTTCTTGAGACC	
P79	M6Probe6-DO	5'GGCAGAGTTCAGAGATGCAACTGC	

4.4 Standard molecular biology methods

4.4.1 Polymerase chain reaction and colony PCR

The polymerase chain reaction (PCR) was used for various applications like the amplification of DNA cassettes for the insertion into BAC vectors, sequencing and genotyping. In a standard protocol 10-100 ng template DNA was amplified with 1x reaction buffer, 2 mM $MgCl_2$, 200 nM each primer, 200 µM dNTP mix and 0.05 U/µl Taq-Polymerase were used (Fermentas Life Sciences except primers). For most applications,

the template DNA was denatured at 95℃ for 5 min followed by 30-35 cycles of 45 sec at 95℃, 1 min at the appropriate annealing temperature and 1 min per kb DNA to be amplified at synthesis temperature (72℃). Amplification was completed with a final synthesis step at 72℃ for 7 min. The optimal annealing temperature of the primers was estimated with the following formula: T_A=59.9+0.41(GC%)-600/L (GC%, GC content in percent, L, total number of base pairs).

Colony PCR was used to verify successful modifications of BAC vectors. Single bacterial cell colonies were resuspended in 5 µl ddH_2O in PCR tubes and pre-incubated at 95℃ for 5 min to lyse the bacteria. 45 µl of the PCR mastermix were added, samples were mixed by tapping and further processed as described above.

4.4.2 DNA sequencing

The sequencing was commercially performed by Seqlab Sequencing Laboratories, Göttingen. 25 ng template DNA/100 bp (maximum 5 µl) was used for each sequencing reaction (usually gel purified PCR products). In case of unpurified PCR products used as templates, the samples were pretreated with 4 U SAP (Shrimp Alkaline Phosphatase) and 10 U Exonuclease I, in order to remove primers and dNTPs. The samples were mixed, centrifuged briefly and incubated for 30 min at 37°C followed by inactivation of SAP and Exonuclease at 80℃ for 30 min. 5 µl of the processed PCR products and 20 pmol of primer were used for sequencing.

4.4.3 Gel purification of DNA fragments

PCR products or DNA restriction fragments were loaded on a 1% agarose gel and submitted to gel electrophoresis. The DNA fragment of interest was cut from the gel and extracted from the agarose matrix using the QIAEX II Gel Extraction Kit (Qiagen, Hilden) following the manufacturer's instructions.

4.4.4 Small and intermediate scale preparation of plasmid DNA

The isolation of small amounts of plasmid DNA was performed according to Qiagen protocols and as described in section 4.5.4 for BAC DNA isolation using buffers P1 to P3.

Higher amounts of plasmid DNA were isolated from bacterial cells using the Qiagen Plasmid Midi Kit following the manufacturer's instructions. The purified plasmid DNA was dissolved in TE buffer pH 8.0 (10 mM TrisCl pH 8.0, 1 mM EDTA).

4.4.5 Quantification of DNA

The concentration of DNA was determined by measuring absorption at 260 nm and 280 nm (A_{260} and A_{280}). An A_{260} of 1 corresponds to a concentration of approximately 50 µg/ml of double stranded DNA. The purity of the DNA can be assessed by calculating

the ratio of A_{260}/A_{280} with 1.8 reflecting pure DNA. A ratio below or above 1.8 indicates protein or RNA contamination, respectively. Alternatively, DNA concentrations were estimated in an agarose gel after electrophoresis by comparing the band intensities with a standard.

4.4.6 Restriction digest

DNA was enzymatically cleaved by restriction endonucleases (NEB and Fermentas Life Sciences) using the appropriate enzyme buffers. Following the manufacturer's instructions, 1 U was used to digest 1 µg of DNA at 37℃ in most instances.

4.4.7 Southern blot

Southern blot analysis was performed according to standard procedures and bound probes were detected by chemoluminescence.

4.4.7.1 Buffers

Liquid Block: Delivered with the Gene Images Random Prime Labeling and CDP-Star Detection Kit (Amersham/GE-Healthcare, Munich). Aliquots were stored at -20℃.

Denaturation and transfer buffer: 0.4 M NaOH, 0.6 M NaCl in ddH_2O

Neutralization buffer: 0.5 M TrisCl, 1 M NaCl in ddH_2O, pH 7.2

20x SSC: 0.3 M NaCitrate, 3 M NaCl in ddH_2O, pH 7.0.

Hybridization buffer: 5x SSC, 0.1% SDS (w/v), 5% Dextransulfate (w/v), 5% Liquid Block (v/v) in ddH_2O, incubate 2 h at 65℃ to facilitate the dissolvin g of the Dextransulfate.

Buffer A: 100 mM TrisCl, 300 mM NaCl in ddH_2O, pH 9.5

Blocking buffer: Liquid Block 1:10 diluted in buffer A, 0.1% NaAzide (w/v)

Anti-fluorescein AP conjugate solution: 0.5% BSA (w/v), AP conjugate (enclosed in the CDP-Star Detection Kit) 1:5000 in buffer A

Wash buffer 1: 1x SSC, 0.1% SDS (w/v) in ddH_2O

Wash buffer 2: 0.5x SSC, 0.1% SDS (w/v) in ddH_2O

Wash buffer 3: buffer A with 0.3% Tween 20 (v/v, Serva)

Substrate: CDP-Star detection reagent enclosed in the CDP-Star Detection Kit

4.4.7.2 Blotting

DNA was digested with restriction enzymes, loaded on a 0.7% agarose gel and submitted to gel electrophoresis in TAE buffer. The gel was cut to an appropriate size and photographed together with a ruler. In order to denature the DNA, the gel was incubated in denaturation/transfer buffer for 30 min. The DNA was transferred to the PoraBlot NY plus membrane (Macherey-Nagel, Düren) by alkaline transfer by capillary force. For this purpose the gel was placed onto three sheets of pre-wetted Whatman paper (3 mm) the margins of which were connected to a reservoir of transfer buffer. The membrane was

placed on top of the gel followed by three additional pre-wetted sheets of Whatman paper and dry paper towels (at least 6 cm in height) topped by a weight. After over night blotting, the membrane was incubated in neutralization buffer for 5 min and subsequently dried at 80°C for 2 h.

4.4.7.3 Probe labeling

Purified PCR products or restriction fragments to be used as probes were labeled with fluorescein coupled dCTPs using the Gene Images Random Prime Labeling Kit following the manufacturer's instructions. Briefly, approximately 100 ng of template DNA was denatured in a volume of 20 µl at 99°C for 5 min and placed on ice. A mastermix consisting of the dNTP mix (which included the labeled dCTPs), the primer mix for random priming and the Klenow fragment, was added to the denatured DNA and the sample was incubated for 1 h at 37°C. The reaction was stopped by addition of EDTA (final concentration 20 mM). The probe was kept on ice or stored at -20°C prior to the hybridization.

4.4.7.4 Hybridization and detection

The hybridization buffer as well as the hybridization tubes were pre-heated at 65°C. The membrane was wetted in 5x SSC, placed into a hybridization tube and pre-incubated in hybridization buffer without probe at 63°C for 2 h in a hybridization oven, before freshly denatured probe was added. After overnight incubation at 63°C, the membrane was washed with wash buffer 1 and subsequently with wash buffer 2 each time for 15 min at 65°C. To reduce unspecific binding of the AP conjugate, the membrane was incubated for 1 h in blocking buffer at RT. During the subsequent incubation of the membrane with anti-fluorescein AP conjugate at RT for 1 h, the antibody bound to the fluorescein labeled dCTPs of the probes. The membrane was washed thrice with wash buffer 3, each step for 15 min at RT. The substrate solution was pipetted onto the membrane and after 5 min, an Amersham Hyperfilm™ was exposed for 15 min to 2 h.

4.5 Molecular biology methods for modification of BAC vectors

4.5.1 BAC clones

BAC clones used in this thesis were part of the RPCI-23 mouse BAC library (library No. 731 (Osoegawa et al., 2000)). Fragments of C57BL/6 genomic DNA, partially digested with *Eco*RI, were cloned into *Eco*RI sites of pBACe3.6 vector. For each clone, both ends of these inserts were sequenced generating "end sequences" which define the chromosomal location of the genomic fragment. The BAC clones indicated in Table 4.4

were purchased from the RZPD (Deutsches Ressourcenzentrum für Genomforschung GmbH, Berlin) and propagated in DH10B *E. coli* cells at 37℃ in chloramphenicol conditioned medium. Glycerol stocks were generated by adding 300 µl of sterile glycerol to 900 µl of an over night culture. The mixture was frozen on dry ice and stocks were stored at -80℃.

BAC clone (RZPD clone ID)	**chromosomal position of genomic inserts [bp]**	**gene of interest**	**synonyms**
RP23-284A14 (RPCIB731A14284Q2)	Chr. 14, 56471619 – 56678625	*Mcpt5*	*Cma1*
RP23-240F3 (RPCIB731F3240Q2)	Chr. 17, 25433400 – 25606599	*Mcpt6*	*Tpsb2*

Table 4.4 BAC clones from the mouse BAC library RPCI-23 used in this thesis

4.5.2 BAC recombineering

The modification of BAC vectors was performed by homologous recombination using the Red/ET recombination system ("ET-cloning", patent-registered by Gene Bridges, Dresden). The Red/ET recombination system relies on the plasmid pRedET encoding the Redα/Redβ protein pair which mediates homologous recombination. In addition the plasmid carries the gene coding for the Redγ protein that prevents the RecBCD complex of the intrinsic recombination system of the BAC host from degrading linear DNA fragments. The genes for the Redαβγ proteins are organized in an operon under the control of the L-arabinose inducible pBAD-promoter. Therefore, transcription is respressed by an AraC dimer until L-arabinose binds to this repressor. The plasmid is a derivate of the thermo-sensitive, low copy pSC101 replicon (oriR101) and includes the RepA protein which is necessary for replication and distribution of the plasmid to the daughter cells. As RepA is temperature-sensitive, cells have to be propagated at 30℃ while the expression of the Redαβγ proteins requires 37℃ and L-arabinose. This has the advantage that the expression of the recombinases can be limited to a short time window since the copy number of the plasmid decreases rapidly at 37℃, thereby minimizing the occurrence of undesired additional recombination events.

In principle, the BAC host is first transformed with the plasmid pRedET (which also encodes a tetracycline resistance) and propagated by 30℃. In a second step, the expression of Red α, β and γ is induced by addition of L-arabinose, the temperature is switched to 37℃ and the BAC host is transformed with a PCR product encompassing the 5' and 3' homology regions (HR) for the homologous recombination and DNA sequence to be integrated into the BAC. The homologous recombination event replaces the sequence of the BAC that is flanked by the HRs (Fig. 4.1).

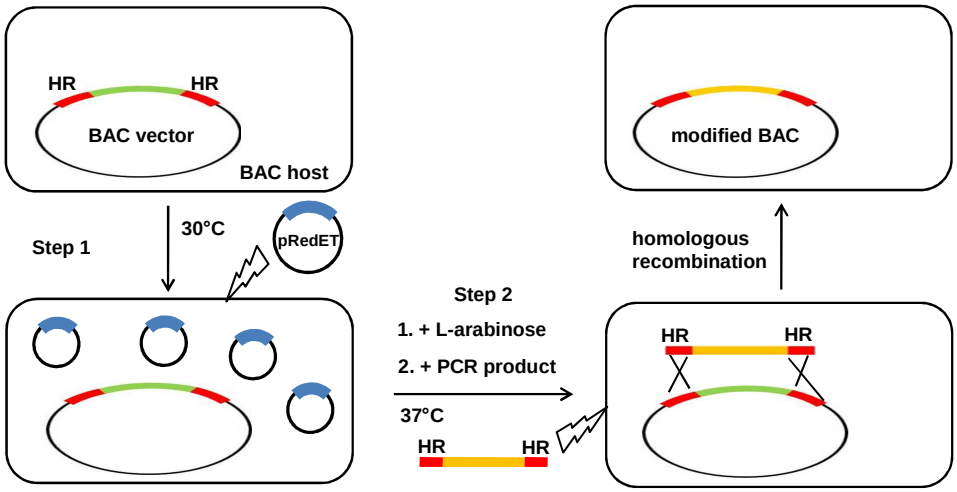

Fig. 4.1 Principle of Red/ET recombination. The BAC host is transformed with the plasmid pRedET and propagated at 30℃. In a second step the expression of the Red α, β and γ is induced by addition of L-arabinose and a temperature switch to 37℃. The PCR product containing homology regions (HR) is electroporated into the BAC host and product recombines with the BAC vector.

4.5.2.1 Templates and sources of DNA cassettes

The selectable markers, i.e. the *ampicillin* (*amp*), *zeocin* (*zeo*) and *neomycin* (*Neo*) resistance cassettes, were amplified from pBluescriptII KS+, psiRNA-hH1zeo (InvivoGen) and pR6K-PGK-gb2-Neo (Gene Bridges), respectively. The minimal vector for subcloning by homologous recombination was based on pACYC184 (NEB). The *iCre* sequence together with the *frt*-flanked estrogen binding domain was subcloned from the plasmid pCreER^{T2}Amp, kindly provided by Giuseppe Testa, Milan.

4.5.2.2 Primer design and generation of the PCR product containing the HRs

Oligonucleotides containing the HR sequences were purchased from Metabion, Martinsried. The HRs were usually 50 bp homologous to a target of the vector to be modified. The design of the primers depended on the application of the BAC recombineering method. The replacement of BAC sequences by a DNA cassette required amplification of the cassette using primers that also contained the HR 5' and 3' of the BAC sequence to be replaced. In addition to the HRs, these primers can optionally contain restriction sites. Thus, from 5' to 3', the primers are composed of (1) the HR, (2) optional restriction site and (3) primer for the amplification of the selectable marker.

In order to subclone DNA sequences from a vector by homologous recombination, a minimal vector that encompasses a resistance gene and an origin of replication was amplified from plasmid DNA. Note, that the forward primer for amplification of the minimal vector contained the HR 3' of the cassette to be subcloned and the reverse primer the 5'

HR, respectively. In this way, the minimal vector replaces the vector backbone and incorporates the desired DNA fragment (see also Fig. 2.3, section 0).

For the generation of these PCR products, the plasmids used as templates were digested with restriction enzymes prior to amplification. About 1-5 µg plasmid DNA were incubated in 20-50 µl samples with restriction endonucleases that do not cleave within the part to be amplified. 1 µl of cleaved plasmid DNA was used as template without further processing. The resulting PCR product was precipitated with 2.5 volumes of 100% ethanol and 0.1 volumes of 3 M NaAc pH 5.2 and washed twice with 70% ethanol. After resuspension of the air dried DNA pellet in ddH_2O, the PCR product was used for electroporation into the BAC host. The cleavage of the plasmid DNA prior to PCR prevents the electroporation of circular template DNA and, thus, reduces the occurrence of false positive colonies containing the template plasmid only.

4.5.2.3 BAC modification protocol

BAC modification was largely done according to the manual of the "Quick and Easy BAC Modification Kit" (Gene Bridges, Dresden) with some modifications. All bacterial cell propagation steps during the BAC modification procedure were performed in selective LB medium in 1.5 ml microcentrifuge tubes with a punctured lid. The bacterial cells were incubated in a thermomixer (Eppendorf, Hamburg) at 1100 rpm. All electroporation steps were done using electroporation cuvettes (Bio-Rad, Munich) with a 1 mm gap and the Electroporator 2510 (Eppendorf, Hamburg). Optimal electroporation results were obtained at a voltage of 1350 V and a time constant of 5-6 ms. Before starting, ddH_2O and electroporation cuvettes were chilled on ice and the benchtop centrifuge was cooled to 2℃. Fast handling of the bacteria and careful c ooling of each sample on ice whenever possible were prerequisites for successful electroporation. The following protocol includes the preparation of electro-competent cells.

Step 1: electroporation of the pRedET plasmid

- Inoculate 1 ml LB medium supplemented with the respective antibiotic (15 µg/ml chloramphenicol (Cm) in case of the BAC clones from the library RPCI-23) with one colony of the BAC host.
- Cultivate cells overnight at 37℃.
- Transfer 30 µl of the overnight culture into 1.4 ml LB-medium containing the same antibiotic and incubate at 37℃ for 2 h.
- Centrifuge for 30 sec at 11,000 rpm, discard supernatant by quickly inverting tube twice, resuspend pellet in 1 ml cold ddH_2O by vortexing.
- Repeat the previous step.
- Centrifuge again and discard supernatant leaving a volume of about 40 µl in the tube.

- Add 1 µl pRedET (0.2 – 0.5 µg).
- Mix briefly by pipetting up and down, transfer the cell/DNA mixture into a chilled cuvette and electroporate.
- Ad 1 ml LB medium without antibiotic to the electroporated cells and transfer them back into the same microcentrifuge tube.
- Incubate at 30°C for 70 min.
- Plate 100 µl of the cells on LB agar plates containing Cm and tetracycline (Tet, 3 µg/ml).
- Incubate at 30°C overnight to 24 h.

Step 2: L-arabinose induction and electroporation of the PCR product

- Inoculate 1 ml LB medium containing Cm and Tet with one colony from the plate obtained in step 1 and incubate overnight at 30°C.
- Inoculate two tubes with 1.4 ml LB-medium conditioned with Cm and Tet with 30 µl of the overnight culture and incubate 2 h at 30°C.
- Add 20 µl 10% (w/v) L-arabinose (Sigma, in ddH_2O, aliquots stored at -20°C) to one tube, incubate 40 min at 37°C. The second tube serves as a negative control without induction of Red/ET recombination.
- Electroporate the PCR product (0.1-0.2 µg in 1-2 µl) as described in step 1.
- Plate cells harboring the modified BAC and uninduced control cells on LB agarose plates containing Cm and the appropriate antibiotic selecting for correctly recombined clones and incubate overnight at 37°C. The ratio of colonies on the induced and uninduced plates should exceed 100:1.
- Identify clones with correct recombination events by colony PCR.

4.5.3 Cre- and Flp-mediated recombination in *E. coli*

In order to remove *loxP*- or *frt*- flanked sequences from BAC vectors in *E. coli*, the BAC hosts were transformed with the expression vector 706-Cre or 706-Flp (Gene Bridges, Dresden). Transformation and further handling of the bacteria were done according to the manufacturer's instructions. Briefly, the transformation was performed by electroporation as described above and successfully transformed bacteria selected for Tet resistance. Bacteria were streaked out on LB agar plates containing the appropriate antibiotics and were incubated for at least 24 h at 30°C. 2 ml LB medium samples were inoculated with single colonies and incubated 2-3 h at 30°C and overnight at 37°C. The temperature switch to 37°C induced the expression of the Cre or Flp recombinase. To test for deletion of the *loxP*- or *frt*-flanked sequence, PCR was performed on 1 µl of the bacterial culture following the protocol for the colony PCR. To be sure that the 2 ml bacterial cultures were each derived from a single colony, BAC DNA was isolated according to the small scale preparation protocol for BAC DNA (section 4.5.4) and re-transformed into DH10B cells by electroporation.

4.5.4 Small scale preparation of BAC DNA

2 ml overnight cultures were prepared in 2 ml Eppendorf tubes with a punctured lid and incubated in a thermomixer at 37°C and 1100 rpm. After centrifugation at 11000 rpm the pellet was resuspended in 200 µl buffer P1 (50 mM TrisCl pH 8.0, 10 mM EDTA, 100 µg/ml RNase A (Sigma)). Bacterial cells were lysed by adding 200 µl of buffer P2 (200 mM NaOH, 1% SDS (w/v)), carefully inverting the tube and incubating at room temperature (RT) for 5 min. 200 µl of buffer P3 (3 M KAc, pH 5.5) were added, samples were gently mixed by inverting and centrifuged at 11000 rpm for 5 min. The supernatant was transferred into 1.5 ml microcentrifuge tubes and DNA was precipitated by adding 0.7 volumes of isopropanol. The samples were mixed by inverting (but not vortexing in order to avoid shearing of the large DNA molecules). DNA was centrifuged and washed once with 70% ethanol, dried briefly and dissolved in TE buffer.

4.5.5 Purification of BAC DNA for pronucleus injection

The isolation and purification of BAC DNA suitable for pronucleus injection were done as described by Sparwasser et al. (Sparwasser et al., 2004) with modifications as detailed in the following.

4.5.5.1 Buffers and reagents

All buffers were prepared in ddH_2O unless otherwise specified and, if possible, autoclaved. All buffers and reagents were exclusively prepared and used for the BAC purification. (*: Buffers freshly prepared prior each BAC DNA preparation)

Solution I: 10 mM EDTA, pH 8.0

Solution II*: 0.2 M NaOH, 1% SDS (w/v) (prepare 1% SDS solution and then add slowly NaOH)

Solution III*: 1.9 M KAc, adjusted to pH 5.5 with glacial acetic acid, pre-cooled on ice (use 7.5 M KAc for fresh preparation of solution III)

Resuspension buffer I: 10 mM TrisCl pH 8.0, 50 mM EDTA, pre-heated to 37°C

Resuspension buffer II: 50 mM TrisCl pH 8.0, 50 mM EDTA

1xTAE: 40 mM TrisCl, 20 mM NaAc, 1 mM EDTA

Injection buffer: 10 mM TrisCl pH 7.5, 0.1 mM EDTA, 100 mM NaCl (autoclaved and further purified by filtration through a 0.2 µm filter)

TE buffer: 10 mM TrisCl pH 8.0, 1 mM EDTA

Reagents: 7.5 M KAc, 10% SDS (w/v), glacial acetic acid, isopropanol, RNase A (10 mg/ml) , phenol/chloroform/isoamylalcohol 25:24:1 (Fluka, Ulm), chloroform

4.5.5.2 Maxi preparation of BAC DNA

- Pellet bacterial cells of a 250 ml over night culture at 6.000 g and 4°C for 15 min.
- Resuspend pellet in 20 ml Solution I, incubate 5 min at RT.
- Carefully add 40 ml of Solution II, mix gently by swirling the bottle for 5 sec, incubate 5 min at RT.
- Carefully add 30 ml Solution III, mix gently by swirling the bottle, incubate 15 min on ice.
- Centrifuge at 6000 g for 20 min at 4°C and filter supernatant through a gauze swab into a clean bottle.
- Centrifuge again at 6000 g for 20 min at 4°C and transfer supernatant into a clean bottle through a 70 µm cell strainer.
- Add 45 ml isopropanol and pour the mixture into a clean bottle allowing the phases to mix.
- Centrifuge at 6000 g for 15 min at 4°C, discard supernatant and aspirate remaining liquid using a water-jet vacuum pump. Air-dry the pellet briefly.
- Resuspend DNA pellet in 9 ml pre-heated resuspension buffer I by swirling gently.
- Pour DNA containing solution into a 30 ml capped centrifuge tube and add 4.5 ml of 7.5 M KAc, mix by inverting the tube gently (precipitate should form). Place the tube at -80°C for 30 min.
- Thaw at RT and centrifuge at 4000 g in swinging buckets for 10 min at 4°C. While spinning, prepare another 30 ml tube with 27 ml 100% ethanol. Pour the supernatant onto the ethanol and mix gently by inverting the tube in order to precipitate the DNA.
- Centrifuge at 4000 g for 10 min, discard the supernatant, aspirate excess supernatant with the water-jet vacuum pump and briefly air-dry the pellet.
- Resuspend DNA in 700 µl resuspension buffer II and add 10 µl RNase A, incubate for 1 h at 37°C.
- Transfer the DNA solution to a 1.5 ml microcentrifuge tube and add 700 µl phenol/chloroform/isoamylalcohol 25:24:1, mix gently until phases are mixed, centrifuge 5 min and transfer the aqueous phase into a clean tube.
- Repeat the previous step.
- Repeat previous step but this time extract with pure chloroform.
- Transfer the aqueous phase into a clean tube and precipitate with 700 µl isopropanol, mix gently, centrifuge for 20 min and discard the supernatant.
- Wash DNA pellet with 500 µl 70% ethanol, centrifuge for 5 min. Discard the supernatant and briefly air-dry the pellet.
- Dissolve BAC DNA in 50-100 µl TE pH 8.0 or ddH_2O (for enzymatic digest).

4.5.5.3 Separation of the BAC insert from the vector backbone

In order to separate the BAC insert from the vector backbone, the BAC DNA was submitted to *Not*I digest (for Mcpt5-Cre and Mcpt5-CreER^{T2}) or *Asc*I/*Bst*BI double digest (for Mcpt6-Cre). For each construct, two digests were prepared, one 200 µl sample for the pronucleus injection containing the total BAC DNA yield of one maxi preparation and one

100 µl sample containing DNA of a second maxi preparation for indicator lanes (see below). Both samples were prepared with 1x reaction buffer, 1x BSA, RNase A (final concentration 10 µg/ml) and enzyme in excess and incubated over night at 37°C.

The gel electrophoresis was performed under ethidium bromide free conditions using a 0.6% (w/v) agarose gel. The total 200 µl sample was loaded into two slots. 20 and 40 µl of the 100 µl sample were loaded into the two adjacent slots on each site of the lanes of interest serving as indicator lanes. Electrophoresis was performed at 5 V/cm for about 4 h at 4°C. Afterwards, the indicator lanes were separated from the lanes containing the DNA for pronucleus injection and were stained with ethidium bromide. To protect the DNA from the UV light, the unstained gel was placed onto a sterile aluminum foil strip on a UV transilluminator with the indicator lanes on both sites allowing the excision of the BAC insert DNA from the unstained gel.

4.5.5.4 Electroelution

The Elutrap® Electroelution System (Whatman) was used to extract the BAC insert DNA from the agarose gel slice. The electroelution device was assembled following the manufacturer's instructions and placed into the same chamber used for the electrophoresis described in the previous section. The electrophoresis chamber was sealed with tape left and right of the Elutrap® device to avoid leakage current. The gel slice was placed into the large compartment of the device and the chamber as well as the Elutrap® device was filled with TAE buffer. A voltage of 6 V/cm for 4.5 h at 4°C was applied. Thereby, the insert DNA passed the BT2 membrane but not the BT1 membrane and, thus, was trapped in the small compartment between both membranes, called the trap (Fig. 4.2). Before recovering the DNA from the trap, the current was inverted for 20 sec to mobilize DNA that may have adhered to the BT1 membrane. The pure DNA was recovered from the trap by pipetting.

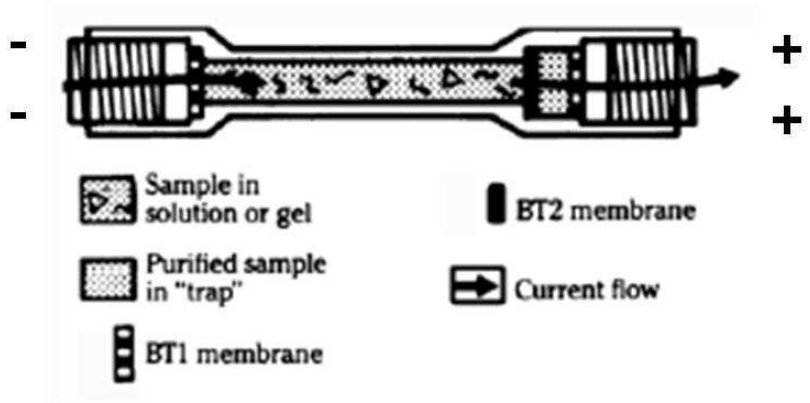

Fig. 4.2 Elutrap® Electroelution System (Whatman). In principle, the DNA is extracted from an agarose gel piece placed in the large compartment by a current directed through the Elutrap device in the indicated direction. While the BT2 membrane is permeable for DNA the BT1 membrane is not, thus, the DNA is collected in the small compartment between the BT2 and BT1 membrane (trap).

4.5.5.5 Drop dialysis

In order to exchange the TAE buffer against the buffer required for pronucleus injection, the recovered DNA from the electroelution was submitted to drop dialysis. For this purpose, a MF-Millipore membrane filter with 25 nm pore size (#VSWP 02500, Millipore, Schwalbach) was placed onto 30 ml injection buffer in a 10 cm cell culture dish. 100 µl of DNA in TAE buffer were pipetted on top of the filter and the dish was capped tightly. After 30 min the drop now containing purified BAC insert DNA dissolved in injection buffer was removed from the filter.

4.5.5.6 Pulsed-field gel electrophoresis

The isolated BAC insert DNA was tested for its integrity und purity by pulsed-field gel electrophoresis (PFGE) using the CHEF-DR III variable angle system (Bio-Rad, München). The PFGE was performed in 0.5x TBE (45 mM Tris-borate, 1 mM EDTA). A 1% PeqGold Pulsed-Field agarose gel (Peqlab, Erlangen) placed in the middle of the hexagonal chamber was loaded with DNA. The Mid Range PFG Marker I embedded in agarose (Peqlab) was used as a size standard. The PFGE was performed with an initial switch time of 0.2 sec, a final switch time of 25 sec, 6 V/cm for 16 h and at a buffer temperature of 12°C. Afterwards, the gel was stained with 0.5 µg/ml ethidium bromide in ddH_2O for 20 min. Excess ethidium bromide was removed by washing with ddH_2O for 10-20 min.

4.5.6 Generation of transgenic mice by pronucleus injection

The pronucleus injection of purified BAC DNA into fertilized C57BL/6 oocytes was done by Ronald Naumann, Transgenic Core Facility, MPI of Molecular Cell Biology and Genetics, Dresden. The injected oocytes were transferred into pseudopregnant foster mice. Transgenic offspring were identified by PCR using genomic tail DNA as template.

4.6 Mice

4.6.1 Mouse strains

All mice were on the C57BL/6 background and crossed exclusively to C57BL/6 mice. Beside the newly generated Mcpt5-Cre and Mcpt6-Cre strains, the following mouse lines were used in this thesis: R26R-EYFP Cre excision reporter (Srinivas et al., 2001), tg(CMV-Cre) that mediates a germline deletion of *loxP*-flanked DNA (Schwenk et al., 1995), transgenic hACTB::FLP ubiquitously expressing the Flp recombinase (Dymecki, 1996a) and ROSA26-iDTR (Buch et al., 2005). Mice were kept under specific pathogen free (SPF) conditions and all experiments were done according to institutional guidelines.

4.6.2 Genotyping

4.6.2.1 Isolation of genomic tail DNA

Mouse tail tips, about 0.5 cm in length, were incubated overnight at 55℃ rocking in 500 µl lysis buffer (200 mM TrisCl, 100 mM NaCl, 1% SDS (w/v), 50 mM EDTA) supplemented with 100 µg Proteinase K (Fermentas Life Sciences). Undigested material was sedimented by centrifugation and the supernatant was poured into a fresh 1.5 ml microcentrifuge tube containing 500 µl isopropanol. The samples were mixed by inverting the tubes several times. The precipitated DNA was pelleted by centrifugation and washed once with 70% ethanol. The air dried DNA pellet was dissolved in TE buffer by incubating at 55℃ shaking for at least 2 h.

4.6.2.2 Genotyping protocols

Mice were genotyped by PCR using the standard PCR program (see section 4.4.1) with varying annealing temperatures (T_A) and cycle numbers. Primers used for genotyping are listed in Table 4.3.

PCR	strain	primer	PCR product	T_A and cycle number
Mcpt5-Cre	Mcpt5-Cre	P1/P3/P4	wt: 224 bp Mcpt5-Cre: 554 bp	T_A=57℃, 30 cycles
Mcpt6-Cre	Mcpt6-Cre	P2/P3	Mcpt6-Cre: 553 bp	T_A=63℃, 12 cycles T_A=58℃, 18 cycles
Mcpt5-CreER^{T2}	Mcpt5-CreER^{T2}	P12/P5	Mcpt5-CreER^{T2}: 1097bp	T_A=63℃, 12 cycles T_A=58℃, 18 cycles
ROSA26-STOP	R26R-EYFP ROSA26-iDTR	P19/P20/P21	wt:600 bp R26-STOP: 300 bp	T_A=54℃, 12 cycles T_A=51℃, 18 cycles
iDTRspez	ROSA26-iDTR	P26/P27	iDTR: 450 bp	T_A=56℃, 12 cycles T_A=52℃, 18 cycles
FlpDel	ACTB::FLP	P22/23	FlpDel: 725 bp	T_A=54℃, 12 cycles T_A=51℃, 18 cycles
DelCre	tg(CMV-Cre)	P24/25	DelCre: 600 bp	T_A=58℃, 35 cycles

Table 4.5 Protocols for genotyping of the indicated mouse strains by PCR, the corresponding primer sequences are listed in Table 4.3 under the respective primer numbers.

Note that in transgenic mice, it is not possible to distinguish between heterozygous and homozygous mice by PCR. Therefore, transgenic mice were never crossed to each other. In case of the Mcpt5-Cre typing, a third primer (P4) was used that amplified together with the upstream primer (P1) a product representing the wt *Mcpt5* locus. This PCR product, which should always be present, served as an internal control of that PCR.

4.6.3 Procedures of animal experimentation

4.6.3.1 Administration of tamoxifen

CreER^{T2} positive mice were treated orally with tamoxifen (free base, Sigma) since it is known that tamoxifen is metabolized in the liver to 4-OH-tamoxifen (Kamal and Goetz, 2007) that binds with high affinity to the ER^{T2} domain (Feil et al., 1997). 400 mg of tamoxifen were suspended in 400 µl 100% ethanol, mixed by vortexing. 19.6 ml sunflower oil (Sigma) were subsequently added to this mixture resulting in a 20 mg/ml tamoxifen suspension. To dissolve the tamoxifen in the oil/ethanol mixture, the suspension was vortexed for 5 min and subsequently sonicated. Single use aliquots were stored at -20℃ and thawed at 56℃. The mice were t reated with 2 mg tamoxifen for five consecutive days by gastric intubation using a feeding needle (1.2 x 4 mm, Heiland, Hamburg). 100 µl tamoxifen were injected directly into the stomach by introducing the feeding needle through the esophagus. The tamoxifen was kept shaking at 56℃ until injected.

4.6.3.2 Administration of diphtheria toxin

The 1 mg/ml stock solution of the diphtheria toxin (DT, Sigma) in pyrogen free ddH_2O was stored in 6 µl aliquots at -80℃. Fresh aliquots we re thawed on ice for each treatment. The working concentration was 5 µg/ml. Thus, the 6 µl-aliquots were diluted 1:200 with 1.2 ml sterile PBS. Mice were injected intraperitoneally (i.p.) with 25-100 ng DT/g bodyweight with varying numbers of injections and treatment intervals. One injection protocol included the application of the H1-antagonist pyrilamine (pyrilamine maleate salt, Sigma) together with the DT. For this purpose 12 µl of a 100 mg/ml pyrilamine stock solution was added to the 1.2 ml DT working solution resulting in a dose of 5 µg/g bodyweight for the H1-antagonist.

4.6.3.3 Back skin biopsies

Mice were anesthetized by i.p. injection of a Rompun (Bayer HealthCare)/Ketanest (Pfizer) solution (5% Rompum (v/v) and 10% Ketanest (v/v) in sterile isotonic saline). 10 µl of this solution per g bodyweight were injected. The mice were shaved and a skin fold was lifted from the back and fixed with two fingers on a sterile pad. One biopsy was taken at the edge of the skin fold using a 4 mm biopsy punch (Stiefel, Wächtersbach).

4.6.3.4 Passive systemic anaphylaxis

In the model of passive systemic anaphylaxis, mice were first sensitized with IgE directed against an allergen thereby loading the high affinity IgE receptor (FcεRI) on mast cells and basophils with allergen-specific IgE. Later, the mice were challenged with the respective allergen. For sensitization 12.5 µg mouse anti-DNP-IgE (clone SPE-7, Sigma) were injected i.p.. 24 h later, mice were challenged by i.p. injection of 400 µg DNP-HSA

(Sigma). The intensity of the anaphylactic response was assessed by measuring the drop of the body temperature every 10 min over a period of 3 h using the thermometer Bio-TK 9882 (Bioseb, France) and the rectal probe BRET3.

4.7 Cell culture

4.7.1 Cell culture media and reagents

Penicillin/Streptomycin: 100 U/ml penicillin, 0.1 mg/ml streptomycin (final concentrations, Biochrom AG, Berlin)

L-Glutamine: 2 mM final concentration (Biochrom AG)

Complete DMEM: DMEM medium (Gibco) supplemented with 10% FBS (Biochrom AG), 50 µM β-mercaptoethanol, L-glutamine, penicillin/streptomycin

WEHI-3B conditioned medium: Supernatant of IL-3 producing WEHI-3B cells purchased from the German Collection of Microorganisms and Cell Cultures (DSMZ, Braunschweig). The medium was prepared by culturing $1x10^5$ WEHI-3B cells in complete IMDM containing 10% FBS, 25 µM β-mercaptoethanol, L-glutamine and penicillin/ streptomycin for 3-4 days until cell density reached about $1x10^6$ cells/ml. Cells were carefully mobilized from the culture dish bottom using a cell scraper, centrifuged and the supernatant was collected. 50 ml aliquots were stored at -20°C.

Complete Opti-MEM: Opti-MEM (Invitrogen, Karlsruhe) supplemented with 10% FBS and penicillin/streptomycin

SCF containing medium: Supernatant of murine SCF secreting CHO transfectants (generated by S. Lyman, Immunex, Seattle, and kindly provided by P. Dubreuil, Marseille). The CHO transfectants were cultivated in DMEM supplemented with 10% FBS, L-glutamine, penicillin/streptomycin, 1 mM sodium pyruvate and splitted 1:10 every 2 days in 10 cm dishes. For collecting the supernatant, cells were seeded on 15 cm dishes and grown to confluency. 72 to 96 h later SCF containing supernatant was harvested. 50 ml aliquots were stored at -20°C.

1x PBS: 10 mM Na_2HPO_4, 1.5 mM KH_2PO_4; 2.6 mM KCl, 136 mM NaCl, pH 7.4

4.7.2 Cultivation of BMMCs

Femur and tibia of both limbs from one mouse were removed under sterile conditions and flushed with complete DMEM using a 24 gauge needle. The bone marrow cells (BMC) were filtered through 70 µm and 40 µm cell strainers, subsequently centrifuged at 1200 rpm for 5 min and washed twice with PBS. In order to lyse erythrocytes, the cell pellet was resuspended in erythrocyte lysis buffer (155 mM NH_4Cl, 10 mM $KHCO_3$, 1 µM EDTA, pH 7.3) and incubated for 5 min at RT. Cells were centrifuged, washed with PBS and the

pellet was resuspended in complete DMEM supplemented with 20% WEHI-3B conditioned medium. BMCs were cultured in a 50 ml culture flask at 37℃ and 5% CO_2. Floating cells were transferred in a clean flask with fresh medium twice a week until no adherent cells were left. Thereafter, cells were fed by replacing half of the volume of the medium by fresh complete DMEM supplemented with WEHI-3B conditioned medium. After four to eight weeks, the culture should consist of more than 90% BMMCs which are identified flow cytometrically by means of their cell surface markers CD117 and FcεRIα (see section 4.8).

4.7.3 Cultivation of PCMCs

Peritoneal cell derived mast cells (PCMC) were generated as recently described by Malbec and coworkers (Malbec et al., 2007). Peritoneal cells were isolated under sterile conditions by peritoneal lavage using RPMI medium without supplements. Cells were sedimented at 1200 rpm for 5 min. The pellet was resuspended in 1 ml complete Opti-MEM freshly supplemented with 4% SCF containing medium. The cells were seeded at a density of $1x10^6$/ml complete Opti-MEM with 4% SCF containing medium into tissue culture dishes of appropriate size. 24 h later, non-adherent cells were removed and fresh medium was added to the adherent cells. In subsequent passages all cells were collected by transferring non-adherent and trypsinized adherent cells in the same Falcon tube. Cells were centrifuged, resuspended in fresh complete Opti-MEM with SCF and seeded at a density of $3x10^5$/ml.

4.8 Flow cytometry

4.8.1 Buffers and reagents

FACS buffer: 1x PBS, 0.5% (w/v) BSA (Serva), 2mM EDTA in ddH_2O

Collagenase IV (Worthington Biochemical Corp., Lakewood, NJ)**:** 2 mg/ml in PBS, freshly prepared before use

Propidium iodide (Sigma): 1mg/ml stock solution in ddH_2O, working dilution 1:100, final concentration 0.5 µg/ml

BD Pharm Lyse (BD biosciences): Erythrocyte lysis buffer, 1:10 diluted in ddH_2O

PBS: see section 4.7.1

4.8.2 Antibodies for flow cytometry

specificity	target cells	host/isotype	clone	dye	final dilution	commercial source
CD117	mast cells	Rat IgG2b κ	2B8	APC	1:500	eBiosciences
CD19	B cells	Rat IgG2a κ	1D3	PE	1:100	BD-Pharmingen
CD3ε	T cells	Armenian hamster IgG1κ	145-2C11	PE	1:100	BD-Pharmingen
CD45	hematopoietic cells	Rat IgG2b κ	30-F11	PE	1:100	BD-Pharmingen
CD49b	basophils/ NK cells	Rat IgM κ	DX5	APC	1:100	eBiosciences
F4/80	macrophages	Rat IgG2a κ	BM8	PE	1:100	eBiosciences
FcεRIα	mast cells/ basophils	Armenian hamster IgG	MAR-1	PE	1:300	eBiosciences
Gr-1	neutrophils	Rat IgG2b κ	RB6-8C5	PE	1:10	Miltenyi Biotec
IgE	mast cells/ basophils	Rat IgG1 κ	23G3	PE	1:20	eBiosciences
NKG2D	NK cells	Rat IgG1 κ	CX5	PE	1:40	eBiosciences
Siglec-F	eosinophils	Rat IgG2a κ	E50-2440	PE	1:100	BD-Pharmingen

Table 4.6 Monoclonal antibodies conjugated either with phycoerythrin (PE) or allophycocyanin (APC) used for flow cytometry. Stock concentrations of all antibodies were 0.2 mg/ml except of anti-IgE (0.1 mg/ml) and anti-Gr-1 (not specified).

4.8.3 FACS staining

The hematopoietic cells in the cell suspensions (described below) were identified by staining for cell surface markers. Unspecific binding of antibodies to Fc receptors via their invariable part of the heavy chain was avoided by blocking with anti-CD16/32 (eBioscience) directed against the FcγIII and the FcγII receptor, respectively. Subsequently, cells were incubated with the antibodies listed in Table 4.6 in 50-100 µl FACS buffer for 30 min on ice. After two washing steps propidium iodide was added (final concentration 0.5 µg/ml) for the detection of dead cells. The samples were analyzed in a BD FACS Calibur equipped with a 488 nm and 633 nm laser.

4.8.4 Single cell suspensions

4.8.4.1 Peritoneal lavage

Mice were sacrificed, the skin was removed from the peritoneum as far as possible and the peritoneal cavity was flushed with 4-7 ml cold FACS buffer. Cells were sedimented and the pellet resuspended in 1 ml FACS buffer.

4.8.4.2 Skin cell suspension

Both ears and 1-2 cm^2 of back skin were excised from shaved adult mice. The fat was removed from the back skin and both, ears and back skin, were minced thoroughly using two scalpels. The tissue mush from one mouse was suspended in 20 ml Collagenase IV (2 mg/ml). The suspension was aliquoted into 2 ml microcentrifuge tubes which were incubated for 1 h at 37°C and 1400 rpm in a thermomixer. During this incubation, the tissue suspensions were mixed twice with a Pasteur pipette. The suspensions were poured over a 70 µm cell strainer and centrifuged at 300 g for 10 min at 4°C. The cell pellet was resuspended in 10 ml FACS buffer and poured over a 40 µm and subsequently over a 30 µm strainer. Cells were finally centrifuged at 250 g for 5 min at 4°C and resuspended in 2 ml FACS buffer.

4.8.4.3 Spleen cell suspension

The spleen was removed from the animal, smashed in a Petri dish containing DMEM medium using a plunger of a 2 ml syringe and rubbed through a 70 µm cell strainer. The Petri dish and the cell strainer were washed once and the resulting suspension was centrifuged. The cell pellet was resuspended and incubated for 5 min at RT in 8 ml 1:10 dilution of BD Pharm Lyse solution in order to lyse erythrocytes. After additional centrifugation, cells were resuspended in 5 ml FACS buffer and finally filtered through a 40 µm strainer.

4.8.4.4 Enrichment of splenic granulocytes

About 80% of spleen cells are B and T cells. Thus, granulocytes, in particular the basophils represent a rare population in this organ (about 0.04% of total spleen cells). In order to enrich granulocytes, spleen cell suspensions were separated into lymphocyte and non-lymphocyte fractions by magnetic activated cell sorting (MACS). T and B cells were labeled with anti-CD3ε-Biotin/anti-Biotin MicroBeads and anti-CD19 MicroBeads (Miltenyi Biotec, Bergisch Gladbach), respectively, and extracted from a total spleen cell suspension using LS columns (Miltenyi Biotec) following the manufacturer's instructions. Briefly, the cells from one spleen (see section 4.8.4.3) were transferred into a FACS tube, centrifuged and resuspended in FACS buffer in the appropriate staining volume. The anti-CD3ε antibody was added at a dilution of 1:25. Cells were incubated for 10 min at 4°C and washed once with FACS buffer. CD19 and anti-Biotin MicroBeads (1:10 and 1:5 final dilutions, respectively) were added to the cells in a total volume of 100 µl per 10^7 cells. After an incubation of 15 min at 4°C, cells were washed once and resuspended in 1 ml FACS buffer. The LS column was equilibrated with 3 ml of degassed FACS buffer. Cells were applied onto the column which was placed in a magnet and washed twice. The flow through was collected as the non-lymphocyte fraction. The T and B cells were recovered

after removing the column from the magnet by flushing it firmly with 5 ml FACS buffer using a plunger.

4.9 Histology

Skin samples were fixed in formalin over night and embedded in paraffin. 6 µm sections were stained with Giemsa following standard protocols. Mast cells were identified in Giemsa stained sections by means of their dark purple cytoplasmic granules. As the granules of mucosal mast cells, in contrast to those of connective tissue mast cells, are sensitive to formalin fixation, samples from the gastrointestinal tract were washed with PBS, fixed for 1 h in Carnoy's solution (ethanol/Chloroform/ glacial acetic acid 6:3:1) and transferred to 100% ethanol and then to xylol for at least 2 h (each step). The tissue was embedded in paraffin and sections were stained with naphthol AS-D chloroacetate (CAE staining) serving as substrate for the chloroacetate esterase present in cytoplasmic granules of neutrophils and mast cells. In sections of the stomach mast cells appeared dark red and were localized between epithelial cells while neutrophils appeared pink and could be distinguished by their segmented nuclei.

Mast cells were quantified as cells/mm^2 by software supported determination of the area in which mast cells were counted (DISKUS software 4.50, Hilgers – Technisches Büro, Königswinter)

5 Abbreviations

Ac	acetate
Amp	ampicillin
APC	allophycocyanin
BAC	bacterial artificial chromosome
BaP	basophil progenitor
BMC	bone marrow cell
BMCP	basophil/mast cell progenitor
BMMC	bone marrow derived mast cells
bp	base pair
BSA	bovine serum albumin
Cm	chloramphenicol
CMP	common myeloid progenitor
Cre	causes recombination
CTMC	connective tissue mast cells
d	day
dCTP	desoxycytidine triphosphate
ddH_2O	bidistilled water
DMEM	Dulbecco's modified Eagle medium
DNA	desoxyribonucleic acid
dNTP	desoxyribonucleoside triphosphate
DT	diphtheria toxin
DTR	diphtheria toxin receptor
E. coli	*Escherichia coli*
EDTA	ethylene diamine tetraacetate
ER	estrogen receptor ligand binding domain
EYFP	enhanced yellow fluorescent protein
FACS	fluorescent activated cell sorting
FBS	fetal bovine serum
g	gravitational acceleration, 9.81 ms^{-1}
GMP	granulocyte/monocyte progenitor
h	hours
i.p.	intraperitoneal
Ig	immunoglobulin
IL	interleukin
kb	kilobases

loxP	locus of crossing (X)-over of P1
LT	leukotriene
MACS	magnetic activated cell sorting
MCP	mast cell progenitor
MMC	mucosal mast cells
mRNA	messenger ribonucleic acid
Neo	neomycin
PAMP	pathogen associated molecular pattern
PBS	phosphate buffered saline
PCMC	peritoneal cell derived mast cell
PCR	polymerase chain reaction
PE	phycoerythrin
PG	prostaglandine
PMA	phorbol 12-myristate 13-acetate
rpm	rounds per minute
RT	room temperature
SDS	sodium dodecylsulfate
Sl	steel locus
SPF	specific pathogen free
SSC	standard saline citrate buffer
T_A	annealing temperature
TE	Tris-EDTA
Tet	tetracycline
TLR	toll-like receptor
TNFα	tumor necrosis factor α
Tris	Tris-(hydroxymethyl-)aminomethan
U	unit
v/v	volume per volume
W	white spotting locus
w/v	weight per volume
wt	wild type
Zeo	zeocin

6 References

Abonia, J.P., Friend, D.S., Austen, W.G., Jr., Moore, F.D., Jr., Carroll, M.C., Chan, R., Afnan, J., Humbles, A., Gerard, C., Knight, P., Kanaoka, Y., Yasuda, S., Morokawa, N., Austen, K.F., Stevens, R.L. and Gurish, M.F. (2005) Mast cell protease 5 mediates ischemia-reperfusion injury of mouse skeletal muscle. *J Immunol*, **174**, 7285-7291.

Abraham, S.N. and Malaviya, R. (1997) Mast cells in infection and immunity. *Infect Immun*, **65**, 3501-3508.

Arase, H., Saito, T., Phillips, J.H. and Lanier, L.L. (2001) Cutting edge: the mouse NK cell-associated antigen recognized by DX5 monoclonal antibody is CD49b (alpha 2 integrin, very late antigen-2). *J Immunol*, **167**, 1141-1144.

Arinobu, Y., Iwasaki, H., Gurish, M.F., Mizuno, S., Shigematsu, H., Ozawa, H., Tenen, D.G., Austen, K.F. and Akashi, K. (2005) Developmental checkpoints of the basophil/mast cell lineages in adult murine hematopoiesis. *Proc Natl Acad Sci U S A*, **102**, 18105-18110.

Bennett, C.L., van Rijn, E., Jung, S., Inaba, K., Steinman, R.M., Kapsenberg, M.L. and Clausen, B.E. (2005) Inducible ablation of mouse Langerhans cells diminishes but fails to abrogate contact hypersensitivity. *J Cell Biol*, **169**, 569-576.

Benoist, C. and Mathis, D. (2002) Mast cells in autoimmune disease. *Nature*, **420**, 875-878.

Berrozpe, G., Agosti, V., Tucker, C., Blanpain, C., Manova, K. and Besmer, P. (2006) A distant upstream locus control region is critical for expression of the Kit receptor gene in mast cells. *Mol Cell Biol*, **26**, 5850-5860.

Besmer, P., Murphy, J.E., George, P.C., Qiu, F.H., Bergold, P.J., Lederman, L., Snyder, H.W., Jr., Brodeur, D., Zuckerman, E.E. and Hardy, W.D. (1986) A new acute transforming feline retrovirus and relationship of its oncogene v-kit with the protein kinase gene family. *Nature*, **320**, 415-421.

Brandt, E.B., Strait, R.T., Hershko, D., Wang, Q., Muntel, E.E., Scribner, T.A., Zimmermann, N., Finkelman, F.D. and Rothenberg, M.E. (2003) Mast cells are required for experimental oral allergen-induced diarrhea. *J Clin Invest*, **112**, 1666-1677.

Buch, T., Heppner, F.L., Tertilt, C., Heinen, T.J., Kremer, M., Wunderlich, F.T., Jung, S. and Waisman, A. (2005) A Cre-inducible diphtheria toxin receptor mediates cell lineage ablation after toxin administration. *Nat Methods*, **2**, 419-426.

Burd, P.R., Rogers, H.W., Gordon, J.R., Martin, C.A., Jayaraman, S., Wilson, S.D., Dvorak, A.M., Galli, S.J. and Dorf, M.E. (1989) Interleukin 3-dependent and -independent mast cells stimulated with IgE and antigen express multiple cytokines. *J Exp Med*, **170**, 245-257.

Butterfield, J.H., Weiler, D., Dewald, G. and Gleich, G.J. (1988) Establishment of an immature mast cell line from a patient with mast cell leukemia. *Leuk Res*, **12**, 345-355.

Cailhier, J.F., Partolina, M., Vuthoori, S., Wu, S., Ko, K., Watson, S., Savill, J., Hughes, J. and Lang, R.A. (2005) Conditional macrophage ablation demonstrates that resident macrophages initiate acute peritoneal inflammation. *J Immunol*, **174**, 2336-2342.

Capecchi, M.R. (1989) The new mouse genetics: altering the genome by gene targeting. *Trends Genet*, **5**, 70-76.

Chen, C.C., Grimbaldeston, M.A., Tsai, M., Weissman, I.L. and Galli, S.J. (2005) Identification of mast cell progenitors in adult mice. *Proc Natl Acad Sci U S A*, **102**, 11408-11413.

Chen, R., Ning, G., Zhao, M.L., Fleming, M.G., Diaz, L.A., Werb, Z. and Liu, Z. (2001) Mast cells play a key role in neutrophil recruitment in experimental bullous pemphigoid. *J Clin Invest*, **108**, 1151-1158.

Choi, I.H., Shin, Y.M., Park, J.S., Lee, M.S., Han, E.H., Chai, O.H., Im, S.Y., Ha, T.Y. and Lee, H.K. (1998) Immunoglobulin E-dependent active fatal anaphylaxis in mast cell-deficient mice. *J Exp Med*, **188**, 1587-1592.

Coussens, L.M., Raymond, W.W., Bergers, G., Laig-Webster, M., Behrendtsen, O., Werb, Z., Caughey, G.H. and Hanahan, D. (1999) Inflammatory mast cells up-regulate angiogenesis during squamous epithelial carcinogenesis. *Genes Dev*, **13**, 1382-1397.

Di Nardo, A., Vitiello, A. and Gallo, R.L. (2003) Cutting edge: mast cell antimicrobial activity is mediated by expression of cathelicidin antimicrobial peptide. *J Immunol*, **170**, 2274-2278.

Dymecki, S.M. (1996a) Flp recombinase promotes site-specific DNA recombination in embryonic stem cells and transgenic mice. *Proc Natl Acad Sci U S A*, **93**, 6191-6196.

Dymecki, S.M. (1996b) A modular set of Flp, FRT and lacZ fusion vectors for manipulating genes by site-specific recombination. *Gene*, **171**, 197-201.

Echtenacher, B., Mannel, D.N. and Hultner, L. (1996) Critical protective role of mast cells in a model of acute septic peritonitis. *Nature*, **381**, 75-77.

Ehrlich, P. (1878) Beiträge zur Theorie und Praxis der histologischen Färbung. Leibzig.

Eklund, K.K., Ghildyal, N., Austen, K.F., Friend, D.S., Schiller, V. and Stevens, R.L. (1994) Mouse bone marrow-derived mast cells (mBMMC) obtained in vitro from mice that are mast cell-deficient in vivo express the same panel of granule proteases as mBMMC and serosal mast cells from their normal littermates. *J Exp Med*, **180**, 67-73.

Enerbäck, L., Kolset, S.O., Kusche, M., Hjerpe, A. and Lindahl, U. (1985) Glycosaminoglycans in rat mucosal mast cells. *Biochem J*, **227**, 661-668.

Feil, R., Brocard, J., Mascrez, B., LeMeur, M., Metzger, D. and Chambon, P. (1996) Ligand-activated site-specific recombination in mice. *Proc Natl Acad Sci U S A*, **93**, 10887-10890.

Feil, R., Wagner, J., Metzger, D. and Chambon, P. (1997) Regulation of Cre recombinase activity by mutated estrogen receptor ligand-binding domains. *Biochem Biophys Res Commun*, **237**, 752-757.

Forlino, A., Porter, F.D., Lee, E.J., Westphal, H. and Marini, J.C. (1999) Use of the Cre/lox recombination system to develop a non-lethal knock-in murine model for osteogenesis imperfecta with an alpha1(I) G349C substitution. Variability in phenotype in BrtlIV mice. *J Biol Chem*, **274**, 37923-37931.

Friend, D.S., Ghildyal, N., Austen, K.F., Gurish, M.F., Matsumoto, R. and Stevens, R.L. (1996) Mast cells that reside at different locations in the jejunum of mice infected with Trichinella spiralis exhibit sequential changes in their granule ultrastructure and chymase phenotype. *J Cell Biol*, **135**, 279-290.

Galli, S.J. (1990) New insights into "the riddle of the mast cells": microenvironmental regulation of mast cell development and phenotypic heterogeneity. *Lab Invest*, **62**, 5-33.

Galli, S.J. and Kitamura, Y. (1987) Genetically mast-cell-deficient W/Wv and Sl/Sld mice. Their value for the analysis of the roles of mast cells in biologic responses in vivo. *Am J Pathol*, **127**, 191-198.

Galli, S.J., Nakae, S. and Tsai, M. (2005) Mast cells in the development of adaptive immune responses. *Nat Immunol*, **6**, 135-142.

Galli, S.J., Zsebo, K.M. and Geissler, E.N. (1994) The kit ligand, stem cell factor. *Adv Immunol*, **55**, 1-96.

Gekara, N.O. and Weiss, S. (2008) Mast cells initiate early anti-Listeria host defences. *Cell Microbiol*, **10**, 225-236.

Gerbaulet, A., Scholten, J., Peschke, K., Naumann, R., Müller, W., Krieg, T., Wickenhauser, C., Hartmann, K. and Roers, A. (submitted) Conditional expression of a constitutively active kit receptor results in aggressive mastocytosis and severe colitis.

Giraldo, P. and Montoliu, L. (2001) Size matters: use of YACs, BACs and PACs in transgenic animals. *Transgenic Res*, **10**, 83-103.

Gordon, J.R. and Galli, S.J. (1990a) Mast cells as a source of both preformed and immunologically inducible TNF-alpha/cachectin. *Nature*, **346**, 274-276.

Gordon, J.R. and Galli, S.J. (1990b) Phorbol 12-myristate 13-acetate-induced development of functionally active mast cells in W/Wv but not Sl/Sld genetically mast cell-deficient mice. *Blood*, **75**, 1637-1645.

Gounaris, E., Erdman, S.E., Restaino, C., Gurish, M.F., Friend, D.S., Gounari, F., Lee, D.M., Zhang, G., Glickman, J.N., Shin, K., Rao, V.P., Poutahidis, T., Weissleder, R., McNagny, K.M. and Khazaie, K. (2007) Mast cells are an essential hematopoietic component for polyp development. *Proc Natl Acad Sci U S A*, **104**, 19977-19982.

Grimbaldeston, M.A., Chen, C.C., Piliponsky, A.M., Tsai, M., Tam, S.Y. and Galli, S.J. (2005) Mast cell-deficient W-sash c-kit mutant Kit W-sh/W-sh mice as a model for investigating mast cell biology in vivo. *Am J Pathol*, **167**, 835-848.

Grimbaldeston, M.A., Metz, M., Yu, M., Tsai, M. and Galli, S.J. (2006) Effector and potential immunoregulatory roles of mast cells in IgE-associated acquired immune responses. *Curr Opin Immunol*, **18**, 751-760.

Grimbaldeston, M.A., Nakae, S., Kalesnikoff, J., Tsai, M. and Galli, S.J. (2007) Mast cell-derived interleukin 10 limits skin pathology in contact dermatitis and chronic irradiation with ultraviolet B. *Nat Immunol*, **8**, 1095-1104.

Gu, H., Marth, J.D., Orban, P.C., Mossmann, H. and Rajewsky, K. (1994) Deletion of a DNA polymerase beta gene segment in T cells using cell type-specific gene targeting. *Science*, **265**, 103-106.

Gurish, M.F. and Boyce, J.A. (2006) Mast cells: ontogeny, homing, and recruitment of a unique innate effector cell. *J Allergy Clin Immunol*, **117**, 1285-1291.

Gurish, M.F., Ghildyal, N., McNeil, H.P., Austen, K.F., Gillis, S. and Stevens, R.L. (1992) Differential expression of secretory granule proteases in mouse mast cells exposed to interleukin 3 and c-kit ligand. *J Exp Med*, **175**, 1003-1012.

Gurish, M.F., Nadeau, J.H., Johnson, K.R., McNeil, H.P., Grattan, K.M., Austen, K.F. and Stevens, R.L. (1993) A closely linked complex of mouse mast cell-specific chymase genes on chromosome 14. *J Biol Chem*, **268**, 11372-11379.

Hallgren, J. and Gurish, M.F. (2007) Pathways of murine mast cell development and trafficking: tracking the roots and routes of the mast cell. *Immunol Rev*, **217**, 8-18.

Heaney, J.D. and Bronson, S.K. (2006) Artificial chromosome-based transgenes in the study of genome function. *Mamm Genome*, **17**, 791-807.

Huang, C., Friend, D.S., Qiu, W.T., Wong, G.W., Morales, G., Hunt, J. and Stevens, R.L. (1998a) Induction of a selective and persistent extravasation of neutrophils into the peritoneal cavity by tryptase mouse mast cell protease 6. *J Immunol*, **160**, 1910-1919.

Huang, C., Sali, A. and Stevens, R.L. (1998b) Regulation and function of mast cell proteases in inflammation. *J Clin Immunol*, **18**, 169-183.

Hunt, J.E., Friend, D.S., Gurish, M.F., Feyfant, E., Sali, A., Huang, C., Ghildyal, N., Stechschulte, S., Austen, K.F. and Stevens, R.L. (1997) Mouse mast cell protease 9, a novel member of the chromosome 14 family of serine proteases that is selectively expressed in uterine mast cells. *J Biol Chem*, **272**, 29158-29166.

Hunt, J.E., Stevens, R.L., Austen, K.F., Zhang, J., Xia, Z. and Ghildyal, N. (1996) Natural disruption of the mouse mast cell protease 7 gene in the C57BL/6 mouse. *J Biol Chem*, **271**, 2851-2855.

Ivanova, A., Signore, M., Caro, N., Greene, N.D., Copp, A.J. and Martinez-Barbera, J.P. (2005) In vivo genetic ablation by Cre-mediated expression of diphtheria toxin fragment A. *Genesis*, **43**, 129-135.

Jung, S., Unutmaz, D., Wong, P., Sano, G., De los Santos, K., Sparwasser, T., Wu, S., Vuthoori, S., Ko, K., Zavala, F., Pamer, E.G., Littman, D.R. and Lang, R.A. (2002) In vivo depletion of CD11c(+) dendritic cells abrogates priming of CD8(+) T cells by exogenous cell-associated antigens. *Immunity*, **17**, 211-220.

Kamal, A.H. and Goetz, M.P. (2007) Tamoxifen: using pharmacogenetics to rediscover an old drug. *Breast Cancer online*, **10**, 1-7.

Kawakami, T. and Galli, S.J. (2002) Regulation of mast-cell and basophil function and survival by IgE. *Nat Rev Immunol*, **2**, 773-786.

Kelly, D.W. and Slikker, W., Jr. (1987) The metabolism and elimination of pyrilamine maleate in the rat. *Drug Metab Dispos*, **15**, 460-465.

Kemp, S.F. and Lockey, R.F. (2002) Anaphylaxis: a review of causes and mechanisms. *J Allergy Clin Immunol*, **110**, 341-348.

Khalil, R.M., Luz, A., Mailhammer, R., Moeller, J., Mohamed, A.A., Omran, S., Dormer, P. and Hultner, L. (1996) Schistosoma mansoni infection in mice augments the capacity for interleukin 3 (IL-3) and IL-9 production and concurrently enlarges progenitor pools for mast cells and granulocytes-macrophages. *Infect Immun*, **64**, 4960-4966.

Kilby, N.J., Snaith, M.R. and Murray, J.A. (1993) Site-specific recombinases: tools for genome engineering. *Trends Genet*, **9**, 413-421.

Kinet, J.P. (1999) The high-affinity IgE receptor (Fc epsilon RI): from physiology to pathology. *Annu Rev Immunol*, **17**, 931-972.

Kissenpfennig, A., Henri, S., Dubois, B., Laplace-Builhe, C., Perrin, P., Romani, N., Tripp, C.H., Douillard, P., Leserman, L., Kaiserlian, D., Saeland, S., Davoust, J. and Malissen, B. (2005) Dynamics and function of Langerhans cells in vivo: dermal dendritic cells colonize lymph node areas distinct from slower migrating Langerhans cells. *Immunity*, **22**, 643-654.

Kitamura, Y. (1989) Heterogeneity of mast cells and phenotypic change between subpopulations. *Annu Rev Immunol*, **7**, 59-76.

Kitamura, Y. and Go, S. (1979) Decreased production of mast cells in S1/S1d anemic mice. *Blood*, **53**, 492-497.

Kitamura, Y., Go, S. and Hatanaka, K. (1978) Decrease of mast cells in W/Wv mice and their increase by bone marrow transplantation. *Blood*, **52**, 447-452.

Knight, P.A., Wright, S.H., Lawrence, C.E., Paterson, Y.Y. and Miller, H.R. (2000) Delayed expulsion of the nematode Trichinella spiralis in mice lacking the mucosal mast cell-specific granule chymase, mouse mast cell protease-1. *J Exp Med*, **192**, 1849-1856.

Koller, B.H. and Smithies, O. (1992) Altering genes in animals by gene targeting. *Annu Rev Immunol*, **10**, 705-730.

Kuhn, R., Schwenk, F., Aguet, M. and Rajewsky, K. (1995) Inducible gene targeting in mice. *Science*, **269**, 1427-1429.

Kulka, M., Alexopoulou, L., Flavell, R.A. and Metcalfe, D.D. (2004) Activation of mast cells by double-stranded RNA: evidence for activation through Toll-like receptor 3. *J Allergy Clin Immunol*, **114**, 174-182.

Kumamoto, T., Shalhevet, D., Matsue, H., Mummert, M.E., Ward, B.R., Jester, J.V. and Takashima, A. (2003) Hair follicles serve as local reservoirs of skin mast cell precursors. *Blood*, **102**, 1654-1660.

Kwan, K.M. (2002) Conditional alleles in mice: practical considerations for tissue-specific knockouts. *Genesis*, **32**, 49-62.

Lahl, K., Loddenkemper, C., Drouin, C., Freyer, J., Arnason, J., Eberl, G., Hamann, A., Wagner, H., Huehn, J. and Sparwasser, T. (2007) Selective depletion of Foxp3+ regulatory T cells induces a scurfy-like disease. *J Exp Med*, **204**, 57-63.

Lakso, M., Sauer, B., Mosinger, B., Jr., Lee, E.J., Manning, R.W., Yu, S.H., Mulder, K.L. and Westphal, H. (1992) Targeted oncogene activation by site-specific recombination in transgenic mice. *Proc Natl Acad Sci U S A*, **89**, 6232-6236.

Langer, S.J., Ghafoori, A.P., Byrd, M. and Leinwand, L. (2002) A genetic screen identifies novel non-compatible loxP sites. *Nucleic Acids Res*, **30**, 3067-3077.

Lee, D.M., Friend, D.S., Gurish, M.F., Benoist, C., Mathis, D. and Brenner, M.B. (2002) Mast cells: a cellular link between autoantibodies and inflammatory arthritis. *Science*, **297**, 1689-1692.

Longley, B.J., Tyrrell, L., Ma, Y., Williams, D.A., Halaban, R., Langley, K., Lu, H.S. and Schechter, N.M. (1997) Chymase cleavage of stem cell factor yields a bioactive, soluble product. *Proc Natl Acad Sci U S A*, **94**, 9017-9021.

Lu, L.F., Lind, E.F., Gondek, D.C., Bennett, K.A., Gleeson, M.W., Pino-Lagos, K., Scott, Z.A., Coyle, A.J., Reed, J.L., Van Snick, J., Strom, T.B., Zheng, X.X. and Noelle, R.J. (2006) Mast cells are essential intermediaries in regulatory T-cell tolerance. *Nature*, **442**, 997-1002.

Lunderius, C. and Hellman, L. (2001) Characterization of the gene encoding mouse mast cell protease 8 (mMCP-8), and a comparative analysis of hematopoietic serine protease genes. *Immunogenetics*, **53**, 225-232.

Lunderius, C., Xiang, Z., Nilsson, G. and Hellman, L. (2000) Murine mast cell lines as indicators of early events in mast cell and basophil development. *Eur J Immunol*, **30**, 3396-3402.

Malaviya, R., Ikeda, T., Ross, E. and Abraham, S.N. (1996) Mast cell modulation of neutrophil influx and bacterial clearance at sites of infection through TNF-alpha. *Nature*, **381**, 77-80.

Malbec, O., Roget, K., Schiffer, C., Iannascoli, B., Dumas, A.R., Arock, M. and Daeron, M. (2007) Peritoneal cell-derived mast cells: an in vitro model of mature serosal-type mouse mast cells. *J Immunol*, **178**, 6465-6475.

Malfait, A.M., Malik, A.S., Marinova-Mutafchieva, L., Butler, D.M., Maini, R.N. and Feldmann, M. (1999) The beta2-adrenergic agonist salbutamol is a potent suppressor of established collagen-induced arthritis: mechanisms of action. *J Immunol*, **162**, 6278-6283.

Marshall, J.S. (2004) Mast-cell responses to pathogens. *Nat Rev Immunol*, **4**, 787-799.

Marshall, J.S. and Jawdat, D.M. (2004) Mast cells in innate immunity. *J Allergy Clin Immunol*, **114**, 21-27.

Matsushima, H., Yamada, N., Matsue, H. and Shimada, S. (2004) TLR3-, TLR7-, and TLR9-mediated production of proinflammatory cytokines and chemokines from murine connective tissue type skin-derived mast cells but not from bone marrow-derived mast cells. *J Immunol*, **173**, 531-541.

McCurdy, J.D., Lin, T.J. and Marshall, J.S. (2001) Toll-like receptor 4-mediated activation of murine mast cells. *J Leukoc Biol*, **70**, 977-984.

McLachlan, J.B., Hart, J.P., Pizzo, S.V., Shelburne, C.P., Staats, H.F., Gunn, M.D. and Abraham, S.N. (2003) Mast cell-derived tumor necrosis factor induces hypertrophy of draining lymph nodes during infection. *Nat Immunol*, **4**, 1199-1205.

McLachlan, J.B., Shelburne, C.P., Hart, J.P., Pizzo, S.V., Goyal, R., Brooking-Dixon, R., Staats, H.F. and Abraham, S.N. (2008) Mast cell activators: a new class of highly effective vaccine adjuvants. *Nat Med*, **14**, 536-541.

McNeil, H.P., Austen, K.F., Somerville, L.L., Gurish, M.F. and Stevens, R.L. (1991) Molecular cloning of the mouse mast cell protease-5 gene. A novel secretory granule protease expressed early in the differentiation of serosal mast cells. *J Biol Chem*, **266**, 20316-20322.

McNeil, H.P., Frenkel, D.P., Austen, K.F., Friend, D.S. and Stevens, R.L. (1992a) Translation and granule localization of mouse mast cell protease-5. Immunodetection with specific antipeptide Ig. *J Immunol*, **149**, 2466-2472.

McNeil, H.P., Reynolds, D.S., Schiller, V., Ghildyal, N., Gurley, D.S., Austen, K.F. and Stevens, R.L. (1992b) Isolation, characterization, and transcription of the gene encoding mouse mast cell protease 7. *Proc Natl Acad Sci U S A*, **89**, 11174-11178.

Metcalfe, D.D., Baram, D. and Mekori, Y.A. (1997) Mast cells. *Physiol Rev*, **77**, 1033-1079.

Metz, M., Grimbaldeston, M.A., Nakae, S., Piliponsky, A.M., Tsai, M. and Galli, S.J. (2007) Mast cells in the promotion and limitation of chronic inflammation. *Immunol Rev*, **217**, 304-328.

Morii, E., Jippo, T., Tsujimura, T., Hashimoto, K., Kim, D.K., Lee, Y.M., Ogihara, H., Tsujino, K., Kim, H.M. and Kitamura, Y. (1997) Abnormal expression of mouse mast cell protease 5 gene in cultured mast cells derived from mutant mi/mi mice. *Blood*, **90**, 3057-3066.

Morii, E., Tsujimura, T., Jippo, T., Hashimoto, K., Takebayashi, K., Tsujino, K., Nomura, S., Yamamoto, M. and Kitamura, Y. (1996) Regulation of mouse mast cell protease 6 gene expression by transcription factor encoded by the mi locus. *Blood*, **88**, 2488-2494.

Müsch, W., Wege, A.K., Mannel, D.N. and Hehlgans, T. (2008) Generation and characterization of alpha-chymase-Cre transgenic mice. *Genesis*, **46**, 163-166.

Muyrers, J.P., Zhang, Y., Testa, G. and Stewart, A.F. (1999) Rapid modification of bacterial artificial chromosomes by ET-recombination. *Nucleic Acids Res*, **27**, 1555-1557.

Nagy, A. (2000) Cre recombinase: the universal reagent for genome tailoring. *Genesis*, **26**, 99-109.

Nakano, T., Sonoda, T., Hayashi, C., Yamatodani, A., Kanayama, Y., Yamamura, T., Asai, H., Yonezawa, T., Kitamura, Y. and Galli, S.J. (1985) Fate of bone marrow-derived cultured mast cells after intracutaneous, intraperitoneal, and intravenous transfer into genetically mast cell-deficient W/Wv mice. Evidence that cultured mast cells can give rise to both connective tissue type and mucosal mast cells. *J Exp Med*, **162**, 1025-1043.

Nigrovic, P.A., Gray, D.H., Jones, T., Hallgren, J., Kuo, F.C., Chaletzky, B., Gurish, M., Mathis, D., Benoist, C. and Lee, D.M. (2008) Genetic Inversion in Mast Cell-Deficient Wsh Mice Interrupts Corin and Manifests as Hematopoietic and Cardiac Aberrancy. *Am J Pathol*.

Ogihara, H., Kanno, T., Morii, E., Kim, D.K., Lee, Y.M., Sato, M., Kim, W.Y., Nomura, S., Ito, Y. and Kitamura, Y. (1999) Synergy of PEBP2/CBF with mi transcription factor (MITF) for transactivation of mouse mast cell protease 6 gene. *Oncogene*, **18**, 4632-4639.

Okayama, Y. and Kawakami, T. (2006) Development, migration, and survival of mast cells. *Immunol Res*, **34**, 97-115.

Osoegawa, K., Tateno, M., Woon, P.Y., Frengen, E., Mammoser, A.G., Catanese, J.J., Hayashizaki, Y. and de Jong, P.J. (2000) Bacterial artificial chromosome libraries for mouse sequencing and functional analysis. *Genome Res*, **10**, 116-128.

Ott, V.L. and Cambier, J.C. (2000) Activating and inhibitory signaling in mast cells: new opportunities for therapeutic intervention? *J Allergy Clin Immunol*, **106**, 429-440.

Pejler, G., Abrink, M., Ringvall, M. and Wernersson, S. (2007) Mast cell proteases. *Adv Immunol*, **95**, 167-255.

Pennock, J.L. and Grencis, R.K. (2004) In vivo exit of c-kit+/CD49d(hi)/beta7+ mucosal mast cell precursors from the bone marrow following infection with the intestinal nematode Trichinella spiralis. *Blood*, **103**, 2655-2660.

Reynolds, D.S., Gurley, D.S., Austen, K.F. and Serafin, W.E. (1991) Cloning of the cDNA and gene of mouse mast cell protease-6. Transcription by progenitor mast cells and mast cells of the connective tissue subclass. *J Biol Chem*, **266**, 3847-3853.

Reynolds, D.S., Stevens, R.L., Gurley, D.S., Lane, W.S., Austen, K.F. and Serafin, W.E. (1989) Isolation and molecular cloning of mast cell carboxypeptidase A. A novel member of the carboxypeptidase gene family. *J Biol Chem*, **264**, 20094-20099.

Rodewald, H.R., Dessing, M., Dvorak, A.M. and Galli, S.J. (1996) Identification of a committed precursor for the mast cell lineage. *Science*, **271**, 818-822.

Saito, M., Iwawaki, T., Taya, C., Yonekawa, H., Noda, M., Inui, Y., Mekada, E., Kimata, Y., Tsuru, A. and Kohno, K. (2001) Diphtheria toxin receptor-mediated conditional and targeted cell ablation in transgenic mice. *Nat Biotechnol*, **19**, 746-750.

Schmidlin, F., Amadesi, S., Dabbagh, K., Lewis, D.E., Knott, P., Bunnett, N.W., Gater, P.R., Geppetti, P., Bertrand, C. and Stevens, M.E. (2002) Protease-activated receptor 2 mediates eosinophil infiltration and hyperreactivity in allergic inflammation of the airway. *J Immunol*, **169**, 5315-5321.

Schmidt-Supprian, M. and Rajewsky, K. (2007) Vagaries of conditional gene targeting. *Nat Immunol*, **8**, 665-668.

Schneider, L.A., Schlenner, S.M., Feyerabend, T.B., Wunderlin, M. and Rodewald, H.R. (2007) Molecular mechanism of mast cell mediated innate defense against endothelin and snake venom sarafotoxin. *J Exp Med*, **204**, 2629-2639.

Scholten, J., Hartmann, K., Gerbaulet, A., Krieg, T., Muller, W., Testa, G. and Roers, A. (2008) Mast cell-specific Cre/loxP-mediated recombination in vivo. *Transgenic Res*, **17**, 307-315.

Schwenk, F., Baron, U. and Rajewsky, K. (1995) A cre-transgenic mouse strain for the ubiquitous deletion of loxP-flanked gene segments including deletion in germ cells. *Nucleic Acids Res*, **23**, 5080-5081.

Schwenk, F., Kuhn, R., Angrand, P.O., Rajewsky, K. and Stewart, A.F. (1998) Temporally and spatially regulated somatic mutagenesis in mice. *Nucleic Acids Res*, **26**, 1427-1432.

Secor, V.H., Secor, W.E., Gutekunst, C.A. and Brown, M.A. (2000) Mast cells are essential for early onset and severe disease in a murine model of multiple sclerosis. *J Exp Med*, **191**, 813-822.

Serafin, W.E., Reynolds, D.S., Rogelj, S., Lane, W.S., Conder, G.A., Johnson, S.S., Austen, K.F. and Stevens, R.L. (1990) Identification and molecular cloning of a novel mouse mucosal mast cell serine protease. *J Biol Chem*, **265**, 423-429.

Serafin, W.E., Sullivan, T.P., Conder, G.A., Ebrahimi, A., Marcham, P., Johnson, S.S., Austen, K.F. and Reynolds, D.S. (1991) Cloning of the cDNA and gene for mouse mast cell protease 4. Demonstration of its late transcription in mast cell subclasses and analysis of its homology to subclass-specific neutral proteases of the mouse and rat. *J Biol Chem*, **266**, 1934-1941.

Shelburne, C.P. and Ryan, J.J. (2001) The role of Th2 cytokines in mast cell homeostasis. *Immunol Rev*, **179**, 82-93.

Shimshek, D.R., Kim, J., Hubner, M.R., Spergel, D.J., Buchholz, F., Casanova, E., Stewart, A.F., Seeburg, P.H. and Sprengel, R. (2002) Codon-improved Cre recombinase (iCre) expression in the mouse. *Genesis*, **32**, 19-26.

Soriano, P. (1999) Generalized lacZ expression with the ROSA26 Cre reporter strain. *Nat Genet*, **21**, 70-71.

Soucek, L., Lawlor, E.R., Soto, D., Shchors, K., Swigart, L.B. and Evan, G.I. (2007) Mast cells are required for angiogenesis and macroscopic expansion of Myc-induced pancreatic islet tumors. *Nat Med*, **13**, 1211-1218.

Sparwasser, T., Gong, S., Li, J.Y. and Eberl, G. (2004) General method for the modification of different BAC types and the rapid generation of BAC transgenic mice. *Genesis*, **38**, 39-50.

Srinivas, S., Watanabe, T., Lin, C.S., William, C.M., Tanabe, Y., Jessell, T.M. and Costantini, F. (2001) Cre reporter strains produced by targeted insertion of EYFP and ECFP into the ROSA26 locus. *BMC Dev Biol*, **1**, 4.

St-Onge, L., Furth, P.A. and Gruss, P. (1996) Temporal control of the Cre recombinase in transgenic mice by a tetracycline responsive promoter. *Nucleic Acids Res*, **24**, 3875-3877.

Stevens, R.L. and Adachi, R. (2007) Protease-proteoglycan complexes of mouse and human mast cells and importance of their beta-tryptase-heparin complexes in inflammation and innate immunity. *Immunol Rev*, **217**, 155-167.

Stevens, R.L., Friend, D.S., McNeil, H.P., Schiller, V., Ghildyal, N. and Austen, K.F. (1994) Strain-specific and tissue-specific expression of mouse mast cell secretory granule proteases. *Proc Natl Acad Sci U S A*, **91**, 128-132.

Strait, R.T., Morris, S.C., Yang, M., Qu, X.W. and Finkelman, F.D. (2002) Pathways of anaphylaxis in the mouse. *J Allergy Clin Immunol*, **109**, 658-668.

Supajatura, V., Ushio, H., Nakao, A., Akira, S., Okumura, K., Ra, C. and Ogawa, H. (2002) Differential responses of mast cell Toll-like receptors 2 and 4 in allergy and innate immunity. *J Clin Invest*, **109**, 1351-1359.

Thakurdas, S.M., Melicoff, E., Sansores-Garcia, L., Moreira, D.C., Petrova, Y., Stevens, R.L. and Adachi, R. (2007) The mast cell-restricted tryptase mMCP-6 has a critical immunoprotective role in bacterial infections. *J Biol Chem*, **282**, 20809-20815.

Theoharides, T.C. and Conti, P. (2004) Mast cells: the Jekyll and Hyde of tumor growth. *Trends Immunol*, **25**, 235-241.

Thomas, K.R. and Capecchi, M.R. (1987) Site-directed mutagenesis by gene targeting in mouse embryo-derived stem cells. *Cell*, **51**, 503-512.

Tkaczyk, C., Okayama, Y., Metcalfe, D.D. and Gilfillan, A.M. (2004) Fcgamma receptors on mast cells: activatory and inhibitory regulation of mediator release. *Int Arch Allergy Immunol*, **133**, 305-315.

Tomimori, Y., Muto, T., Fukami, H., Saito, K., Horikawa, C., Tsuruoka, N., Saito, M., Sugiura, N., Yamashiro, K., Sumida, M., Kakutani, S. and Fukuda, Y. (2002a) Chymase participates in chronic dermatitis by inducing eosinophil infiltration. *Lab Invest*, **82**, 789-794.

Tomimori, Y., Muto, T., Fukami, H., Saito, K., Horikawa, C., Tsuruoka, N., Yamashiro, K., Saito, M., Sugiura, N., Sumida, M., Kakutani, S. and Fukuda, Y. (2002b) Mast cell chymase regulates dermal mast cell number in mice. *Biochem Biophys Res Commun*, **290**, 1478-1482.

Trautmann, A., Toksoy, A., Engelhardt, E., Brocker, E.B. and Gillitzer, R. (2000) Mast cell involvement in normal human skin wound healing: expression of monocyte chemoattractant protein-1 is correlated with recruitment of mast cells which synthesize interleukin-4 in vivo. *J Pathol*, **190**, 100-106.

Trong, H.L., Newlands, G.F., Miller, H.R., Charbonneau, H., Neurath, H. and Woodbury, R.G. (1989) Amino acid sequence of a mouse mucosal mast cell protease. *Biochemistry*, **28**, 391-395.

Tsai, M., Shih, L.S., Newlands, G.F., Takeishi, T., Langley, K.E., Zsebo, K.M., Miller, H.R., Geissler, E.N. and Galli, S.J. (1991) The rat c-kit ligand, stem cell factor, induces the development of connective tissue-type and mucosal mast cells in vivo. Analysis by anatomical distribution, histochemistry, and protease phenotype. *J Exp Med*, **174**, 125-131.

Voehringer, D., Liang, H.E. and Locksley, R.M. (2008) Homeostasis and effector function of lymphopenia-induced "memory-like" T cells in constitutively T cell-depleted mice. *J Immunol*, **180**, 4742-4753.

von Köckritz-Blickwede, M., Goldmann, O., Thulin, P., Heinemann, K., Norrby-Teglund, A., Rohde, M. and Medina, E. (2008) Phagocytosis-independent antimicrobial activity of mast cells by means of extracellular trap formation. *Blood*, **111**, 3070-3080.

Vooijs, M., Jonkers, J. and Berns, A. (2001) A highly efficient ligand-regulated Cre recombinase mouse line shows that LoxP recombination is position dependent. *EMBO Rep*, **2**, 292-297.

Waskow, C., Terszowski, G., Costa, C., Gassmann, M. and Rodewald, H.R. (2004) Rescue of lethal c-KitW/W mice by erythropoietin. *Blood*, **104**, 1688-1695.

Weller, K., Foitzik, K., Paus, R., Syska, W. and Maurer, M. (2006) Mast cells are required for normal healing of skin wounds in mice. *Faseb J*, **20**, 2366-2368.

Wolters, P.J., Mallen-St Clair, J., Lewis, C.C., Villalta, S.A., Baluk, P., Erle, D.J. and Caughey, G.H. (2005) Tissue-selective mast cell reconstitution and differential lung gene expression in mast cell-deficient Kit(W-sh)/Kit(W-sh) sash mice. *Clin Exp Allergy*, **35**, 82-88.

Wolters, P.J., Pham, C.T., Muilenburg, D.J., Ley, T.J. and Caughey, G.H. (2001) Dipeptidyl peptidase I is essential for activation of mast cell chymases, but not tryptases, in mice. *J Biol Chem*, **276**, 18551-18556.

Wong, G.W., Yasuda, S., Morokawa, N., Li, L. and Stevens, R.L. (2004) Mouse chromosome 17A3.3 contains 13 genes that encode functional tryptic-like serine proteases with distinct tissue and cell expression patterns. *J Biol Chem*, **279**, 2438-2452.

Yamada, N., Matsushima, H., Tagaya, Y., Shimada, S. and Katz, S.I. (2003) Generation of a large number of connective tissue type mast cells by culture of murine fetal skin cells. *J Invest Dermatol*, **121**, 1425-1432.

Yamazaki, M., Tsujimura, T., Morii, E., Isozaki, K., Onoue, H., Nomura, S. and Kitamura, Y. (1994) C-kit gene is expressed by skin mast cells in embryos but not in puppies of Wsh/Wsh mice: age-dependent abolishment of c-kit gene expression. *Blood*, **83**, 3509-3516.

Yu, M., Tsai, M., Tam, S.Y., Jones, C., Zehnder, J. and Galli, S.J. (2006) Mast cells can promote the development of multiple features of chronic asthma in mice. *J Clin Invest*, **116**, 1633-1641.

Zhang, Y., Buchholz, F., Muyrers, J.P. and Stewart, A.F. (1998) A new logic for DNA engineering using recombination in Escherichia coli. *Nat Genet*, **20**, 123-128.

Zhang, Y., Muyrers, J.P., Testa, G. and Stewart, A.F. (2000) DNA cloning by homologous recombination in Escherichia coli. *Nat Biotechnol*, **18**, 1314-1317.

Zhou, J.S., Xing, W., Friend, D.S., Austen, K.F. and Katz, H.R. (2007) Mast cell deficiency in Kit(W-sh) mice does not impair antibody-mediated arthritis. *J Exp Med*, **204**, 2797-2802.

Acknowledgements

I would like to thank Prof. Krieg and Prof. Pasparakis for reviewing my thesis and Prof. Krieg for providing me the opportunity to join his department and for supporting me.

Many sincere thanks to my supervisor Axel Roers who gave me the opportunity to join his group. I am very grateful for his professional support, for his motivating enthusiasm and also for giving me the opportunity to present my data on various congresses.

I also wish to thank Werner Müller for his particularly helpful advice.

I also like to thank all members of the lab for creating this friendly atmosphere. I am especially grateful to Alexander Gerbaulet, Karin Hartmann, Carmen Berns, Tobias Häring and Lisa Siewe for constructive discussions and technical support.

Many sincere thanks to my husband, Lars, for his great support and many thanks to my mother for her support during my whole studies.

Erklärung

Ich versichere, dass ich die von mir vorgelegte Dissertation selbständig angefertigt, die benutzten Quellen und Hilfsmittel vollständig angegeben und die Stellen der Arbeit − einschließlich Tabellen, Karten und Abbildungen −, die anderen Werken im Wortlaut oder dem Sinn nach entnommen sind, in jedem Einzelfall als Entlehnung kenntlich gemacht habe; dass diese Dissertation noch keiner anderen Fakultät oder Universität zur Prüfung vorgelegen hat; dass sie − abgesehen von unten angegebenen Teilpublikationen − noch nicht veröffentlicht worden ist sowie, dass ich eine solche Veröffentlichung vor Abschluss des Promotionsverfahrens nicht vornehmen werde. Die Bestimmungen der Promotionsordnung sind mir bekannt. Die von mir vorgelegte Dissertation ist von Prof. Dr. Dr. Thomas Krieg betreut worden.

Köln, den

_____

Julia Scholten

Teilpublikation:

Scholten, J., Hartmann, K., Gerbaulet, A., Krieg, T., Müller, W., Testa, G. and Roers, A. (2008) Mast cell-specific Cre/*loxP*-mediated recombination in vivo. *Transgenic Res*, **17**, 307-315

Lebenslauf

Nachname, Vorname	Scholten, Julia
Geburtsdatum	11. Mai 1977
Geburtsort	Duisburg

Promotion

Seit Mai 2004	Novel tools for mast cell research: Mast cell-specific Cre-mediated gene inactivation and inducible ablation of mast cells *in vivo.* Im Institut von Prof. T. Krieg in der Arbeitsgruppe von Prof. A. Roers

Biologie-Studium

Mai 2003 bis Mai 2004	Diplomarbeit; Thema: „Molekulargenetische und zellbiologische Untersuchung des Par-4-Interaktionspartners Amida“, Institut für Genetik, Rheinische Friedrich-Wilhelms Universität Bonn
März bis April 2003	Diplomprüfungen im Rahmen des Biologiestudiums an der Rheinischen Friedrich-Wilhelms-Universität Bonn; Hauptfach: Molekulargenetik, Nebenfächer: Immunbiologie und Biochemie
November 1998	Vordiplom der Biologie, Rheinische Friedrich-Wilhelms Universität Bonn
Oktober 1996	Aufnahme des Biologiestudiums an der Rheinischen Friedrich-Wilhelms-Universität Bonn

Medizin-Studium

August 2002	Erstes Staatsexamen der Medizin, Rheinische Friedrich-Wilhelms Universität Bonn
März 2001	Ärztliche Vorprüfung (Physikum), Rheinische Friedrich-Wilhelms Universität Bonn
April 1999	Aufnahme des Medizinstudiums an der Rheinischen Friedrich-Wilhelms-Universität Bonn

Schulische Ausbildung

Juni 1996	Lise-Meitner-Gymnasium, Geldern, Abitur